# AN ABRASIVE-CORROSIVE WEAR EVALUATION OF SOME ALUMINIUM ALLOYS

by

G.D. Meyer-Rödenbeck

A thesis submitted to the Faculty of Engineering, University of Cape Town
in fulfillment of the degree of Master of Science in Engineering

Department of Materials Engineering
University of Cape Town

January 1989

## ABSTRACT

This investigation evaluates the abrasive-corrosive wear behaviour of aluminium alloys with the aim of establishing a data base of performance and guide lines for material optimisation. Wear test apparatus and standard tests developed by previous research programmes were utilised (Noel and Allen, 1981; Barker, 1988). Further tests were then devised for a more detailed characterisation of wear behaviour.

Tests conducted showed that aluminuim alloys have approximately a quarter to half the abrasion resistance of mild steel. Poor microfracture properties of Al-Si cast alloys were observed as a result of coarse and brittle silicon rich phases contained in the aluminium matrix. Non heat-treatable wrought alloys exhibit ductile micro-deformation characteristics whilst heat-treatable alloys, having the best abrasion resistance, possess better combinations of strength, hardness and toughness.

Tests with combined corrosion and wear showed that most aluminium alloys are subject to pitting corrosion due to localised differences in electrode potentials at constituent sites. Higher series alloys with a large number of constituent particles exhibit higher pitting densities. Due to the high electrode potentials of silicon phases and copper and zinc solid solutions, the alloys LM6+Sr, 2014 and 7075 have poor corrosion resistance and are subject to localised and pitting attack. As a consequence the alloys 2014, 7075 and LM6+Sr show a decrease in wear performance under abrasive-corrosive conditions. In contrast the good corrosion resistance of the alloys 5083, 6261 and 7017 provide a significant improvement in wear performance under conditions of long corrosion periods with light abrasive intervals.

This study concludes that the abrasion resistance of wrought alloys may be optimised by designing an alloy with a good combination of tensile strength, fracture toughness and hardness together with an intermediate microstructural size distribution of second phase particles in the aluminium matrix. Ageing of heat treatable alloys improves abrasion resistance significantly, peak hardness and strength conditions resulting in optimum abrasion properties.

## ACKNOWLEDGEMENTS

I would like to thank the following people for their help and advice during the course of this thesis:

Professor A Ball, my supervisor.

Mr N Dreze and Mr G Newins for their technical assistance.

Dr K C Barker for his invaluable advice.

Mr J Peterson and Mr B Greeves for the photographic work.

Mrs H Bohm for her help in the preparation of the final manuscript.

Mrs J Geldenhuys and Mrs A C Ball for typing of the final manuscript.

Hulett Aluminium (Pty.) Ltd. is gratefully acknowledged for the provision of the research bursary and materials supplied.

CONTENTS Page

## GLOSSARY OF SYMBOLS AND ABBREVIATIONS

| | |
|---|---|
| AFSA | Aluminium Federation of South Africa |
| G | slope of curve |
| d | sample diameter |
| D | average grit diameter |
| $D_1$ | transition grit diameter |
| n | constant which depends on sample and grit size |
| p | average pressure on the sample surface |
| pH | $\log[H^+]^{-1}$ |
| ppm | concentration in parts per million |
| R | wear rate |
| $R_1$ | value of R at transition point |
| S | slope of the curve |
| RAR | Relative Abrasion Resistance |
| RWR | Relative Abrasive-Corrosive Wear Resistance |
| RWR#1,2 | Standard Relative Wear Resistance |
| SEM | Scanning Electron Microscope |
| t | time |

# AN ABRASIVE-CORROSIVE WEAR EVALUATION OF SOME ALUMINIUM ALLOYS

by

G.D. Meyer-Rödenbeck

A thesis submitted to the Faculty of Engineering, University of Cape Town
in fulfillment of the degree of Master of Science in Engineering

Department of Materials Engineering
University of Cape Town

January 1989

# CHAPTER 1

## INTRODUCTION

### 1.1 PROJECT MOTIVATION

Hulett Aluminium (Pty) Ltd. of South Africa produces a wide range of cast and wrought products for industrial and domestic applications; new application areas are continuously being asessed and promoted. One of these new application areas is the mining industry. In view of escalating production and maintenance costs, the efficiency of traditional construction and wear application metals are being evaluated. New development steels are being introduced and tested and as a part of a drive for increased usage of aluminium components in the mining industry Hulett Aluminium have initiated a cooperative research project with the aim of establishing a data base of wear performance for aluminium alloys. The work described herein represents the initial assessment of existing alloys in terms of microstructural parameters.

### 1.2 THE APPROACH TAKEN

Protheroe, Ball and Heathcock (1982) considered the practical requirements for material selection in a mining environment. See fig. 1.1.

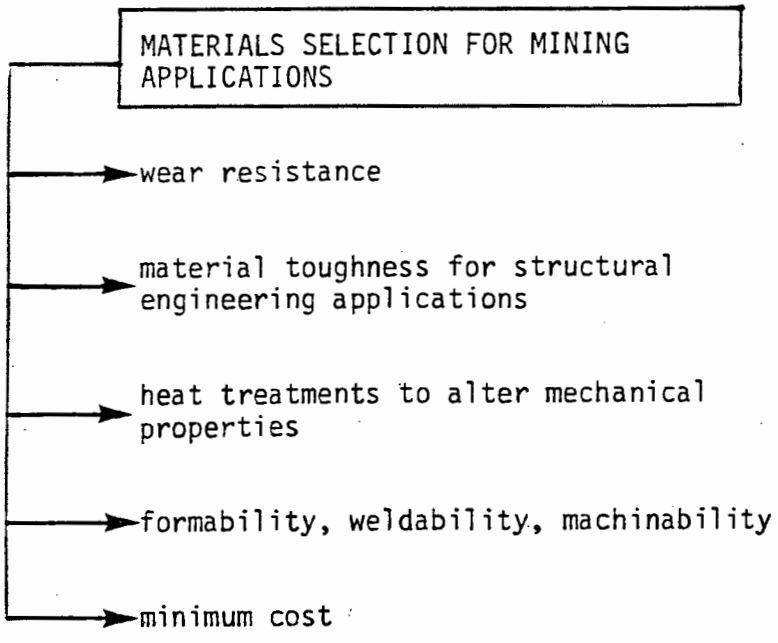


FIGURE 1.1 : Materials selection requirements.

The approach taken was to establish the basic wear characteristics of aluminium alloys utilising test apparatus developed by previous research programmes (Noel, Allen, 1981). Particular strengths and weaknesses could then be assessed and investigated with reference to microstructural and physical properties. An initial evaluation of the alloys tested in terms of the criteria set out in fig. 1.1 and the identification of optimum performance conditions could then be achieved.

## 1.3 PROJECT OBJECTIVES

This investigation involves the accumulation and evaluation of wear data for aluminium alloys. As the range of test alloys is extensive (14 alloys) and little information is presently available on the abrasive-corrosive wear of aluminium alloys, a broad rather than detailed characterisation is required. The following objectives have been set :

i) Accumulation of wear data:
   (a) to establish the effect of load, speed and grit size parameters on dry abrasive wear.
   (b) obtain a measure of dry abrasive and abrasive-corrosive wear performance relative to mild steel.
   (c) conduct tests for a more detailed corrosive and abrasive-corrosive wear characterisation of some alloys.

ii) Evaluation of wear data:
   (a) evaluate and explain weaknesses and strengths in terms of microstructural and physical properties.
   (b) ranking the materials with respect to abrasion resistance and abrasion-corrosion resistance.
   (c) identify wear conditions and material properties for optimum material performance.

# CHAPTER 2

## LITERATURE SURVEY

### 2.1 PURPOSE AND SCOPE

The purpose of this literature survey is to provide the reader with the background knowledge that was required and used to interpret, discuss and conclude on experimental results. The three wear mechanisms relevant to this investigation, namely abrasion, corrosion and abrasion-corrosion, are described.

Metal deterioration in any of the above wear environments depends on both the wear properties of the material and the type and severity of the wear conditions. These factors are discussed with specific reference to aluminium alloys and the previous work done to characterise the wear behaviour of these alloys.

### 2.2 DRY ABRASION

In this section a model of 2-body abrasive wear is presented. The effect of material properties, external factors and heat treatments on abrasive wear performance is discussed. Figure 2.1 gives a schematic layout of the wear variables involved.

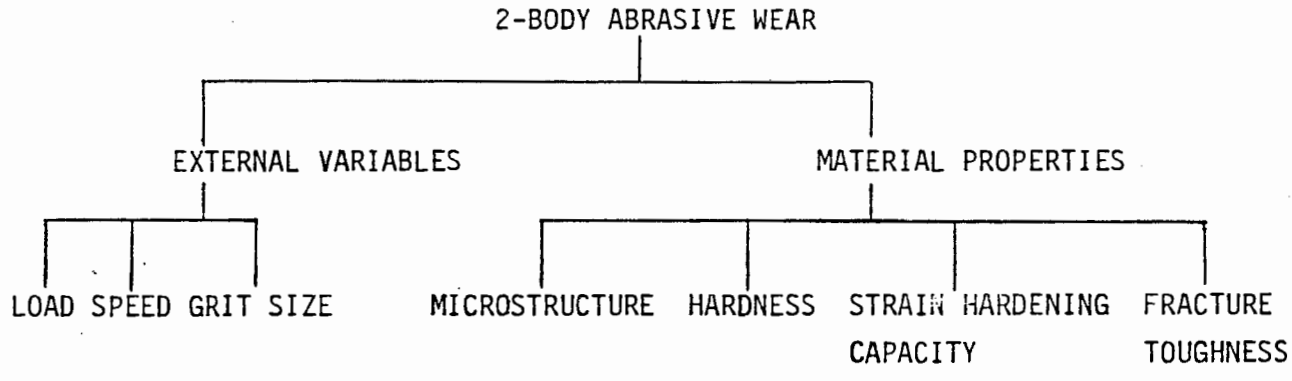


FIGURE 2.1 : Abrasive wear variables.

### 2.2.1 2-Body Abrasive Wear

Abrasion, by definition, is the removal of material by hard particles or protuberances. The ability of a metal to accommodate the stresses and strains imposed by abrasive wear without appreciable material loss is termed abrasion resistance. 2-body abrasive wear is characterized by the movement of hard particles over a metal surface. See fig. 2.2.

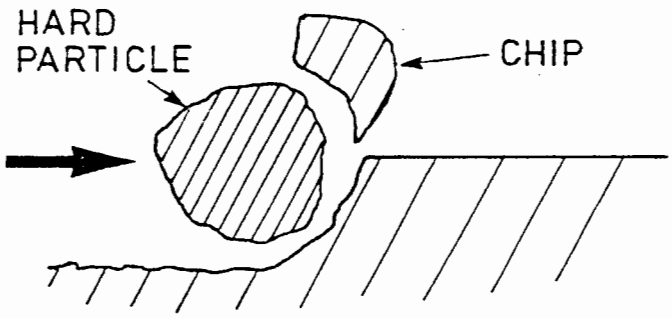


FIGURE 2.2 : 2-body abrasive wear.

Volume loss occurs in a two-stage process; initially critical strains are accumulated through plastic deformation and then either ductile or brittle microfracture occurs. During steady-state abrasion these two processes occur simultaneously and continuously.

### 2.2.2 Effect of Material Properties on Abrasive Wear Resistance

#### Hardness

Simple models of abrasive wear are based on resistance to indentation, or hardness. Moore (1980) concludes that, in practice, the hardness of a worn surface does influence wear properties but provides no measure of deformation characteristics and susceptibility to ductile or brittle microfracture. These two important factors influence the mechanism and ease of material removal during abrasive wear.

Horn and Ziegler (1983) considered the effects of hardness on the abrasive wear behaviour of aluminium alloys. Although in general, alloys having low hardness show higher wear and wear decreases appreciably with increasing hardness for some alloys, no definite trends are identifiable.

A plot of abrasion resistance versus hardness for a wide range of metals also demonstrates the inadequacy of hardness as a primary measure of abrasion resistance. Figure 2.3 shows that alloys with vastly different hardness values can have similar abrasion resistnce and conversely, alloys with the same hardness can wear at very different rates.

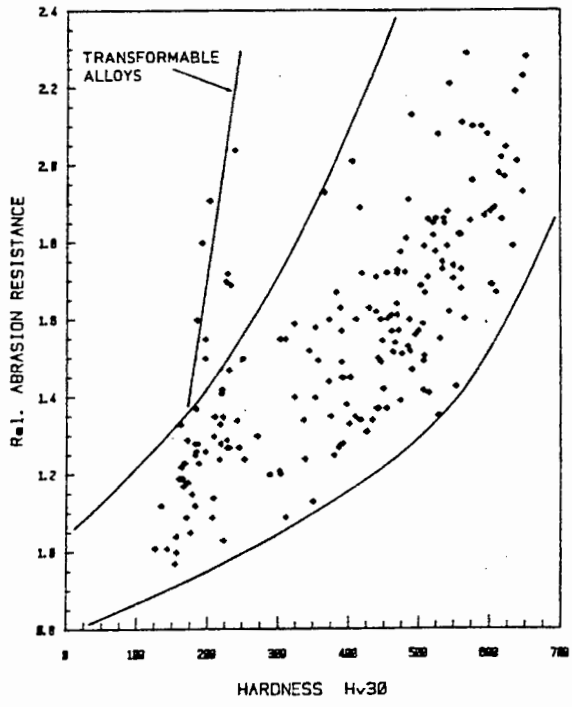


FIGURE 2.3 : Abrasion resistance of alloys in dry conditions relative to the abrasion resistance of mild steel plotted against bulk hardness (combined plot of materials tested at Dept. of Materials Engineering, UCT, Sept. 1985).

Strain hardening capacity

During abrasive wear, localised regions on the metal surface experience high stresses, strains and strain rates. The ability of a material to withstand strain and to resist microfracture is influenced by strain hardening capacity. Ball (1986) discusses the interaction of abrasive wear and strain-hardening for different classes of materials. Fig. 2.4 shows the stress-strain curves and a basic model of the wear behaviour of Materials A, B and C.

Stress-strain curve A is representative of hard and brittle solids. During abrasive wear microfracture is initiated by small defects in the material and low resistance to crack propagation of the microstructure results in high wear losses.

Material C represents soft, ductile metals. The mean level of stress associated with abrasive wear ($\sigma m$), is such that critical stresses and strains required for microfracture are easily achieved and wear loss occurs by ductile cutting. Clearly these materials have poor wear resistance.

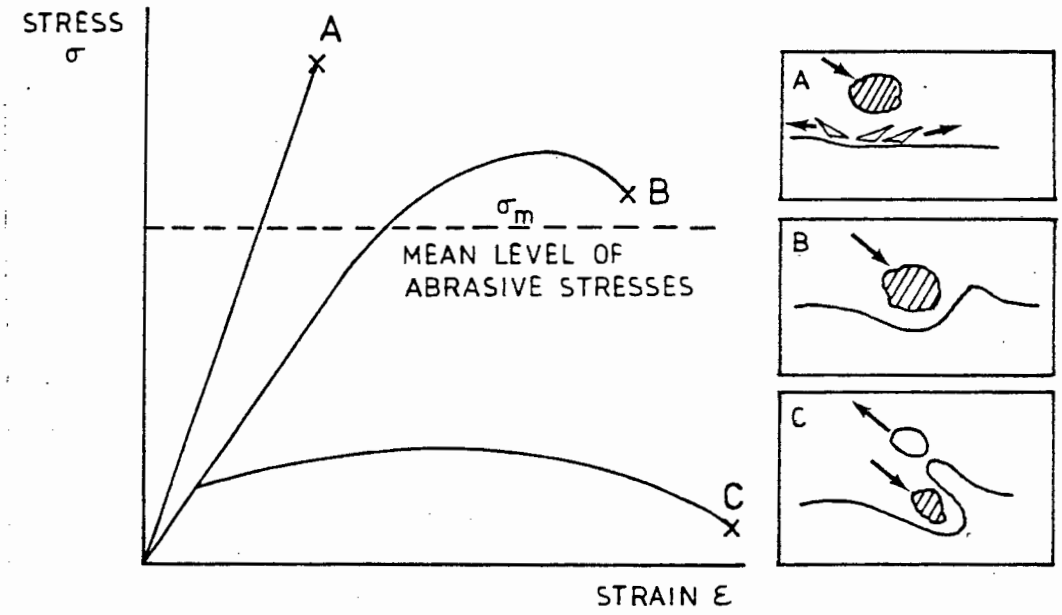


FIGURE 2.4 : Strain hardening characteristics (after Ball, 1986).

The rapidly rising stress-strain curve of Material B indicates a good combination of strength and strain-hardening capacity. In this case, abrasive stress levels are such that localised regions on the metal surface accumulate strain and become work-hardened. Strength-and-hardness increases through work-hardening also affords a degree of toughness and in effect, a higher resistance to wear is achieved. The importance of work-hardening capacity is thus clearly illustrated.

Narasimha Rao and Sekhar (1986) examined the differences in mechanical properties of aluminium alloys to explain their wear behaviour. A plot of truestress versus truestrain for these alloys

showed that the slope or strain-hardening index was similar for all alloys, regardless of their strength value. Table 2.1 lists the work-hardening exponent of some wear application steels and the value for aluminium alloys as obtained by Rao and Sekhar.

TABLE 2.1 : Work-hardening exponents.

| MATERIAL | WORK-HARDENING EXPONENT |
|---|---|
| Aluminium alloys | 0.10-0.15 |
| Wearalloy 500 | 0.077 |
| Roqlast AH400 | 0.067 |
| AISI 304 | 0.45-0.50 |
| 3CR12 | 0.173 |

Fracture-toughness

Since microfracture plays an important part in the abrasive wear process, the effect of fracture toughness needs to be evaluated. Zum Gahr (1978) rationalizes the contribution of microfracture by a plot of wear resistance and hardness versus fracture toughness. See fig. 2.5.

Bearing in mind the wear behaviour of Materials A,B and C referred to in fig. 2.4, the wear resistance curve can be divided into three regions. Over Region I brittle wear behaviour as characterised by Material A is predominant, and material loss is strongly dependent on fracture toughness. As hardness decreases with increasing toughness, wear resistance increases. For Region II wear resistance increases to a maximum as an optimum combination of fracture toughness and hardness is attained. Material B is representative. Further increase in toughness and corresponding decrease of hardness (Region III) results in ductile wear behaviour characterised by Material C. Wear resistance then decreases and becomes dependent on hardness.

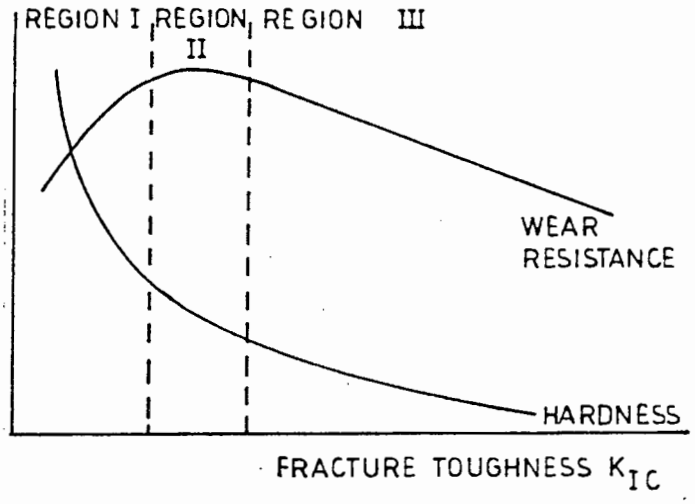


FIGURE 2.5 : Schematic relationship between wear resistance, hardness and fracture toughness (after Zum Gahr, 1978).

### 2.2.3 The Effect of External Factors on Wear Rates

Load

The effect of applied load on wear rates is usually stated to be directly proportional. Jasim and Dwarakadasa (1986) report a linear relationship between load and wear rate for Al-Si alloys under dry sliding conditions, distinguishing between mild and severe wear regimes. See fig. 2.6.

Larsen-Basse (1978) investigated the effect of load on wear rates for metallic abrasion using copper samples. Taking into account the effect of grit and sample size, he established the following relationship for loads up to 1000g :

$$R = S_1 p^n \quad \text{.....eqn. (1)}$$

where $R$ = wear rate ($mm^3/m$)

$S_1, n$ = constants which depend on sample and grit size

$p$ = average pressure on the sample surface ($g/mm^2$)

General trends obtained showed that, for sample diameters greater than 6 - 7 mm, n approached a value of 1.0. A minor variation of n values with grit size was observed.

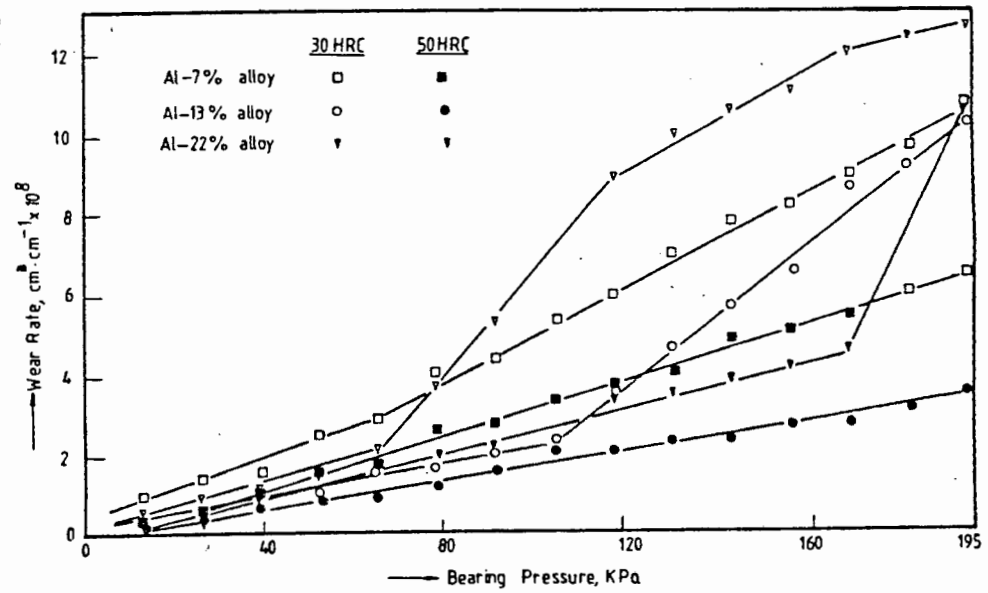


FIGURE 2.6 : Variation of dry sliding wear rates of Al-Si alloys as a function of applied load or bearing pressure (after Jasim and Dwarakadasa, 1986).

Speed

Tanouye and Larsen-Basse (1978) found an inverse relationship between wear rate and sliding velocity for aluminium alloys. See fig. 2.7. It was concluded that an increase in abrasion velocity (increased rate of strain) affects the flow stress of a material by making deformation more difficult, thus reducing the wear rate.

Allen, Protheroe and Ball (1981) found that certain grades of stainless steels showed significant wear rate increases at higher velocities. This result was attributed to an increase in friction temperature leading to easier slip and deformation characteristics.

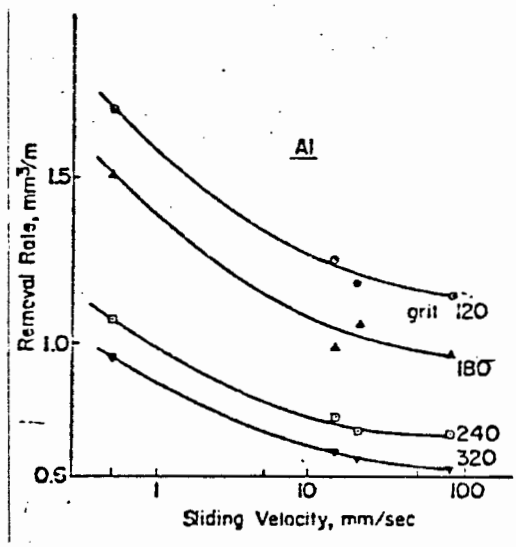


FIGURE 2.7 : A plot of wear rate versus sliding velocity for aluminium alloys using different grit size abrasives (after Tamouye and Larsen-Basse, 1978).

Grit Size

The effect of abrasive grit size on wear rates has been characterized in the following manner : wear rate increases rapidly with grit size until a critical grit diameter is reached. Above this value, wear increases linearly with grit size, but at a slower rate. A physical explanation for the increasing trend is that, for larger grit sizes, fewer abrasive particles are in contact with the metal surface, resulting in higher loads per unit area, larger wear grooves and thus higher wear rates.

Three explanations are forwarded for the critical grit diameter effect. Avient, Goddard and Wilman (1960) found that chips removed by abrasion fill all or part of the interstices between abrasive grits, limiting their cutting action. This effect was more pronounced for finer grit sizes. Mulhearn and Samuels (1962) found that grains of finer grit size abrasives contained a large number of cracks, reducing their ability to remove material. Larsen-Basse (1978) concluded that some abrasive grains are in contact with the metal surface only plastically and do not contribute to cutting of the metal. This was more pronounced for finer grit sizes and virtually disappeared for grit diameters above the critical value.

Horn and Ziegler (1983) investigated the effect of SiC grain size on wear of aluminium alloys and found a less pronounced critical grit diameter effect for the lower wear rate and higher hardness alloys. See fig. 2.8.

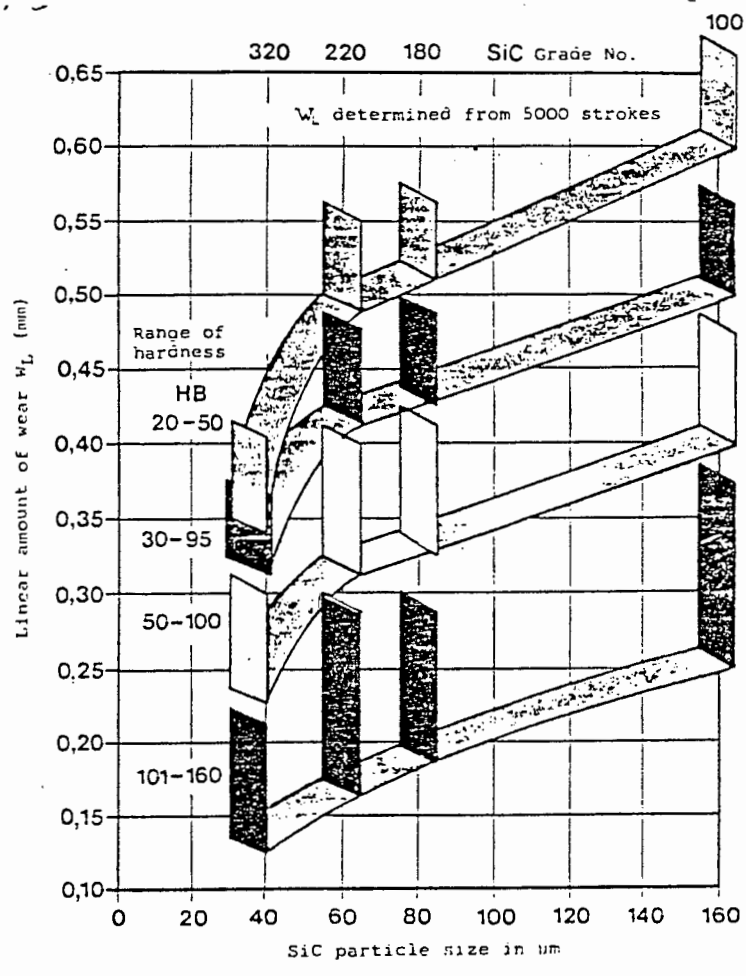


FIGURE 2.8 : Wear loss versus SiC grain size and hardness for some aluminium alloys (after Horn and Ziegler, 1983).

## 2.2.4 The Effect of Microstructure and metallurgical treatments on Abrasion Resistance

Microstructural parameters such as the coherency, hardness and distribution of second phase particles are determined by the type of thermal or metallurgical treatments employed. Abrasive wear resistance is influenced by these parameters through their effect on mechanical properties and microfracture behaviour.

Moore (1980) cites two important effects of microstructure on abrasive wear : when the size of microstructural features is small in comparison to groove size or depth of abrasive particle indentation, micro-influences both bulk properties and crack initiation. Micro-structural features comparable in size to abrasive groove width or depth, influence wear through their individual properties, rather than through their cumulative effect on bulk properties.

Horn and Ziegler (1983) investigated the effect of thermal and metallurgical treatments on aluminium alloys and found that ageing of heat-treatable wrought alloys after solution treating increases their wear resistance appreciably since the coherent and semi-coherent precipitates are smaller and more effectively anchored in the aluminium matrix to resist abrasive particle wear. In the case of non heat-treatable alloys cold work does not improve wear behaviour significantly. Second phase particles contained in the soft Al-matrix are broken out by abrasive particle wear without appreciable resistance. Solution hardening of the Al-matrix by addition of suitable alloying elements increases wear resistance more effectively.

## 2.3 CORROSION

This section introduces the reader to the principles of corrosion involved and the most likely form of corrosive attack that will occur in the case of aluminium alloys. The influence of alloy composition and surface condition on the corrosion resistance of aluminium alloys is also discussed.

### 2.3.1 General

Deterioration of a metal by corrosion takes many forms, depending on the nature of the alloy and characteristics of the corrosive medium. Consider an aluminium alloy as the corroding metal and an aqueous solution as the corrosive medium. Corrosion will take place by means of an electrochemical process and is associated with the flow of electric current between anodic and cathodic regions. The resulting corrosive attack is not uniform, but confined to localised

sites on the metal surface where heterogenerity of either the metal or the corrosive medium is present. See Figure 2.9.

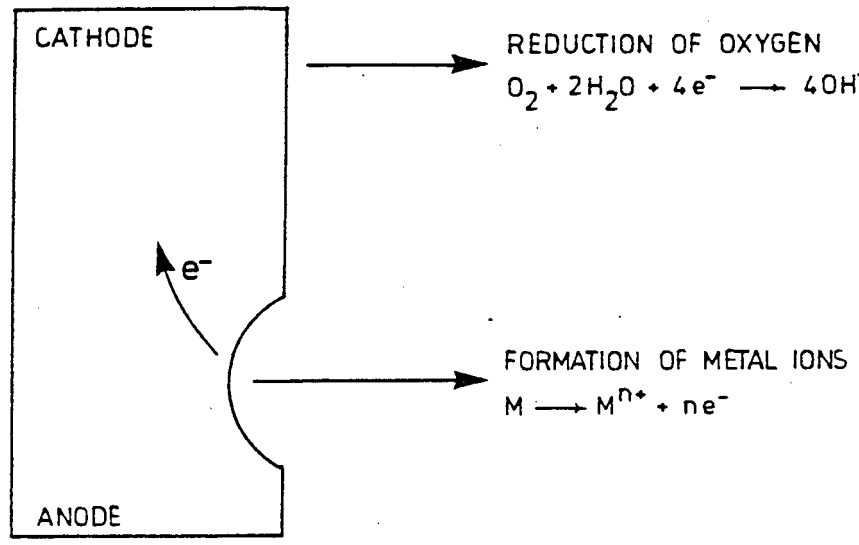


FIGURE 2.9 : Reduction of oxygen and the formation of metal ions in an aqueous solution.

In the case of aluminium, the most common form of corrosive attack is localised corrosion or pitting. Several factors are basic in determining the size and distribution of corrosion pits:

i) Alloy composition, combined with metallurgical and thermal treatments, determine the composition of microconstituents their distribution, quantity and continuity. The resulting cathodic or anodic potentials relative to adjacent regions may initiate pitting at a constituent particle, an inclusion or a grain boundary.

ii) The mechanical deformation associated with an abraded surface influences the quality and continuity of the oxide film. Local discontinuities in this protective film may then act as pit initiation sites.

iii) The nature of the corrosive medium influences both the severity and type of corrosive attack. For an aqeous solution, the amount of dissolved ions, the presence of oxygen, temperature of the solution and velocity of movement are important characteristics.

## 2.3.2 Effect of Alloying Elements and Impurities

Alloying elements may be present in the microstructure of aluminium alloys as solid solutions with aluminium or as microconstituents comprising the element itself. Table 2.2 lists the electrode potentials of various solid solutions and microconstituents that are found in commercially produced aluminium alloys.

Using Table 2.2 it is possible to predict whether the micro constituents of a particular alloy will behave anodically or cathodically with respect to the aluminium solid solution. Localised regions where preferential attack may take place, can thus be identified.

TABLE 2.2 : Electrode potentials of Al-solid solutions and constituents.

| Solid solution or constituent | Potential, v(a) | Solid solution or constituent | Potential, v(a) |
|---|---|---|---|
| $Mg_2Al_3$ | −1.24 | 99.95 Al | −0.85 |
| Al + 4 $MgZn_2$(b) | −1.07 | Al + 1 $Mg_2Si$(b) | −0.83 |
| Al + 4 Zn(b) | −1.05 | Al + 1 Si(b) | −0.81 |
| $MgZn_2$ | −1.05 | Al + 2 Cu(b) | −0.75 |
| $CuMgAl_2$ | −1.00 | $CuAl_2$ | −0.73 |
| Al + 1 Zn(b) | −0.96 | Al + 4 Cu(b) | −0.69 |
| Al + 7 Mg(b) | −0.89 | $FeAl_3$ | −0.56 |
| Al + 5 Mg(b) | −0.88 | $NiAl_3$ | −0.52 |
| Al + 3 Mg(b) | −0.87 | Si | −0.26 |
| $MnAl_6$ | −0.85 | | |

(a) 0.1*N* calomel scale, measured in an aqueous solution of 53 g per liter NaCl + 3 g per liter $H_2O_2$ at 25 C. (b) Solid solution.

## 2.3.3 Corrosion Rates

When an abraded metal surface is exposed to a corrosive environment, material loss may occur through various types of corrosive attack, and at various rates. Barker (1988) identifies three types of corrosion behaviour for materials in the abraded state under identical corrosive conditions. These are : general corrosion, localised corrosion and pitting corrosion. Figure 2.10 shows schematic representations of accumulative material loss by corrosion for three different Materials A, B and C.

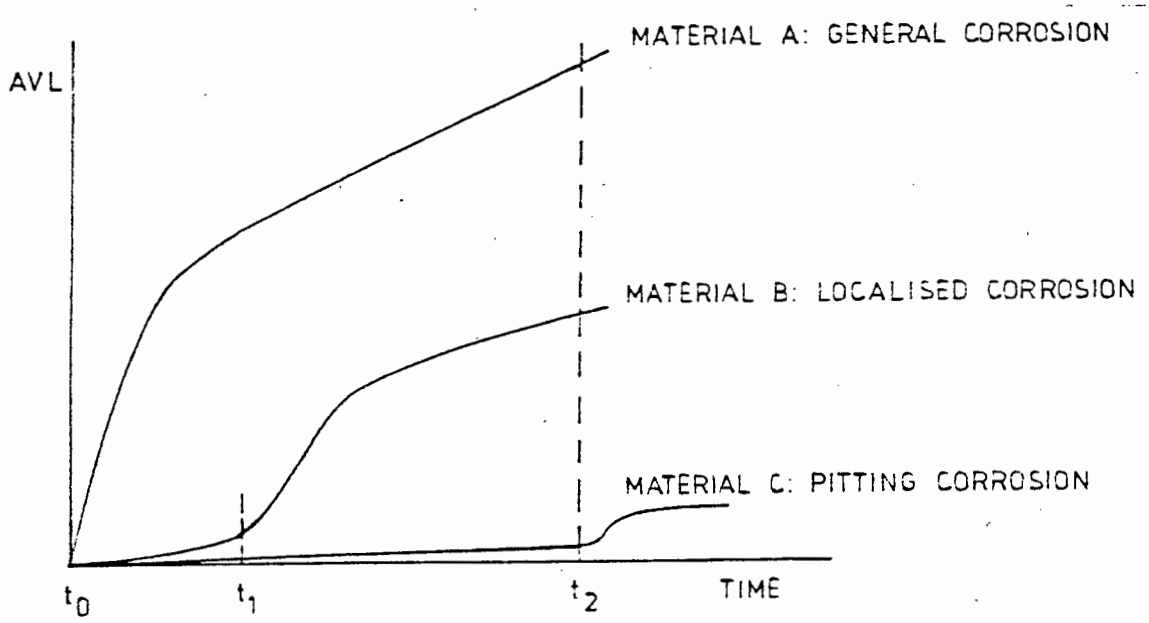


FIGURE 2.10 : Accumulative volume loss by corrosion for Materials A, B and C (after Barker, 1988).

Two definitions are important:

(i) Induction period : defined as the time required for the rate of material loss by corrosion from a freshly abraded metal surface to reach a maximum.

(ii) Passivity : under certain conditions, a small amount of soluble compound of the metal may form an adhering and dense protective film, rendering the corrosion rate negligibly small.

Volume loss of Material A occurs by general corrosion. Material is lost at an accelerated rate immediately after abrasion and the induction period is equal to zero ($t_0$). As thickening of the oxide film occurs, corrosion rate will be controlled by diffusion of oxygen ($O_2$) through the rust and oxide layer. When the rate of decay by corrosion equals the rate of growth of the oxide layer, steady state conditions are achieved. A good example is mild steel.

The formation of a passive oxide layer allows Material B to resist corrosive attack for a certain period of time until localised breakdown of the passive film occurs . After the induction period $t_1$ (see fig. 2.10), accumulative material loss by corrosion increases until steady state conditions are reached. Steels containing chromium of up to 12% are good examples.

The oxide layer of Material C passivates almost immediately and a long induction period ($t_2$) elapses before measurable quantities of material is lost through pitting corrosion. Steels with chromium in excess of 12% are good examples. Under the corrosive conditions relevant to this investigation Materials B and C are most likely to represent the corrosion behaviour of wrought and cast aluminium alloys.

### 2.3.4 The Effect of Surface Condition on Corrosion Rates

The condition of a metal surface prior to corrosion depends on the severity of mechanical deformation associated with abrasion. Barbosa and Scully (1982) investigated the effect of surface finish on the relative size and distribution of corrosion pits using AISI 304 stainless steel and concluded that pit nucleation is primarily a consequence of attack at inclusions and second phase particles rather than a slow rate of film formation at scratched areas.

Noel (1981) conducted similar experiments using mild steel specimens and found that single scratch abrasions on a polished surface produced selective pitting at the deformed ridges of the abrasion groove. It was concluded that the passivating layer and its characteristics are different at abraded regions, changing the corrosion kinetics considerably. As a consequence, selective pitting at abraded regions occurs.

## 2.4 ABRASION-CORROSION

Having introduced the principles of dry abrasion and corrosion, and having discussed the influence of material properties and external factors on wear resistance, it is necessary to look at the combined effect of these two wear mechanisms, termed abrasive-corrosive wear.

Laboratory test simulations of mineral processing operations by Noel (1981), Dunn (1985) and Schumacher (1985) showed that the combined action of these wear mechanisms result in a mutual reinforcement of their effectiveness, known as synergism. Barker (1988), in a study confirming the observed synergistic effects, cites two extreme examples of mining equipment exposed to abrasive-corrosive wear :

(i) A semi-continuous abrasive action which is halted for a certain period of time (high frequency abrasion).
(ii) Long idle times in the presence of a corrosive environment that are periodically interrupted by abrasive action.

Consider the abrasive-corrosive wear performance of Material A characterised in section 2.3.3 for each of the above conditions. From fig. 2.10 it is evident that the corrosion rate is highest for a short period of time $t_1$. Thus, for high frequency abrasive actions and short corrosion times where frequent exposure of the freshly abraded surface to the corrosive environment occurs, the overall rate of material loss is maximised. Conversely, longer corrosion times and lower frequency abrasions will decrease the overall rate of material loss. See fig. 2.11.

Unlike the wear behaviour of Material A, fig. 2.10 shows that the corrosion rate of Material B is low for short exposure times $t_1$, increasing only for periods exceeding $t_2$. The rate of material loss is thus minimised by short corrosion times and frequent abrasions, whilst longer corrosion times result in accelerated corrosion rates and greater overall volume loss rates. See fig. 2.12.

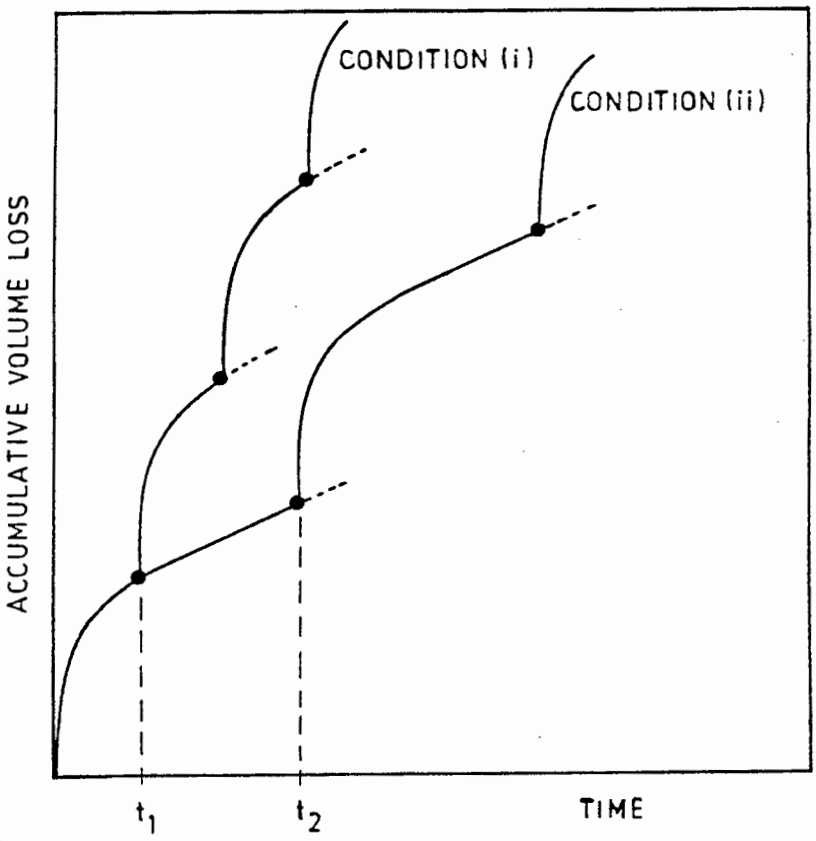


condition (i) : frequent abrasions and short corrosion times ($t_1$) result in high wear rates.

condition (ii): lower frequency abrasions and longer corrosion times ($t_2$) result in lower wear rates.

FIGURE 2.11 : Wear behaviour of Material A for conditions (i) and (ii) (after Barker and Ball to be published in British Corrosion Journal).

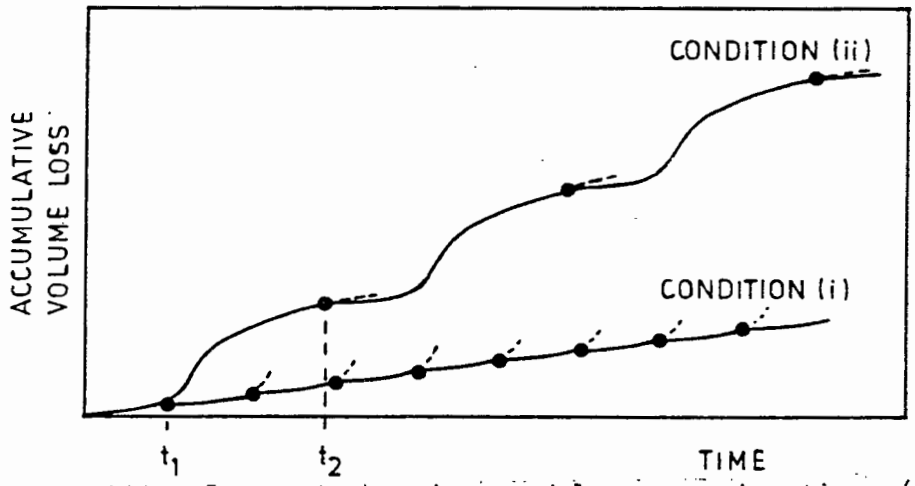


condition (i) : frequent abrasions and low corrosion times ($t_1$) result in low wear rates.

condition (ii): lower frequency abrasions and longer corrosion times ($t_2$) result in higher wear rates.

FIGURE 2.12 : Wear behaviour of Material B for conditions (i) and (ii) (after Barker, 1988).

# CHAPTER 3

## EXPERIMENTAL OVERVIEW

In this section an overview of the test apparatus, experiment variables and test ranges is given. The standard wear tests developed by previous research programmes that were used for this investigation are presented. Criteria for the setting up of further wear tests is also discussed.

## 3.1 DESCRIPTION OF TEST APPARATUS

### 3.1.1 Dry Abrasion Test Rig

The abrasion rig is a Rockwell belt-sander modified to function as a semi-automatic abrasion tester (see fig. 3.1). A schematic sketch of the dry abrasion test and the test variables involved are shown in fig. 3.2.

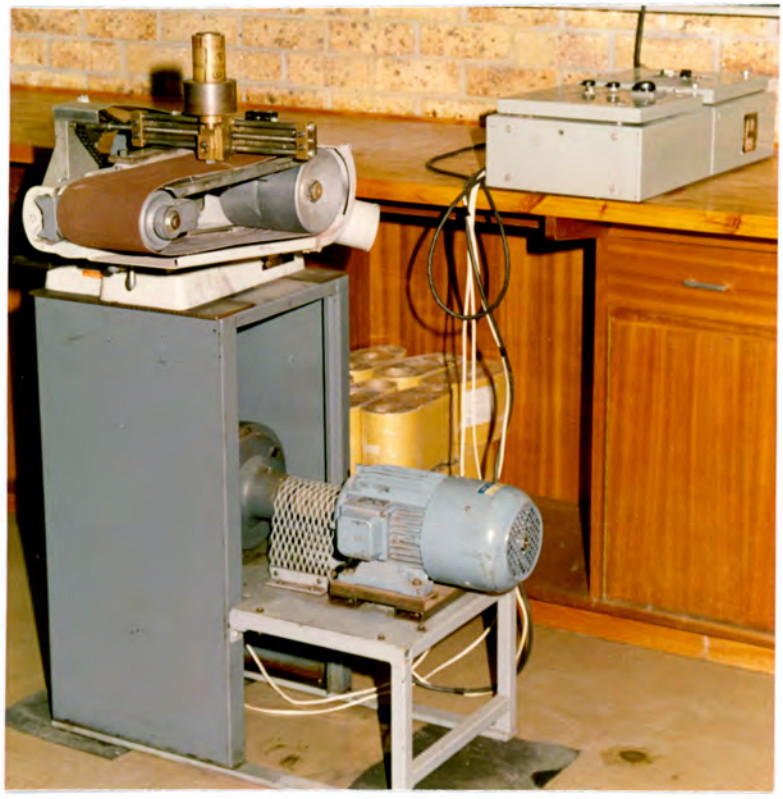

FIGURE 3.1 : Dry abrasion test rig.

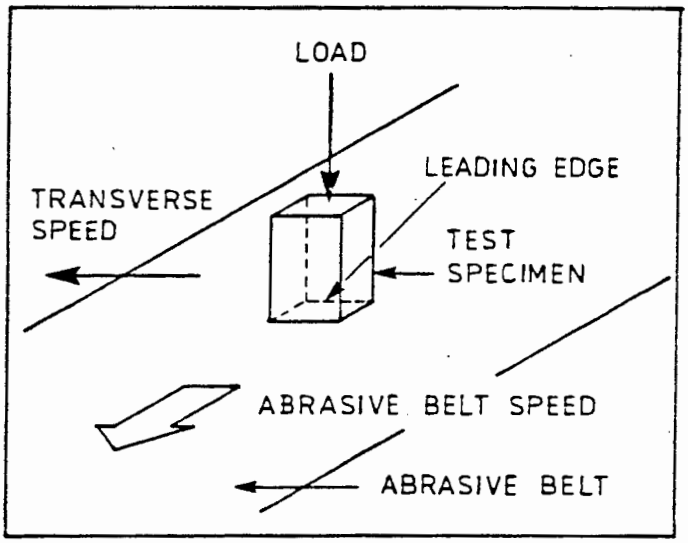


| TEST VARIABLES |
| --- |
| abrasive belt speed<br>load<br>abrasive belt grit size<br>abrasion length |

FIGURE 3.2 : Dry abrasion test and test variables.

Important features of the test rig are:

i) test specimens are clamped in a slider-holder and abraded under load against continuous feed abrasive paper.

ii) for a continuous fresh abrasive belt supply, transverse feed of the test specimen is facilitated by a drive screw arrangement from the main drive.

iii) abrasive belt speed, together with the transverse feed, is thyristor controlled. Stop and start buttons enable control of the abrasion path length.

### 3.1.2 Corrosion Test Rig

The basic principle of the corrosion rig is to circulate simulated mine water using a pump, filter, pipes and reservoir and to pass it over a test panel containing the test samples. See fig. 3.3. A photograph of the test rig is shown in fig. 3.4.

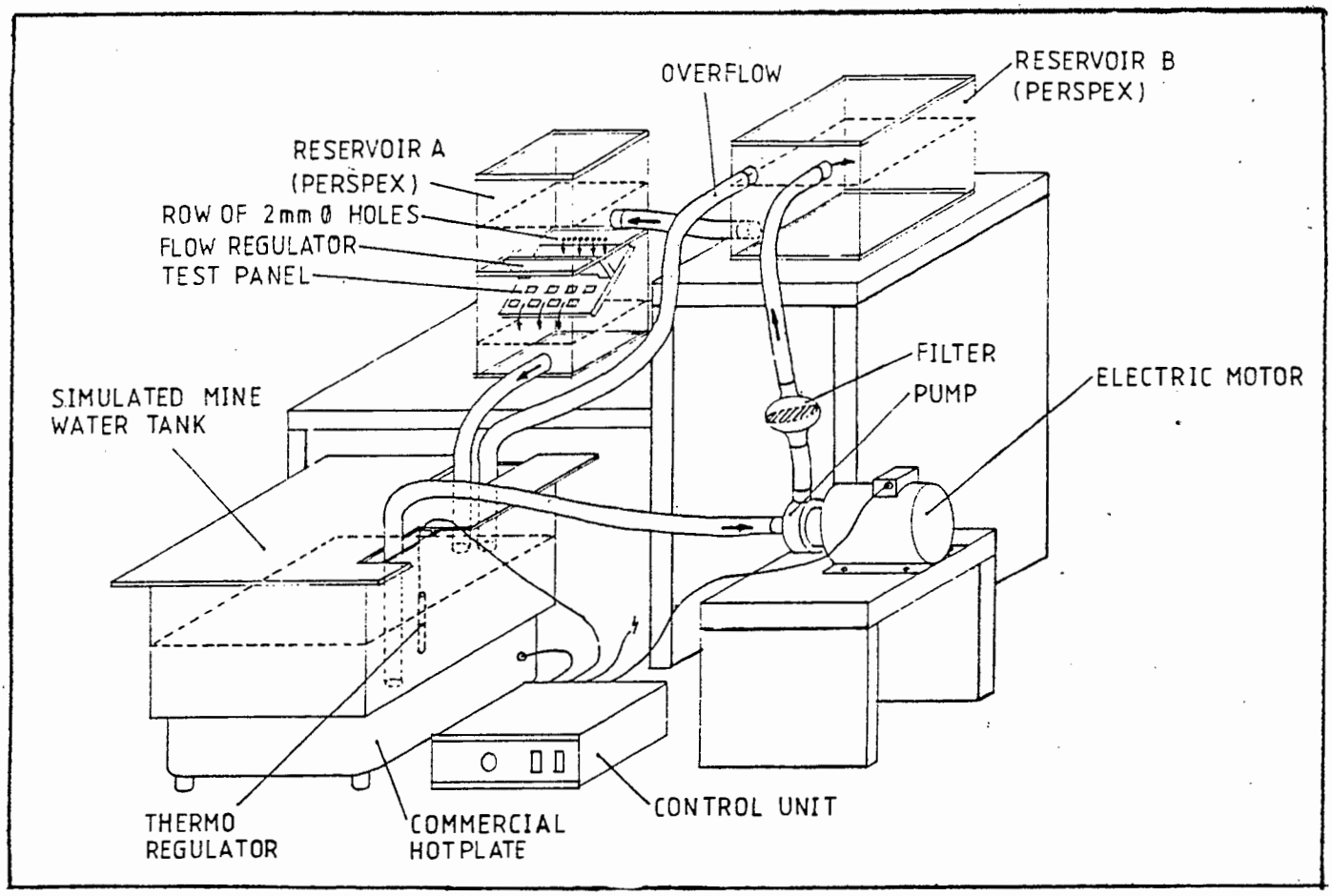


| TEST VARIABLES |
| --- |
| corrosion time<br>corrosion solution<br>temperature<br>flow rate |

FIGURE 3.3 : Schematic diagram of the corrosion rig and test variables.

FIGURE 3.4 : Corrosion rig.

The following features are important:

i) the circulated mine water is maintained at constant temperature using a conventional hotplate and thermo-regulating unit.

ii) the overflow facility of reservoir B (see fig.3.3) ensures a constant flowrate.

iii) test specimens are mounted on the test panel so that only the abraded surface is exposed to the corrosive environment. Unabraded sides of the test specimen are coated with a lacquer to prevent unwanted corrosion.

iv) a sintered glass filter with porosity 41-100 microns maintains a low level of corrosion product in the circulating fluid.

## 3.2 STANDARD TESTS

Based on work done concerning dry abrasion and abrasion-corrosion of metals such as mild steel, stainless steels and other heat treated alloys, standard wear tests using the test rigs described were established in the Materials Engineering Department at the University of Cape Town.

Initial test parameters were selected to simulate the abrasive-corrosive wear conditions at the base of Shaker coveyors in gold mines. These tests were subsequently modified to minimise experiment error.

Noel (1981) developed three standard laboratory tests, using mild steel as reference alloy, which allowed a wide range of materials to be tested and ranked according to their relative dry abrasion resistance and relative abrasive-corrosive wear resistance. Detailed test procedures are contained in Appendix A1.

### (1) Relative abrasion resistance (RAR) test

The RAR test utilises only the dry abrasion test rig. The basic test procedure involves an initial run-in to obtain a uniformly abraded surface, after which specimens are cleaned (ultrasonically) and weighed to an accuracy of 0.1 mg. Subsequent abrasion under conditions listed in Table 3.1 and re-weighing allows the volume loss per meter of abrasion to be determined. Relative abrasion resistance is then defined as:

$$RAR = \frac{\text{volume loss per metre of mild steel}}{\text{volume loss per metre of test material}}$$

TABLE 3.1 : RAR test conditions.

| | |
|---|---|
| Specimen size | 10 x 10 mm X-section |
| Abrasion speed | 0.275 m/s |
| Load | 3.665 kg |
| Abrasive belt | 80 grit Aloxite |
| Abrasion length | 3.66 m |

(2) Standard relative wear resistance tests (RWR#1, RWR#2)

RWR tests utilise both the dry abrasion rig and the corrosion rig. The basic idea is to separate the wear variables involved by a repetitive procedure of abrading a specimen and subsequently corroding it. This allows the dry abrasion and corrosion parameters to be controlled separately, whilst their combined effect is monitored by weight loss measurements between change-overs from abrasion to corrosion.

From an analysis of mine service water over a one year period, Noel (1981) selected a corrosion solution to be used for all standard wear tests. Table 3.2 gives a comparison between the standard corrosion solution selected and mine water. Since corrosion Solution A is an average representation of the corrosivity of mine waters, it was decided to use this solution for all tests.

TABLE 3.2 : Comparison between standard corrosion solution selected and mine water.

| | MINE WATER | CORROSION SOLUTION A |
|---|---|---|
| Langelier Index | -1.3 | -1.0 |
| pH | 6.7 | 6.7 |
| Sulphate (ppm) | 1232 | 715 |
| Chloride (ppm) | 337 | 350 |
| Calcium (ppm) | 150 | 175 |

The two standard wear tests are differentiated by corrosion time and abrasion length only. See test parameters, Table 3.3. Using mild steel as reference alloy, the relative abrasive-corrosive wear resistance is defined as:

$$\text{RWR\#1,2} = \frac{\text{total volume loss of mild steel}}{\text{total volume loss of test material}}$$

TABLE 3.3 : RWR test parameters.

| TEST PARAMETER | RWR#1 | RWR#2 |
|---|---|---|
| Abrasion load | 3.665 kg | 3.665 kg |
| Abrasion speed | 0.275 m/s | 0.275 m/s |
| Abrasion grit size | 80 grit | 80 grit |
| Abrasion length | 4 x 0.25 m | 4 x 1 m |
| Corrosion solution | Soln. A | Soln. A |
| Temperature | 30 °C | 30°C |
| Corrosion time | 4 x 48 hrs. | 4 x 22 hrs. |

## 3.3 FURTHER WEAR TESTS

Before a test programme is initiated, it is necessary to establish all test variables and ranges. The main criteria for the selection of test ranges are:

(i) physical limitations of the test rig
(ii) expected conditions of maximum material performance
(iii) minimum experimental error

Using these criteria, ranges for further dry abrasive wear tests were established. See Table 3.4.

TABLE 3.4 : Test ranges for dry abrasion.

| TEST VARIABLE | RANGE |
|---|---|
| Abrasive belt speed | 0.165 - 0.466 m/s |
| Abrrasion load | 1.334 - 3.665 kg |
| Abrasive grit size | 60 - 220 grit |
| Abrasion length | 0.25 - 3.66 m |

For further abrasive-corrosive wear tests, where parameters are changed a different reference alloy, namely 3CR12 is used. A brief description of this alloy is presented in Chapter 4. Two additional terms are defined:

$$\text{RWR (relative 3CR12)} = \frac{\text{total volume loss of 3CR12}}{\text{total volume loss of test material}}$$

$$\%\ \text{corrosion 3CR12} = \%\ \text{of total volume loss by corrosion for 3CR12}$$

## 3.4 SUPPLEMENTARY TESTS

### Optical Metallography

Polishing and etching of aluminium alloys was done using conventional polishing equipment and Keller's etchant. Micrographs were taken under 250X magnification using a stereo optical microscope with fittted 35 mm Nikon camera.

### Scanning Electron Microscopy

Specimens were examined in a Cambridge S200 scanning electron microscope (SEM) after wear tests. An attached Tracor EDAX system was used for semi-quantitative element analysis after corrosion wear tests.

### Mechanical and Physical Properties

Vickers hardness values were obtained using a ESEWAY hardness tester set at 30 kg load. Values are abbreviated as HV30.

Values of material density ($g/cm^3$) were determined using the liquid immersion method. A 5-digit Mettler scale and ethanol was employed for this purpose.

Microhardness measurements using the Shimaden microhardness tester and a 200 g load were carried out. Values are abbreviated as MHV200.

Charpy-V-notch impact tests were undertaken to obtain a measure of material toughness at high strain rates according to BS131:1972 (striking velocity = 5 m/s, room temperature).

Tapered Sections

Hardness values as a function of depth through abraded surfaces were obtained by polishing specimens using a 10 degree taper jig. The Shimaden tester was used to make microhardness indents.

Heat Treatments

Most alloy samples were machined and tested in the as-received condition. Some annealing, solution treating and artificial ageing treatments were performed using a conventional Naber air furnace. Temper conditions are detailed in Chapter 5.

## 3.5 REPRODUCIBILITY OF STANDARD TESTS

Primary sources of error for the standard tests conducted are identified :

(i) inconsistency of grit size and bonding strength of abrasive belts may vary from batch to batch and influence the wear losses measured

(ii) the following factors may influence corrosion kinetics and thus volume losses obtained for corrosion tests:
   (a) ± 5°C water temperature variation
   (b) exact amount of ions dissolved in solution may vary due to weighing and mixing inaccuracies

Reproducibility of the RAR test was analysed using mild steel. Table 5.7 gives results for 6 tests and the error data calculated.

TABLE 3.5 : Reproducibility of RAR test.

| | VOLUME LOSS/m FOR MS |
|---|---|
| Test 1 | 1.48 |
| Test 2 | 1.29 |
| Test 3 | 1.36 |
| Test 4 | 1.49 |
| Test 5 | 1.40 |
| Average | 1.40 |

Standard deviation = ±0.084 % error = ±6%

Using a set of nine mild steel specimens, Noel (1981) showed that the reproducibility of the RWR#1 test was within 3.7%. Subsequent tests by Barker (1988) for two materials at opposite ends of the performance range, namely mild steel and UA200 (development alloy containing 8.7% chromium) showed error margins of 5.2% and 12.7% respectively. From the standard test wear data obtained for aluminium alloys, it can be conservatively estimated that a 5-15% error range is applicable to results obtained for this investigation.

# CHAPTER 4

## TEST MATERIALS

A range of 14 aluminium alloys, 10 wrought and 4 cast alloys, were supplied by Hulett Aluminium (Pty) Ltd. for this investigation. This section briefly introduces relevant alloy designations, temper conditions and microstructures.

### 4.1 ALLOY DESIGNATIONS

Wrought aluminium alloys are classified by a 4-digit system, the first digit indicating the alloy group in terms of major alloying elements. Remaining digits identify alloys within each group. See Table 4.1. Cast alloys do not fall under the same alloy designation system but are included for completeness.

TABLE 4.1 : Alloy designations.

| ALLOY DESIGNATION | MAJOR ALLOYING ELEMENTS |
|---|---|
| 1xxx | Al of 99% minimum purity |
| 2xxx | Cu |
| 3xxx | Mn |
| 5xxx | Mg |
| 6xxx | Mg + Si |
| 7xxx | Zn + Mg or Zn + Mg + Cu |
| KS (Karl Schmidt)<br>LM6 (UK BS1490) | Al-Si cast alloys |

### 4.2 TEMPER CONDITIONS

Wrought alloys, those in which the metal is mechanically worked by processes such as rolling, drawing, extruding or forging, are divided into heat-treatable and non heat-treatable alloys. Two temper conditions are relevant to this investigation:

i) T6 temper : solution heat-treated and artifically aged

All heat-treatable alloys, those in which mechanical properties are changed by heat treatments and cold working, were received in the T6 temper condition. This heat treatment consists of heating the alloy to a predetermined temperature just below its melting point, and holding at this temperature until some of the alloy constituents are dissolved and taken into solid solution. To ensure that elements are retained in solution, the material is quenched rapidly to produce a supersaturated solid solution.

As this condition is usually unstable, these alloys are then artificially age-hardened to develop maximum mechanical properties as quickly as possible. The temperature range for optimum control of the precipitation reaction is approximately 120 - 180 degrees and depends on variables such a alloy type, properties desired and production schedule. See fig. 4.1. Careful control of the age hardening process is essential since overageing may result in hardening constituents becoming too coarse, affecting strength properties adversely.

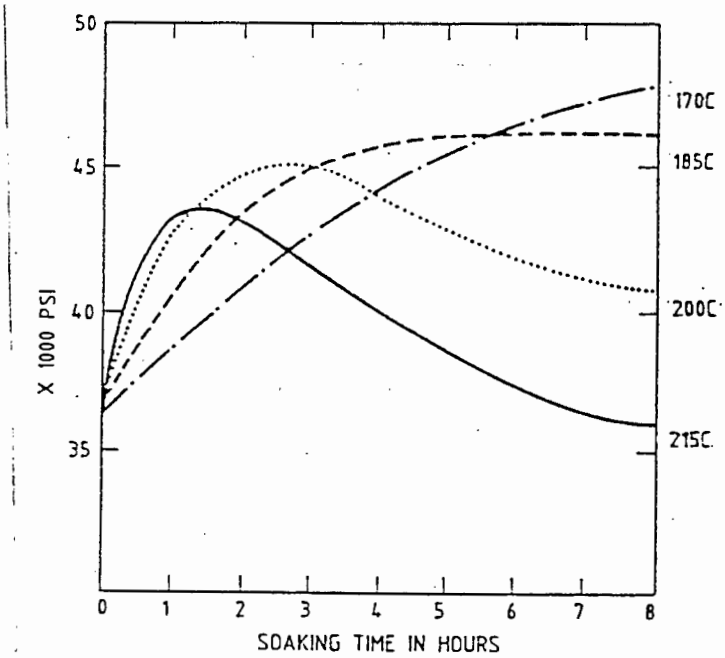


FIGURE 4.1 : Schematic ageing curves for 6082 showing the effect of soaking temperatures on the development of optimum strength properties. (Hulett Aluminium (Pty) Ltd.).

ii) H2 temper : quarter-hard cold worked condition

All non heat-treatable alloys, those in which mechanical properties are enhanced by cold working only, were received in the H2 temper condition. An approximately 10% reduction in cross-sectional area is achieved by initial cold work operations. After final annealing alloys in this condition receive the temper designation 'O'. See fig. 4.2.

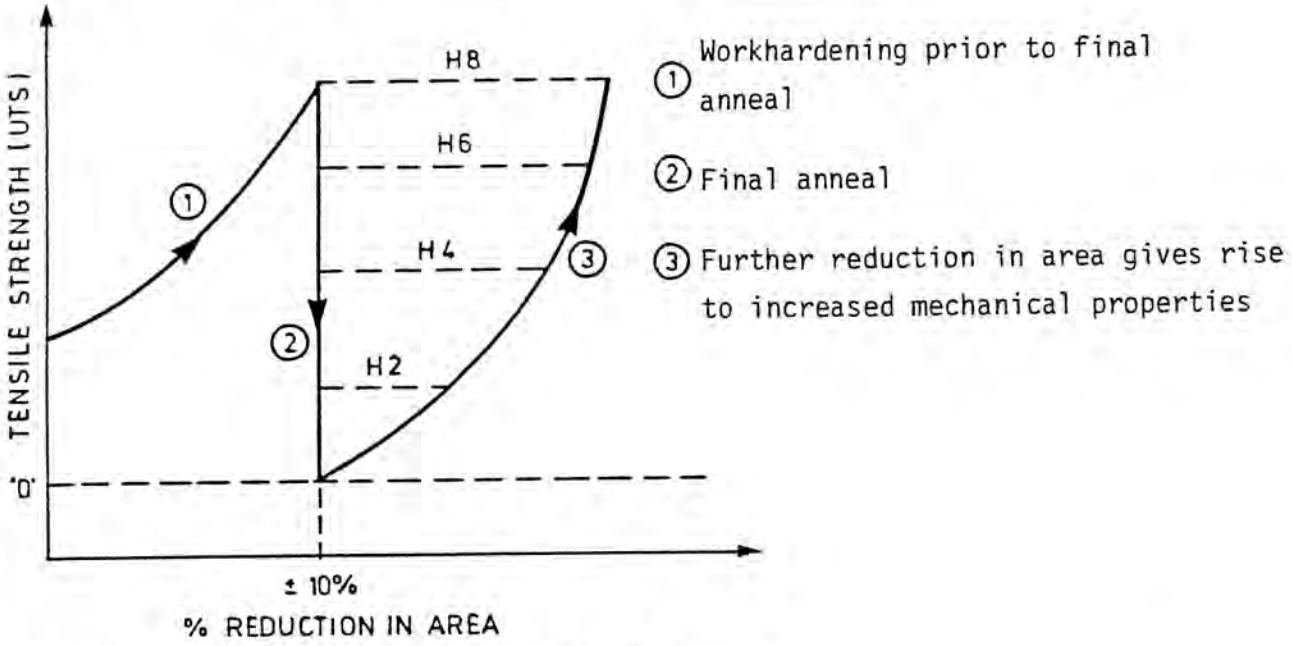


FIGURE 4.2 : Work hardening curve of 'H' tempers. (Hulett Aluminium (Pty) Ltd.).

Subsequent maximum amount of coldwork performed that is commercially practical for the particular alloy leads to the temper condition H8. Between the annealed and H8 state intermediate levels of hardness are obtainable, the temper designation H2 referring to the quarter hard condition.

## 4.3 PRESENTATION OF MATERIALS

The materials are presented under four headings, namely reference alloys, Al-Si cast alloys, heat-treatable wrought alloys and non heat-treatable wrought alloys. A diagram of the test alloys is shown in fig. 4.3.

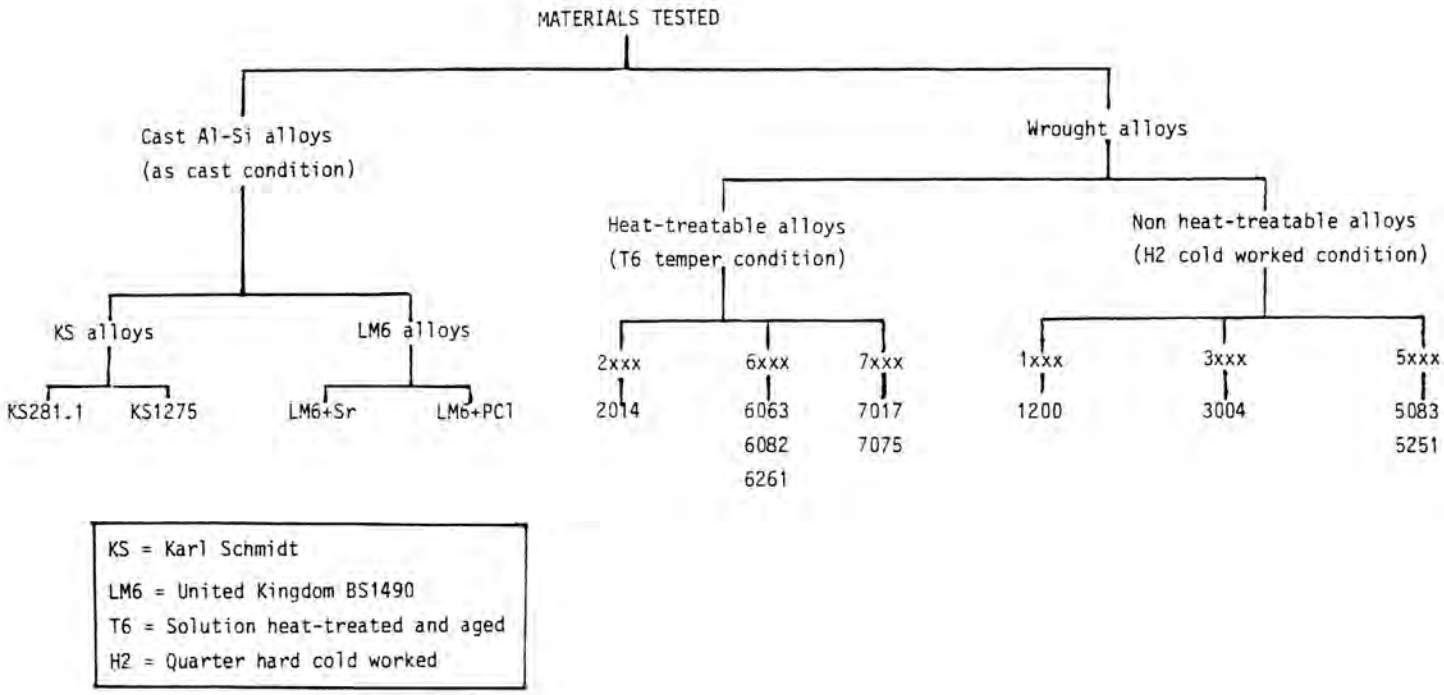


FIGURE 4.2 : Flow-diagram of materials tested

FIGURE 4.3 : Diagram of materials tests.

Most wrought alloy samples were received in either the hot or cold rolled condition. Test specimens of 10x10mm cross section and ± 20mm length were machined from plate samples in the long transverse (LT) direction. See fig. 4.4. AFSA data on alloying elements is presented in Appendix A2. Mechanical properties, temper conditions and fabrication routes are given in Appendix A3.

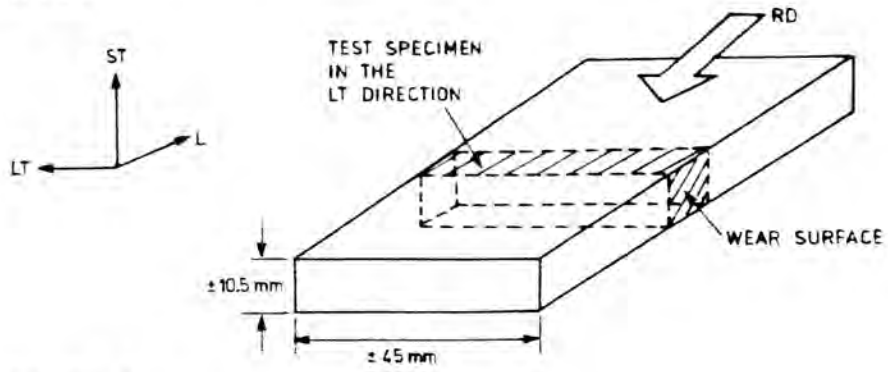


L = Longitudinal
LT = Long transverse
ST = Short transverse

FIGURE 4.4 : Test specimen orientation.

Reference alloys

Two reference alloys, mild steel (070M20, normalised) and 3CR12 (hot rolled), were employed. 3CR12 is an 11% chromium containing steel with a dual phase, ferritic-martensitic microstructure. Allen, Protheroe and Ball (1981) established its potential as an abrasive-corrosive wear resistant steel in certain applications. Table 4.2 gives the approximate chemical compostion of the 3CR12 type alloy and mild steel. Material properties and standard wear test results are contained in Appendix A4.

TABLE 4.2 : Approximate chemical composition of 3CR12 and mild steel (070M20).

| MATERIAL | CHEMICAL COMPOSITION (%wt) | | | | | | | | | |
|---|---|---|---|---|---|---|---|---|---|---|
| | C | Cr | Mn | Ni | Mo | V | Ti | Si | S | P |
| 3CR12 | .022 | 11.3 | 1.14 | .62 | - | - | .20 | .37 | .015 | .016 |
| MS(070M20) | .15 | .02 | .5 | .03 | .01 | .01 | .01 | .35 | .06 | .06 |

Al-Si cast alloys

These alloys are the most important of the cast aluminium alloys because of high fluidity of the melt that gives excellent casting characteristics. The microstructure consists essentially of large plates or needles of silicon in a continuous aluminium matrix. Refinement of the microstructure may be achieved by rapid cooling processes or the addition of certain alkali fluorides to the melt prior to pouring. Microstructures are shown in figs. 4.4 and 4.5.

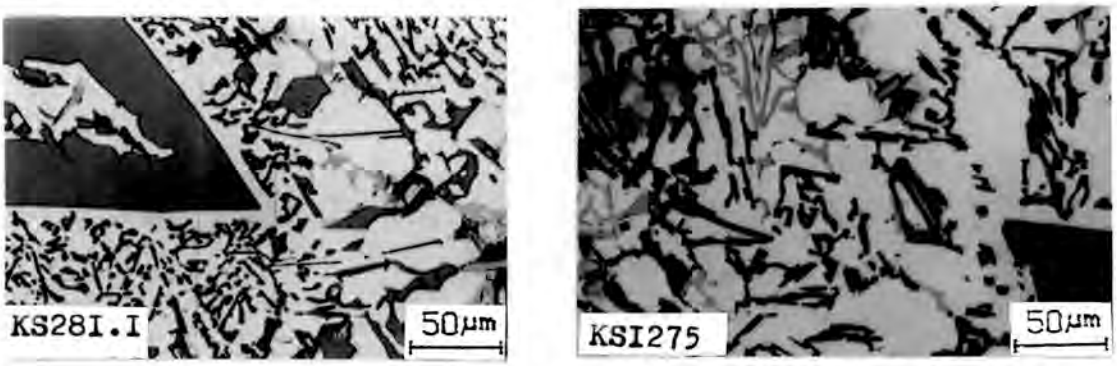


FIGURE 4.4: Microstructures of KS281.1 and KS1275 consisting of silicon (small, angular grey particles in eutectic, and large primary particles) and $Mg_2Si$ (black constituent). Primary silicon phases are larger for the 16% silicon containing alloy KS281.1.

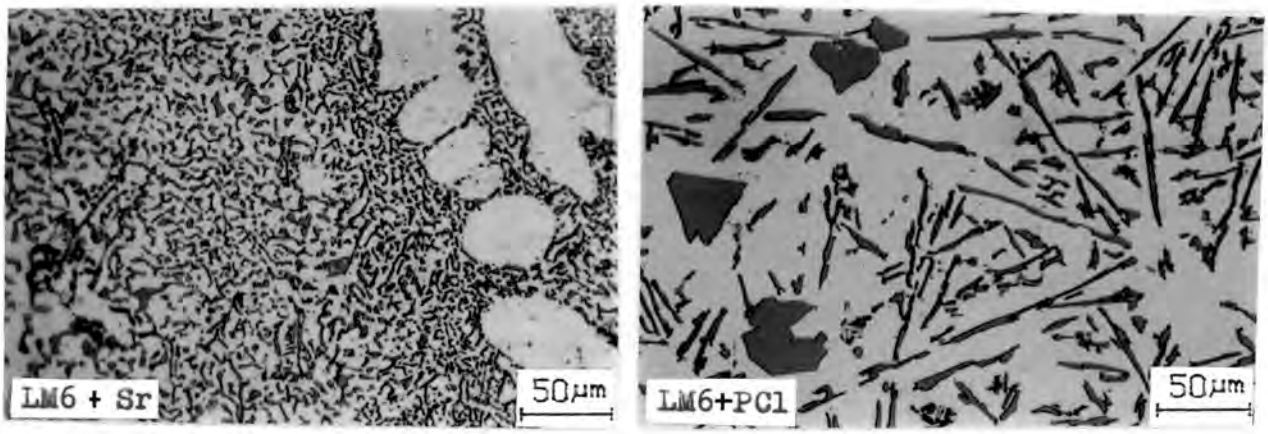


FIGURE 4.5 : Microstructures of LM6+Sr and LM6+PCl comprising a network of silicon particles (grey, sharp) formed in the interdentritic Al-Si eutectic. Addition of strontium or phosphorus to the melt serves to refine the particles of silicon in the eutectic, making them smaller and less angular.

Heat-treatable wrought alloys

Wrought alloys that respond to strengthening by heat treatment are the 2,6 and 7-series alloys. The 6-series alloys and 7017 (Zn-Mg-Al) have medium strength and are readily weldable. The 2-series alloys and 7075 (Zn-Mg-Cu-Al) have high strength and are used primarily for aircraft construction but have limited weldability. These alloys contain soluble phases, which show in various amounts and at various locations in the microstructure, depending on thermal history. Micrographs of the alloys 2014, 6082, 7017 and 7075 are shown below.

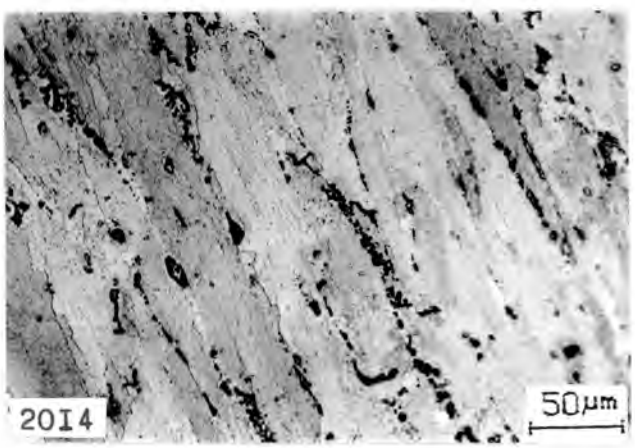


FIGURE 4.6 : Microstructure of 2014 (Al-Cu) consisting of soluble phases of Al with Cu or Mg and insoluble phases of Al-Mg-Si-Mg. Fine precipitates of Al-Cu are contained in the matrix.

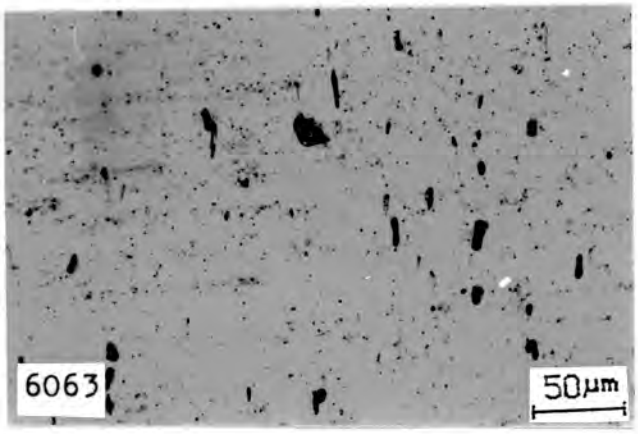


FIGURE 4.7 : Microstructure of 6063(Al-Mg-Si) showing particles of Al-Si-Fe and Mg-Si, the most common intermetallic phase for this alloy.

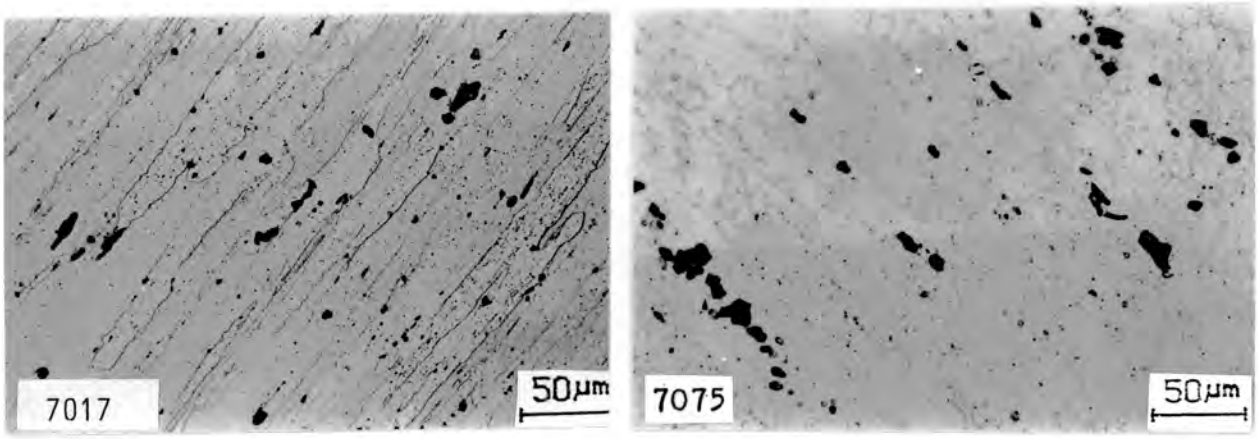


FIGURE 4.8 : Microstructures of 7017 (Al-Zn-Mg) and 7075 (Al-Zn-Mg-Cu). Mg-Zn particles are the principle soluble phase, with a fine dispersion of precipitates, Cr containing phases and Mg-Si particles.

Non-heat-treatable alloys

Wrought alloys that do not respond to strengthening by heat treatment comprise the 1,3 and 5-series alloys. Strength is developed by strain hardening (cold work) in association with dispersion hardening (Al-Mn), or solid solution hardening (Al-Mg), or both (Al-Mn-Mg). Micrographs of the alloys 1200, 3004 and 5083 are shown overleaf.

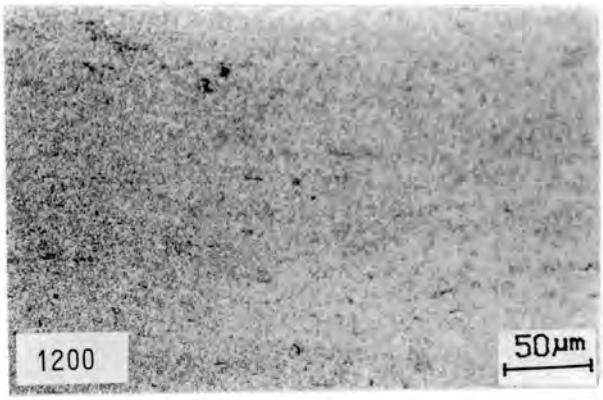


FIGURE 4.9 : Microstructure of 1200 (99% minimum Al). Fine dispersion of particles consist of impurity phases that contain Fe and Si.

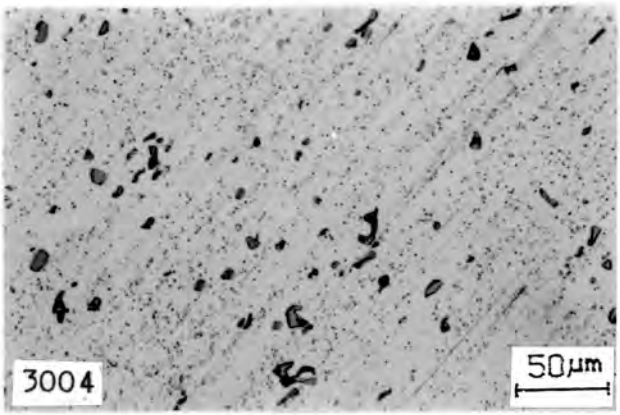


FIGURE 4.10 : Microstructure of 3004 (Al-Mn). Primary and eutectic particles consist of intermetallic phases of Mn with Al, Si and Fe.

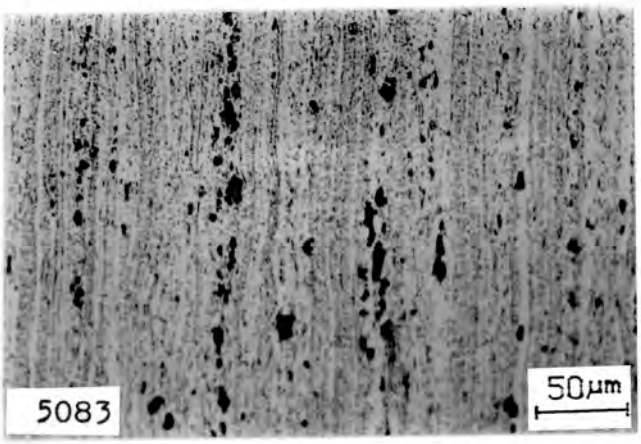


FIGURE 4.11 : Microstructure of 5083 (Al-Mg) consisting of eutectic particles of Al with Mg and Si and intermetallic phases containing Cr and Mg.

# CHAPTER 5

## RESULTS

In this section the results of standard wear tests described in Section 3.2 are presented. Tests to determine the effect of external factors, material properties and heat treatments on wear rates are included. Results of additional corrosion and abrasion-corrosion tests to establish further wear trends are also presented. It is important to remember that the wear data generated is specific to the test apparatus described in Section 3.1. The reader should thus be familiar with the test methods and conditions of testing employed before analysing the results obtained.

## 5.1 THE INFLUENCE OF EXTERNAL FACTORS ON DRY ABRASIVE WEAR RATES

### Load

Figure 5.1 illustrates the effect of load on wear rates. Tests were run at standard grit size and speed settings (80 grit, 0.275 m/s). Within the load range tested (1000-4000g), direct proportionality between load and wear rate is observed for the alloys LM6+Sr, KS281.1, 3004, 6082, 6063 and 7075. Extrapolation to zero gives a small zero off-set. Equation (2) shows the relationship; values of $S_1$ are listed in Table 5.1. The alloys KS1275 and LM6+PCl show a more rapid increase in wear rate for loads greater than 3000g.

$$R = S_1 p \quad \text{.....eqn. (2)}$$

where : $R$ = wear rate ($mm^3/m$)

$p$ = average pressure on sample surface ($g/mm^2$)

$S_1$ = slope of the curve

TABLE 5.1 : Values of $S_1$, $R_1$ and $S_2$.

| ALLOY | $S_1$ $(\frac{mm^3/m}{g/mm^3})$ | $R_1$ $(mm^3/m)$ | $S_2$ $(\frac{mm^3/m}{m})$ |
|---|---|---|---|
| MS | 0.027 | 0.98 | 1.36 |
| 7075 | 0.071 | 2.31 | 4.09 |
| 6082,63 | 0.088 | 2.84 | 4.77 |
| 3004 | 0.100 | 3.33 | 6.56 |
| LM6 + Sr | 0.132 | 5.20 | 10.23 |
| KS2811 | 0.144 | 5.60 | 11.45 |
| LM6 + Sr | 0.165 | 6.40 | 11.45 |
| KS1275 | 0.178 | 5.56 | 11.86 |

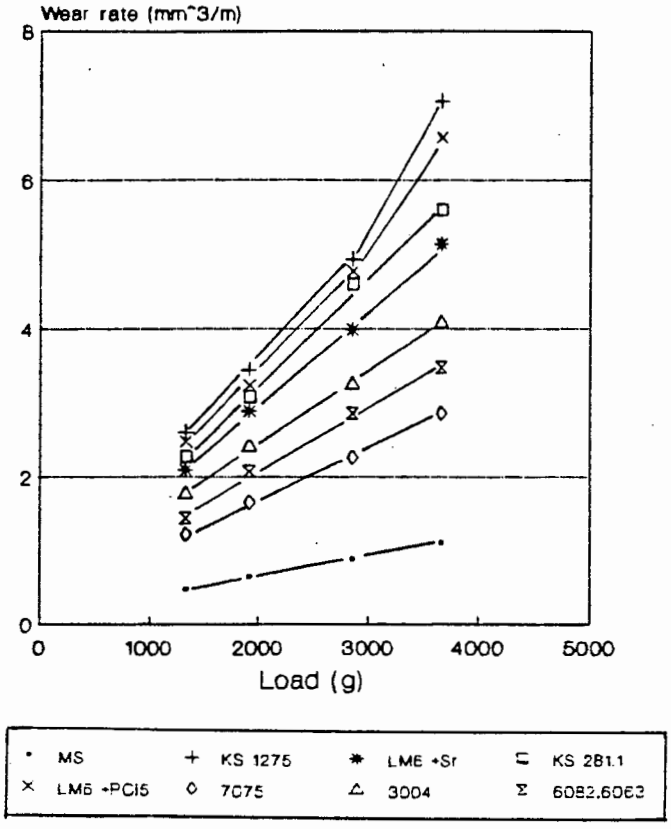


FIGURE 5.1 : Plot of wear rate versus load for the alloys 7075, 6082, 6083, 3004, LM6+Sr, KS281.1, LM6+PCl and KS1275. Grit size 320 $\mu$m, abrasion speed 0.275 m/s.

Speed

The influence of sliding speed on wear rate is illustrated by fig. 5.2. Standard 80 grit belts and a load of 2850 g were used. For the speed range 0.1 - 0.5 m/s, wear rate is seen to be approximately independent of abrasive belt speed.

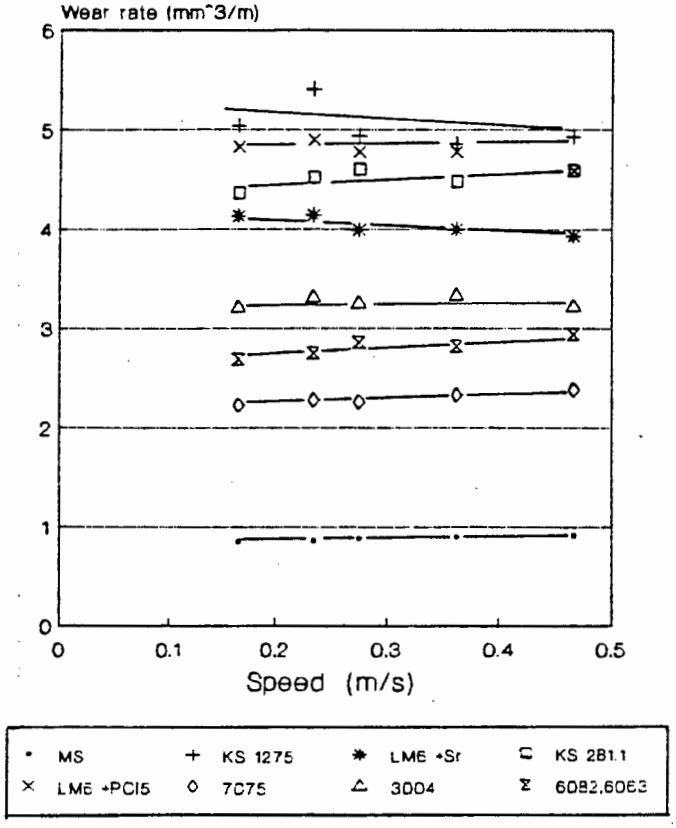


FIGURE 5.2 : Plot of wear rate versus speed for the alloys 7075, 6082, 6083, 3004, LM6+Sr, KS281.1, LM6+PCl and KS1275. Grit size 320$\mu$m, abrasion load 2850g.

Grit Size

Figure 5.3(a) and (b) illustrates the effect of abrasive grit size on wear rates of cast and wrought alloys. Abrasive belts are designated by a grit number which is inversely proportional to the average size of abrasive particles. The range of abrasive belts used and their respective particle sizes are tabulated overleaf.

TABLE 5.2 : Abrasive belt grit sizes.

| Abrasive belt designation | Grit size ($\mu$m) |
|---|---|
| 40 grit | 640 |
| 60 grit | 420 |
| 80 grit | 320 |
| 100 grit | 250 |
| 120 grit | 210 |
| 150 grit | 170 |
| 180 grit | 140 |
| 220 grit | 120 |

For the grit size range 120 - 640 $\mu$m, the following trend is observed: wear rate increases rapidly with grit size until a critical grit diameter of approximately 200 $\mu$m is reached. In the case of cast alloys wear rate increases with grit size above this value, but at a slower rate. Figure 5.3(c) shows a SEM photograph of an abraded wear surface of the alloy KS281.1.

For values above 200 $\mu$m, equation (3) is applicable; values of $R_1$ and $S_2$ are given in Table 5.1. Wrought alloys show a non-linear increase in wear rate above the critical grit diameter.

$$R = R_1 + S_2(D-D_1) \quad \text{.....eqn. (3)}$$

where : $R$ = wear rate ($mm^3/m$)

$R_1$ = value of R at the transition point ($mm^3/m$)

$S_2$ = slope of the curve

$D$ = average grit diameter ($\mu$m)

$D_1$ = critical grit diameter ($\mu$m)

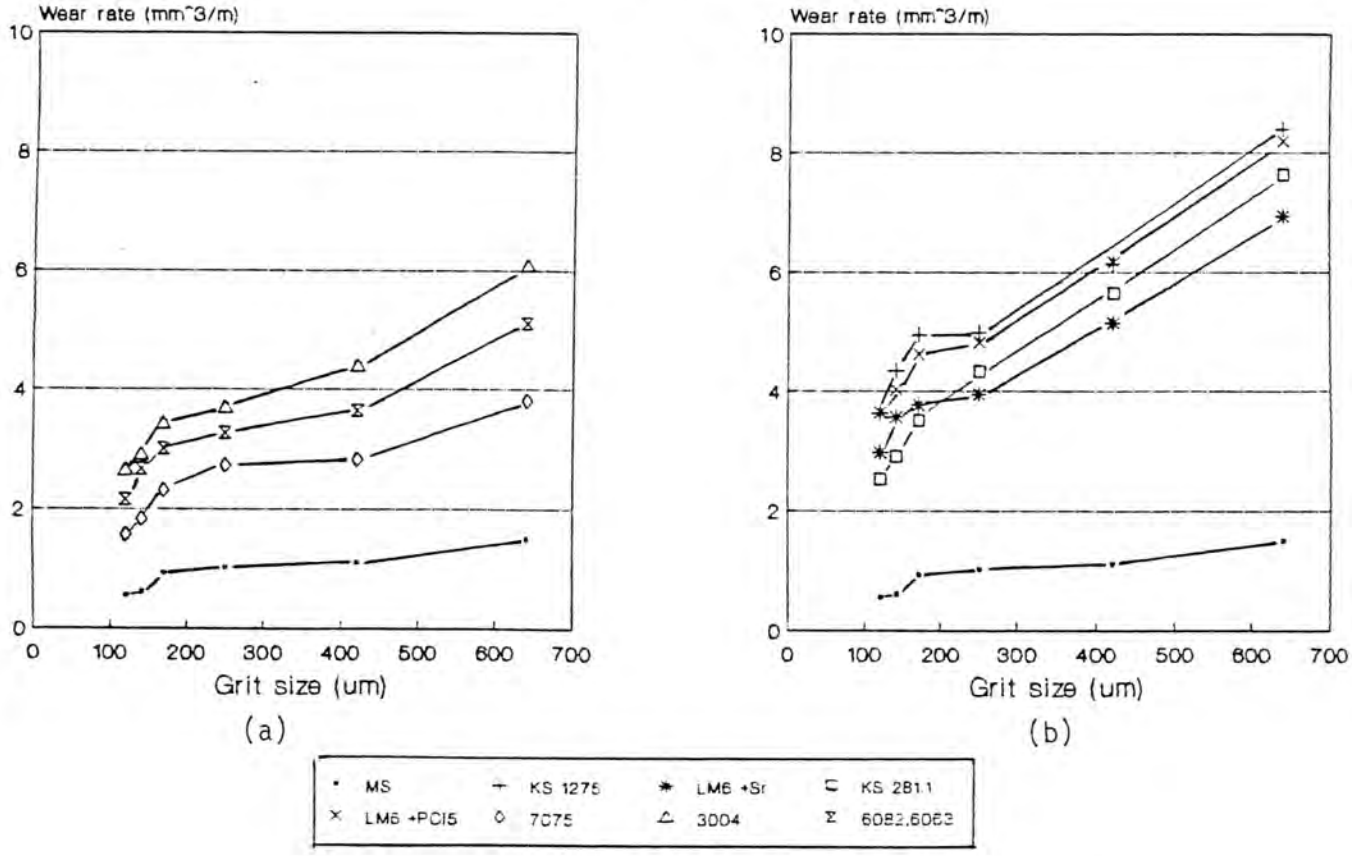


FIGURE 5.3 : (a) Plot of wear rate versus grit size for the wrought alloys 7075, 6063, 6082 and 3004.
(b) Plot of wear rate versus grit size for the Al-Si cast alloys LM6+Sr, KS281.1, LM6+PCl and KS1275. Abrasion speed 0.275 m/s, load 1800 g.

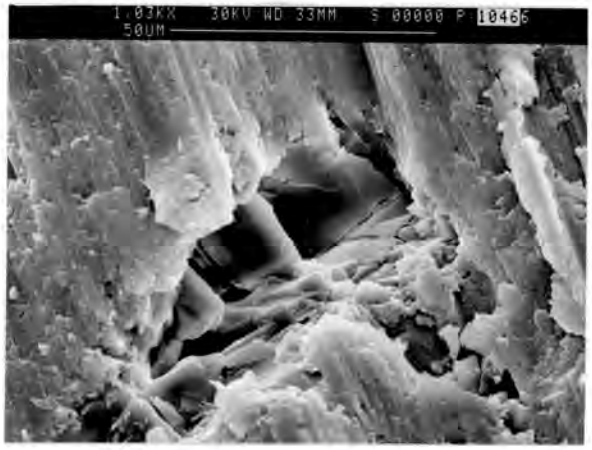


(c)

FIGURE 5.3 : (c) Wear surface of KS281.1 showing brittle microfracture of hard primary silicon phases. Grit size 320$\mu$m, load 2850g.

## 5.2 THE INFLUENCE OF MATERIAL PROPERTIES ON ABRASION RESISTANCE

### Hardness

Vickers hardness values are listed in Appendix A4. Figure 5.4 gives a plot of abrasion resistance versus bulk hardness for both wrought and cast alloys. Microhardness tests were done on polished specimens of two cast alloys, KS281.1 and LM6+Sr, to establish the hardness of phases present in the microstructures. Table 5.3 lists the microhardness values obtained. The etched microstructures of these alloys are shown in figs. 4.4 and 4.5.

TABLE 5.3 : Microhardness values for LM6+Sr and KS281.1.

| | | MICROHARDNESS VALUES (MHV200) | | |
|---|---|---|---|---|
| ALLOY | MACRO-HARDNESS (HV30) | Al-Si SOLID SOLUTION | SOLID SOLUTION + DENDRITES | PRIMARY Si-NEEDLES |
| KS281.1 (16%Si) | 140 | + 95 | 110 | + 950 |
| LM6+Sr (12%Si) | 69 | + 65 | + 78 | - |

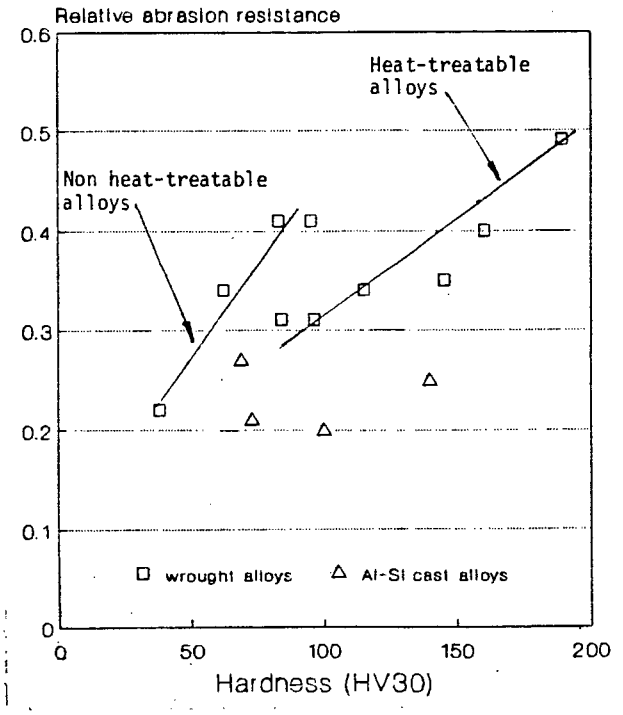


FIGURE 5.4 : Plot of relative abrasion resistance (RAR) versus hardness for Al-Si cast alloys, heat-treatable wrought alloys and non heat-treatable wrought alloys.

Microstructure

Samples of all alloys were polished, etched and examined under the optical microscope to identify trends regarding the influence of microstructure on abrasion resistance. It was found that aluminium alloys with a very coarse or very fine distribution of second phase particles have low abrasion resistance. Good examples are the cast and 1-series alloys respectively. See figs. 4.4, 4.5 and 4.9. Better abrasion resistance is provided by aluminium alloys with an intermediate size and distribution of second phase particles. The heat-treatable wrought alloys are good examples. See figs. 4.6, 4.7 and 4.8.

Tensile Strength

A plot of tensile strength versus RAR (fig. 5.5(a)) yields no definite relationship but the following trend is noticeable: the low strength 1-series and cast alloys show poor abrasion resistance, whilst the higher strength heat-treatable alloys have the best abrasion resistance. Direct proportionality between UTS and hardness is observed. See fig. 5.5(b). Equation (4) gives the relationship.

$$UTS = 3.3 \times HV30 \quad \text{.....eqn. (4)}$$

where : UTS = Ultimate Tensile Strength (MPa)
HV30 = 30 kg Vickers Hardness
3.3 = Slope of the curve (MPa/HV30)

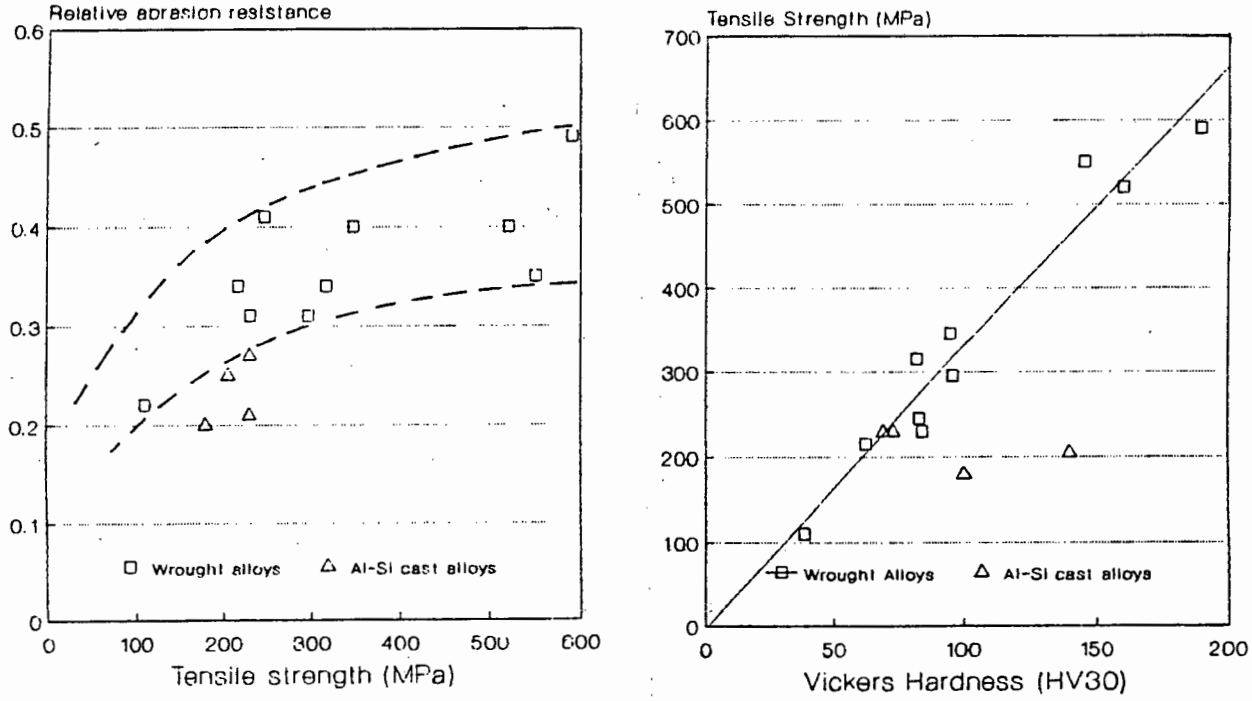


(a) (b)

FIGURE 5.5 : (a) Plot of relative abrasion resistance (RAR) versus tensile strength for wrought and Al-Si cast alloys.
(b) Plot of tensile strength versus hardness for wrought and Al-Si cast alloys.

Workhardening capacity

The extent of workhardening by abrasive wear of six wrought aluminium alloys was investigated. Specimens were abraded using 40 grit abrasive paper and a 3.66 kg load. 10 degree taper-sections were polished and micro-hardness profiles established. Plots of micro-hardness versus depth below the abraded surface for heat-treatable and non heat-treatable alloys are shown in fig. 5.6. The ratio of maximum hardness to bulk hardness gives a measure of workhardening capacity. Values obtained are listed in Appendix A4. Figure 5.7 gives a plot of RAR versus work hardening capacity.

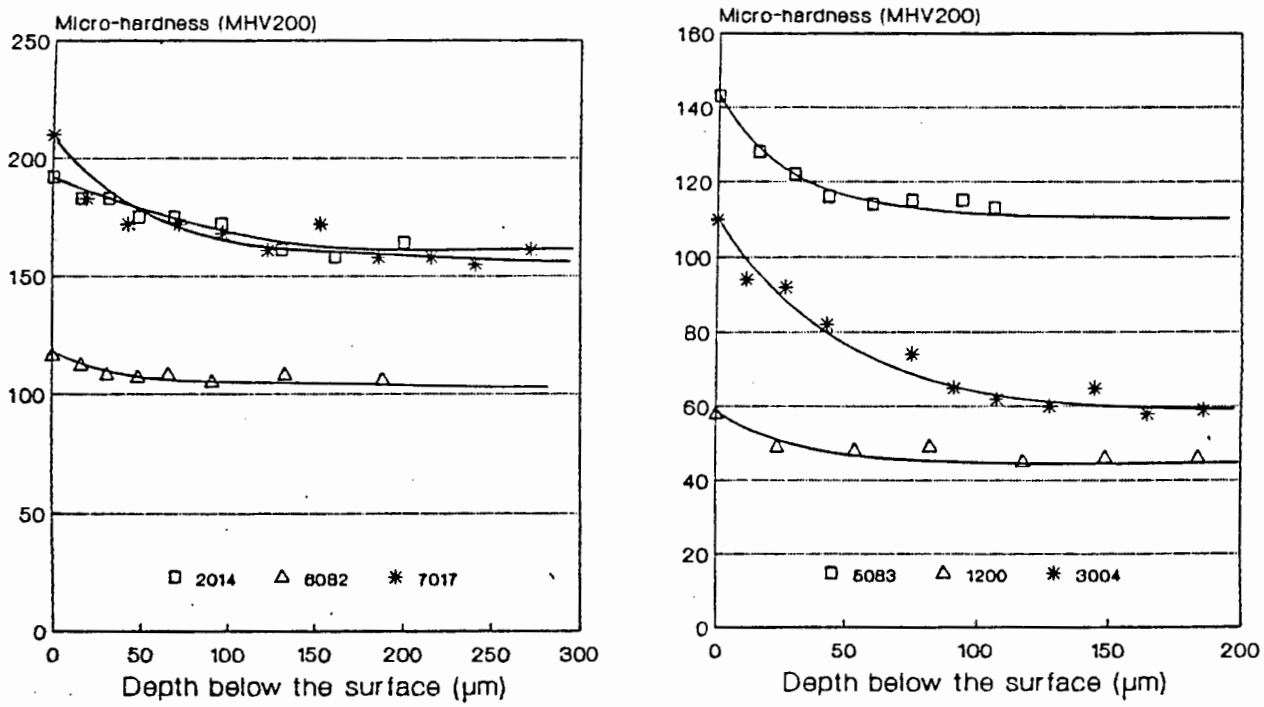


FIGURE 5.6 : (a) Plot of micro-hardness versus depth below the surface for the heat-treatable alloys 2014, 6082 and 7017.
(b) Plot of microhardness versus depth below the surface for the non heat-treatable alloys 1200, 3004 and 5083. Grit size 640 m, load 3.66 kg.

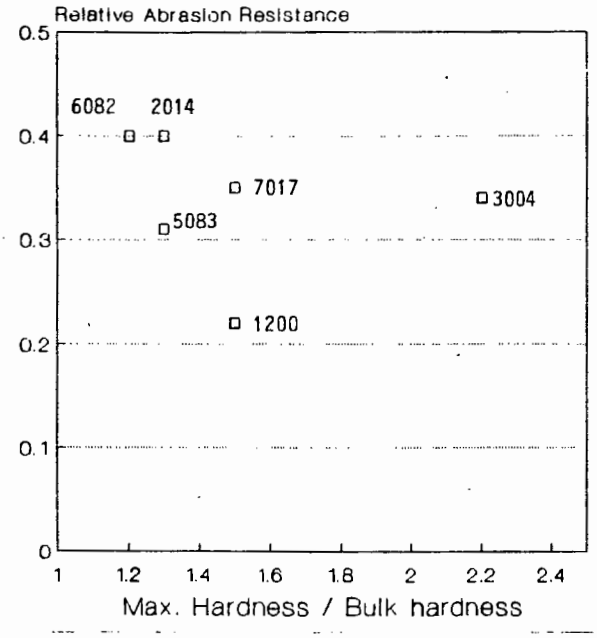


FIGURE 5.7 : Plot of relative abrasion resistance (RAR) versus the ratio of maximum to bulk hardness for the alloys 1200, 3004, 5083, 2014, 6082 and 7017.

Toughness

Notched bar Charpy impact tests were done to obtain an approximate measure of notch toughness for wrought and cast alloys. Specimens tested were those for which the correct dimensions were available. (55 mm length, 10 X 10 mm X-section). Figure 5.8 shows plots of Charpy Impact energy (J) versus RAR and hardness (HV30). SEM photographs of some Charpy fracture surfaces are shown in fig. 5.9.

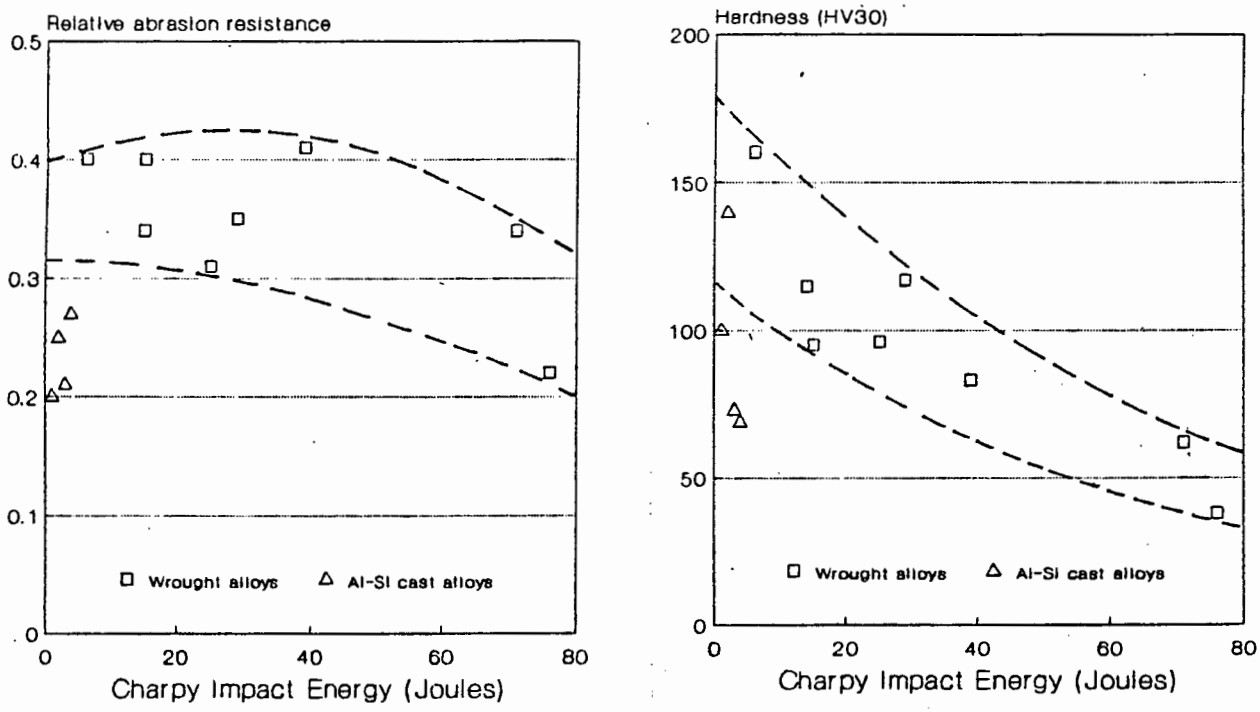


FIGURE 5.8 : (a) Plot of relative abrasion resistance (RAR) versus Charpy Impact toughness for wrought alloys and Al-Si cast alloys. (b) Plot of Charpy Impact toughness versus hardness for the same alloys.

## 5.3 THE EFFECT OF AGEING TIME ON RAR

Three heat-treatable wrought alloys, 6082, 6261 and 7017 were selected to investigate the effect of ageing time after solution treatments on abrasion resistance. AFSA data on temper conditions was used. Table 5.4 lists the details. Figures 5.10, 5.11 and 5.12 show plots of RAR and hardness versus ageing time for the alloys tested.

FIGURE 5.9 : Charpy Impact fracture surfaces for KS281.1, 2014, 5053 and 7017. Energy to fracture of mild steel = 37 Joules

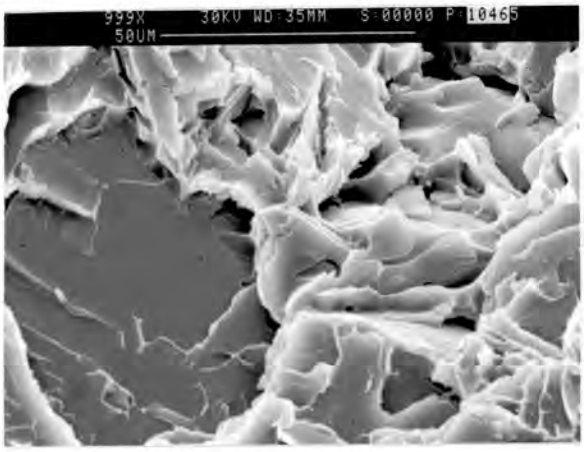


(a) KS281.1 : Energy to fracture = 2 Joules
Brittle micro-fracture of a Si-needle visible on the left and smaller, angular and sharp Si-phases on the right.

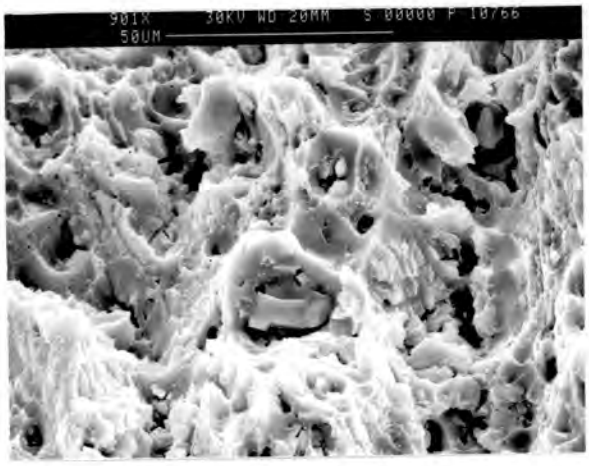


(b) 2014 : Energy to fracture = 6 Joules
Brittle-ductile fracture : Angular and jagged appearance indicates brittle fracture but voids characteristic of ductile fracture also visible.

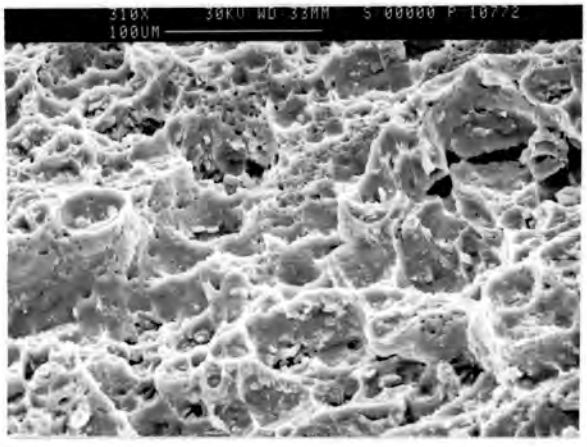


(c) 5083 : Energy to fracture = 25 Joules
Ductile fracture with cup-shaped voids. Average void size (±50 μm) corresponds to grain size.

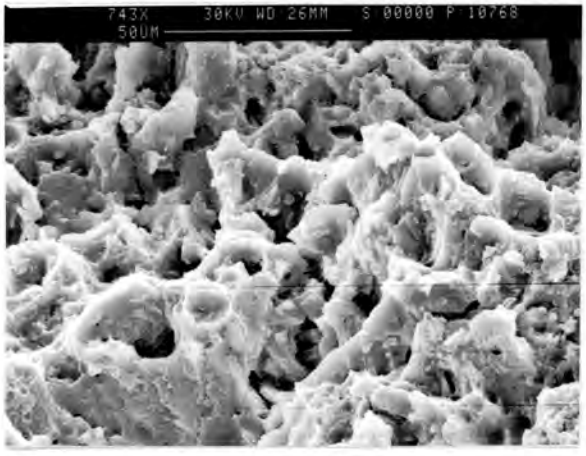


(d) 7017 : Energy to fracture = 29 Joules
Ductile fracture : Void size (10-20 μm) corresponds to grain size.

FIGURE 5.10 : RAR versus ageing time (hrs) for 6082
Solution heat-t. temp.= 520°C
Ageing temp.= 200°C

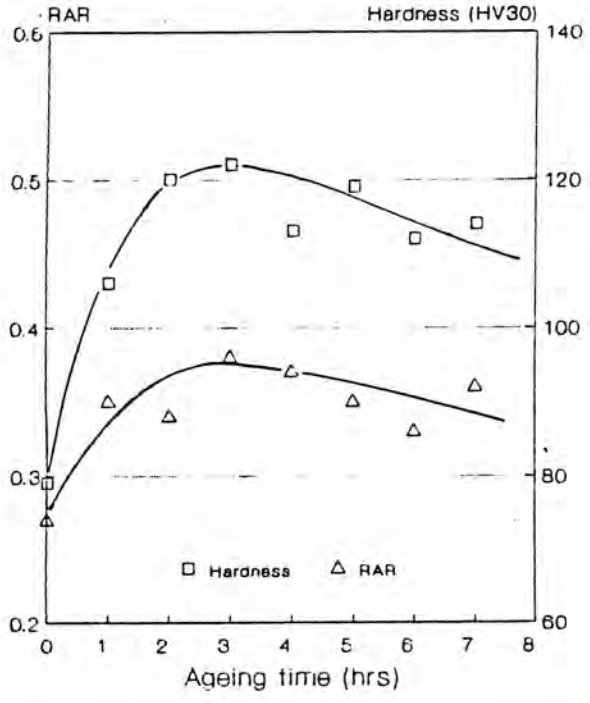


FIGURE 5.11 : RAR versus ageing time for 6261
Solution heat-t. temp.= 520°C
Ageing temp.= 170°C

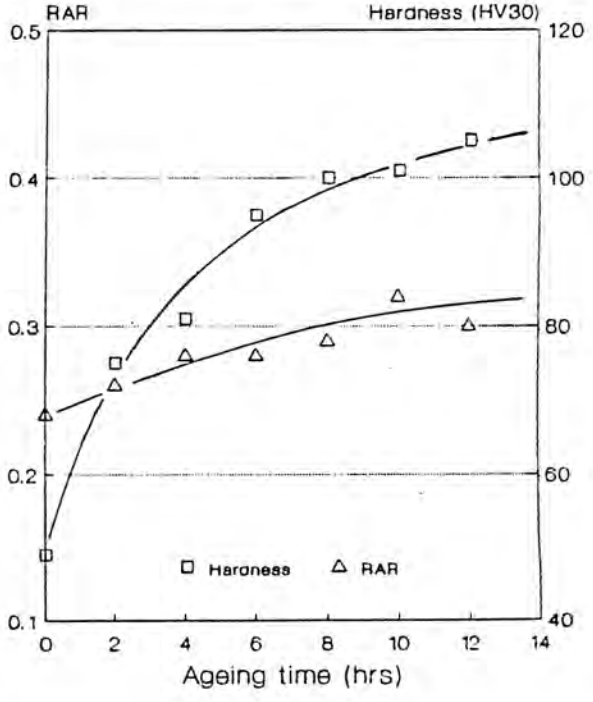


FIGURE 5.12 : RAR versus ageing time (hrs) for 7017
Solution heat-t. temp.= 450°C
Ageing temp.= 150°C

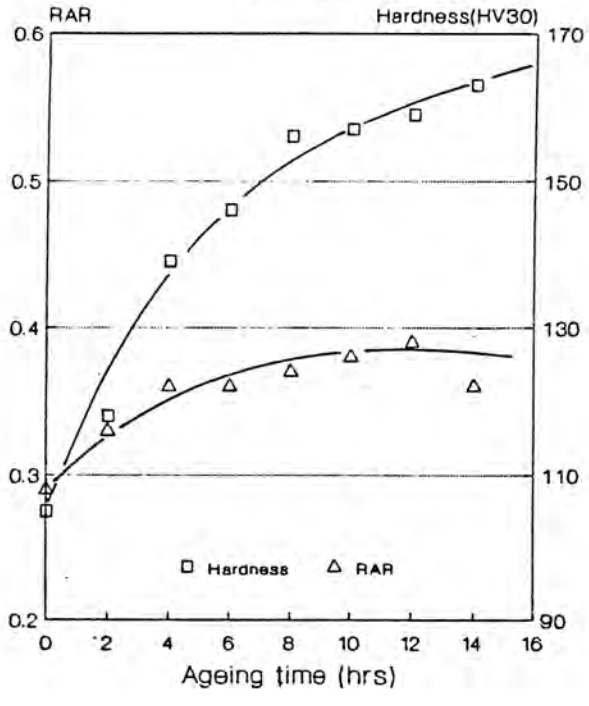

TABLE 5.4 : Temper conditions

| ALLOY | SOLUTION HEAT-TREATMENT TEMP.(°C) (water quench) | AGEING TEMP. (°C) | AGEING TEMP. (nrs) |
|---|---|---|---|
| 6082 | 520 | 200 | 0-7 |
| 6261 | 520 | 170 | 0-12 |
| 7017 | 450 | 150 | 0-14 |

## 5.4 CORROSION TESTS

Tests were conducted to establish the type of corrosive attack i.e. general, localised or pitting, that occurs for tne various aluminium alloys under RWR test conditions:

(i) Seven alloys, namely 1200, 2014, 3004, 5083, 7017, 7075 and LM6+Sr were polisned to a 1 micron finish and corroded for 48 hours in the corrosion rig. Single scratches using a Vickers diamond indenter under 500g load were done to establish to effect of work-hardened regions on the proximity and severity of corrosive attack. SEM photographs are shown in figs. 5.13 and 5.14. Table 5.5 gives a summary of wear test observations.

TABLE 5.5 : Corrosive wear test observations.

| ALLOY | TYPE OF CORROSIVE ATTACK OBSERVED | PREFERENCE OF PITTING ATTACK TO SCRATCHED REGION |
|---|---|---|
| 1200<br>3004<br>5083<br>6082<br>7017 | pitting attack<br>pit size ± 2-10μm<br>pit density increases as series number increases | no preference of pitting attack to workhardened regions |
| LM6+PC1 | severe localised and pitting attack | extensive preferential attack of scratched regions |
| 2014<br>7075 | severe general and pitting attack<br>pit size ± 20-80μm | extensive pitting attack at scratched regions |

FIGURE 5.13 SEM photographs of wear surfaces after the 48 hr corrosion test. Specimens polished to 1 μm surface finish. Corrosion solution A.

(a) 1200 showing isolated pitting attack. Pit size approx. 2-10 μm.

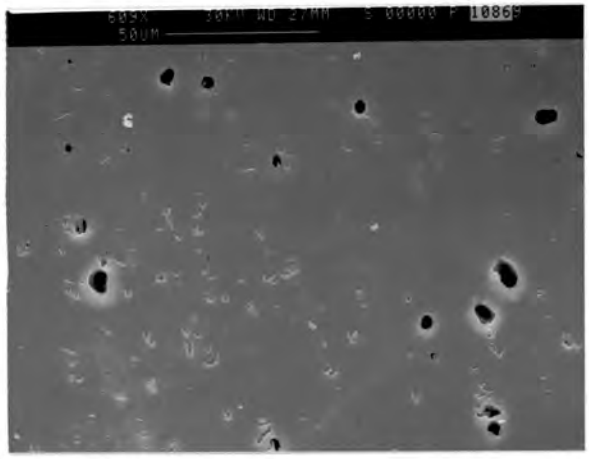

(b) 3004 wear surface shows higher density of pitting attack than 1200. Pit size approximately 5-10 μm.

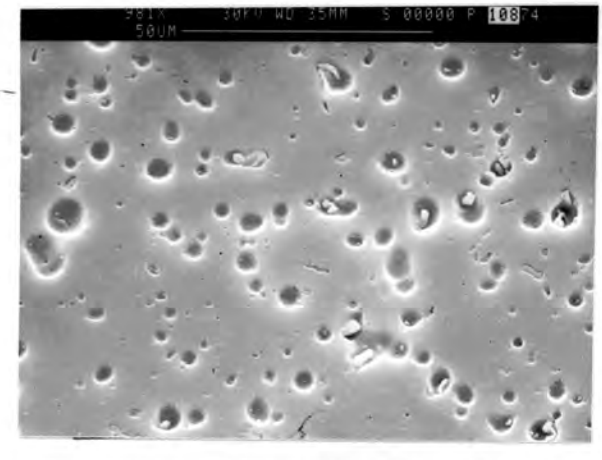

(c) 6082 showing high pitting density. Pit size approximately 2-10 μm. Although pit size remains constant for these alloys, pit density increases for increasing series number.

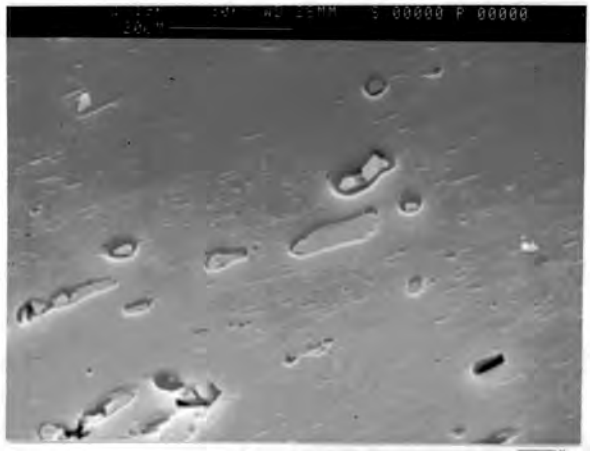

(d) Corroded surface of 5083 showing pit nucleation at precipitates and other constituent particles.

Figure 5.14 : SEM photographs of wear surfaces after the 48 hr corrosion test. Corrosion solution A.

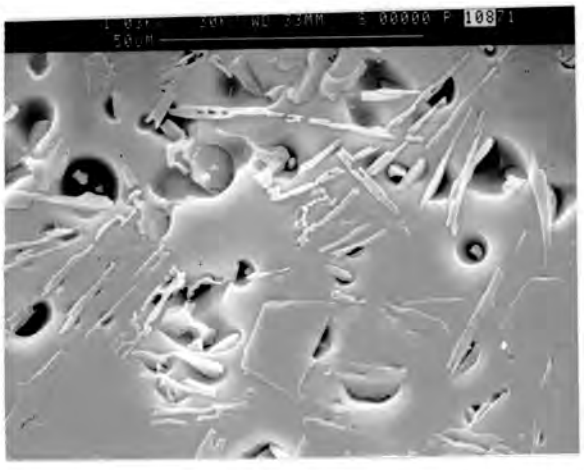

(a) Severe localised attack of the Al-Si solid solution of LM6+PCl. Si-phases behave cathodically.

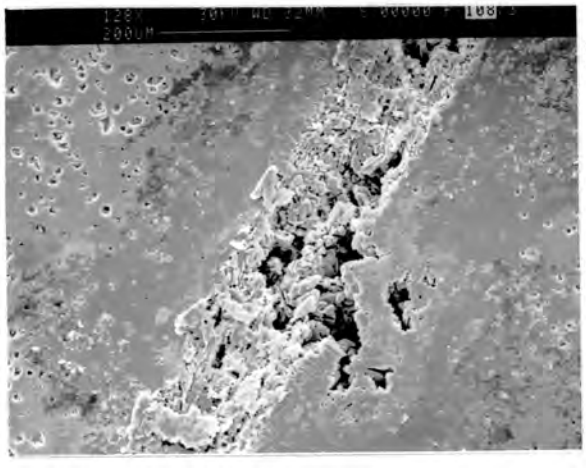

(b) LM6+PCl showing extensive attack at scratched regions.

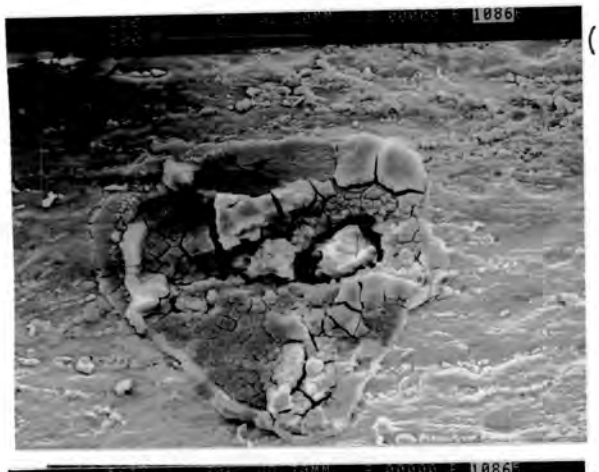

(c) Wear surface of 2014 showing preferential corrosion of the solid solution around a particle constituent, breakdown of the surrounding oxide layer and general attack.

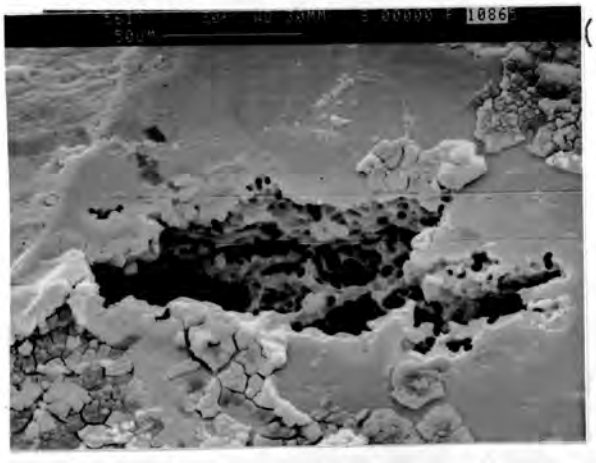

(d) Pitting attack of the 2014 wear surface. Note the breakdown of the oxide layer and resulting general attack in the top left hand corner.

FIGURE 5.15 : Volume loss by corrosion versus time for 6082, LM6+Sr and mild steel.

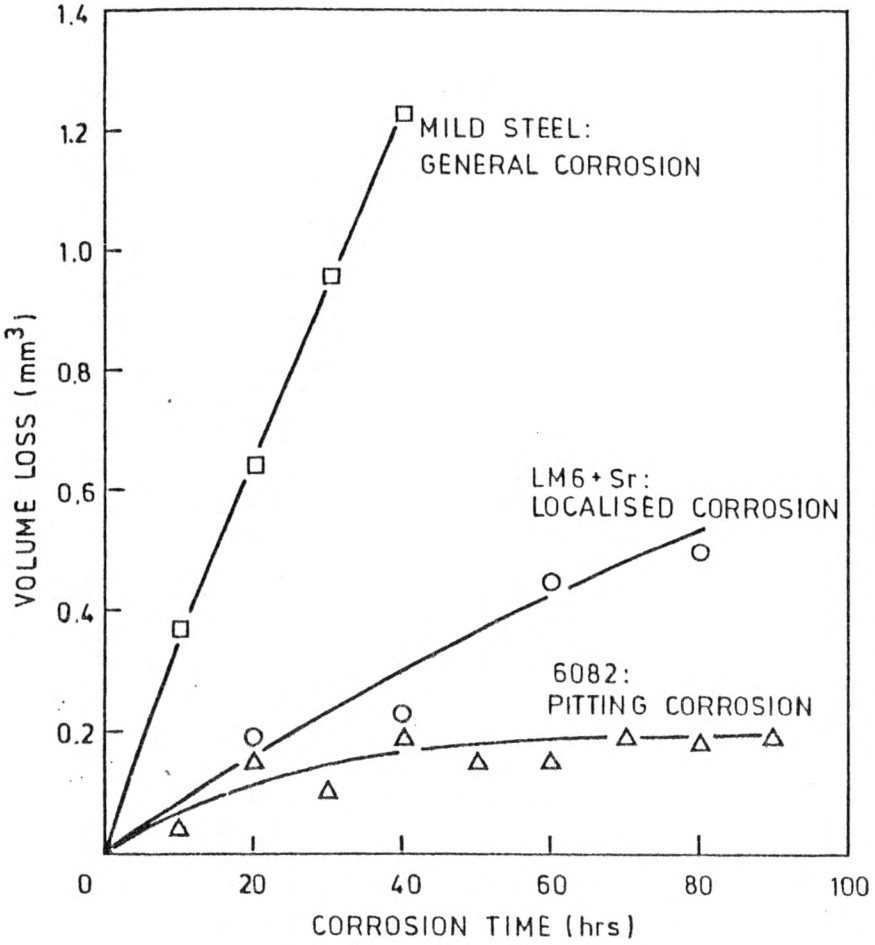



(a) LM6+Sr after 40 hrs corrosion showing extensive localised attack of Al-Si solid solution

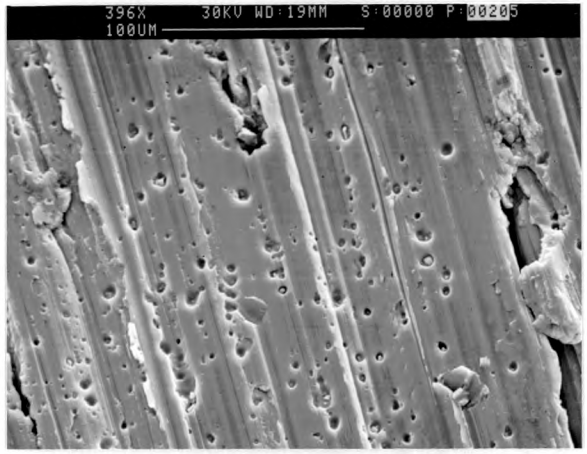


(b) 6082 after 20 hrs corrosion showing small pitting sites (±4μm) initiated at precipitates or second phase particles

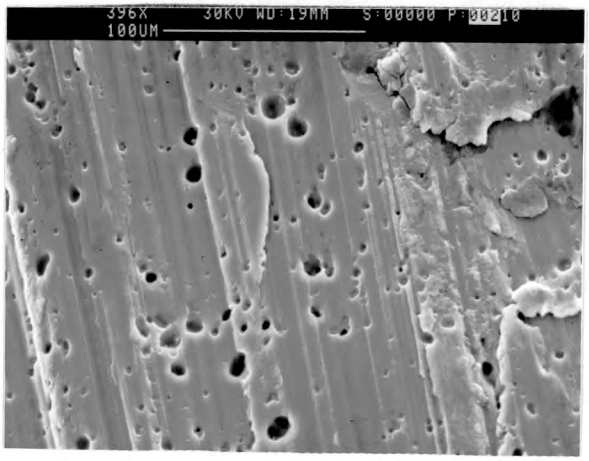


(c) 6082 after 80 hrs corrosion. Pitting sites have become larger (±8μm) but pitting density remains the same. Note that the precipitates have been eroded from the pitting sites.

(ii) Specimens of wrought and cast alloys with 80 grit surface finish were corroded for a period of 0-90 hours to establish the effect of corrosion time on volume losses. Figure 5.15 gives plots of volume loss versus corrosion time for LM6+Sr and 6082, representative of alloys that are subject to localised and pitting corrosion respectively.

## 5.5 ABRASION-CORROSION TESTS

### RWR#1 and RWR#2 Tests

Results obtained for the two standard wear tests are tabulated in Appendix A4. Fig. 5.15 gives a plot of RWR#1 and RWR#2 versus RAR. Plots of accumulative volume losses for the RWR#1 test are presented in fig. 5.16. Corrosion losses are representd by the hatched areas whereas dry abrasion losses are indicated by the area below the hatched areas. No measureable weight losses by corrosion were recorded for the alloys 5083 and 6063.

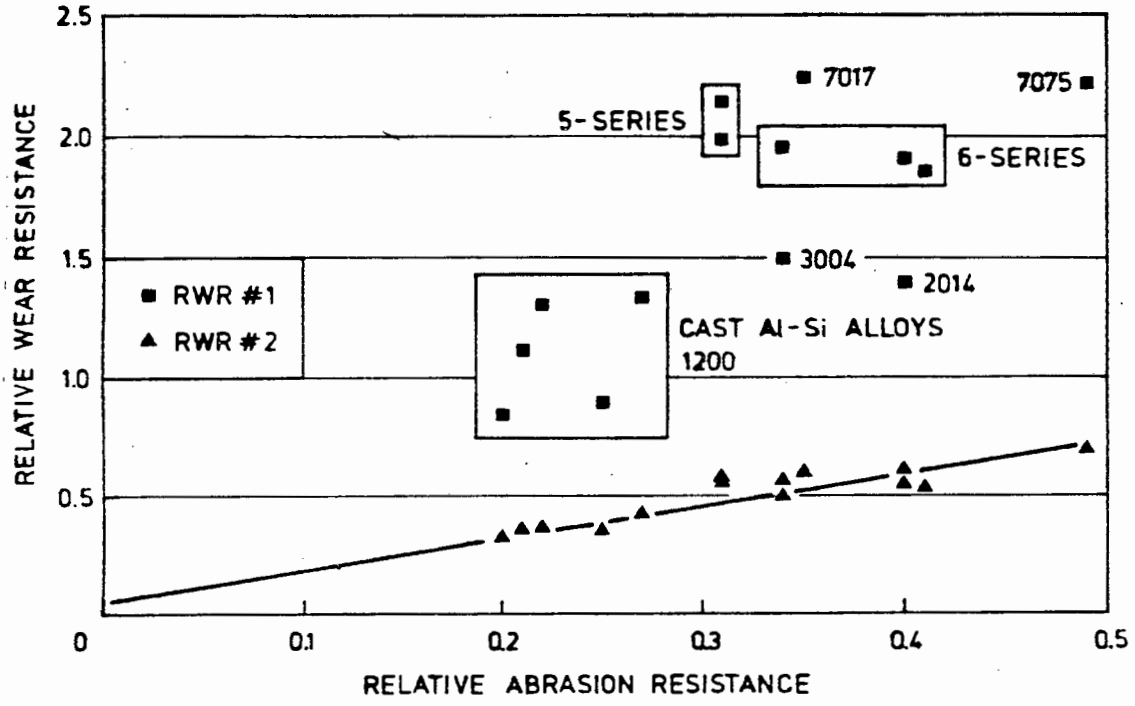


FIGURE 5.15 : Plot of relative wear resistnce (RWR#1,2) versus relative abrasion resistance (RAR) for wrought and cast Al-Si alloys.

FIGURE 5.16 : Accumulative abrasion and abrasion-corrosion volume losses for the RWR#1 test

(1) MILD STEEL

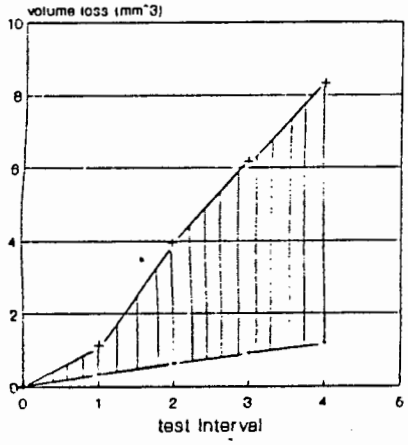


(2) LM6+Sr

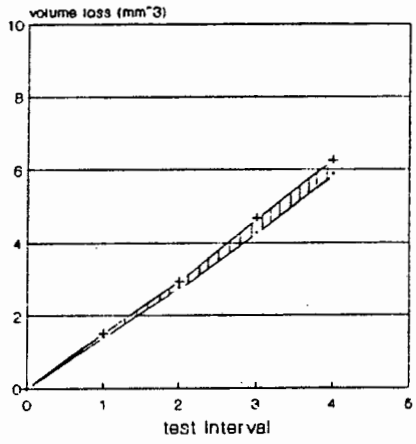


(3) 1200

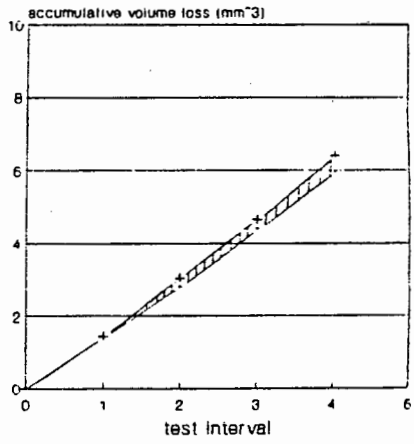


(4) 2014

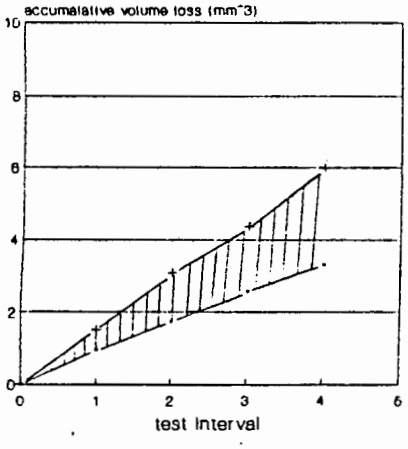


(5) 3004

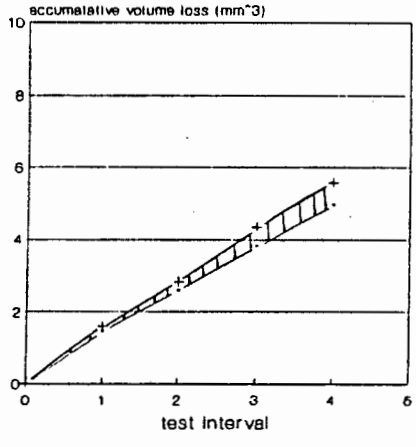


(6) 5083

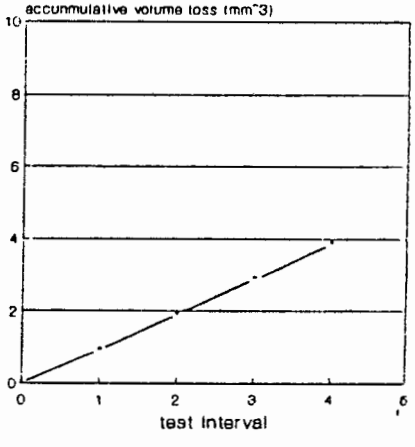


(7) 6063

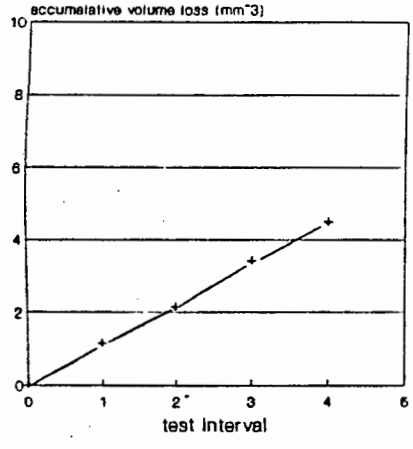


(8) 7017

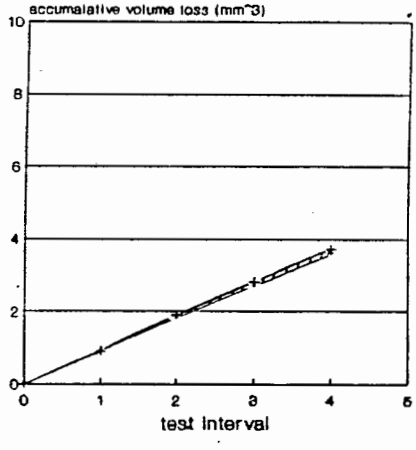


(9) 7075

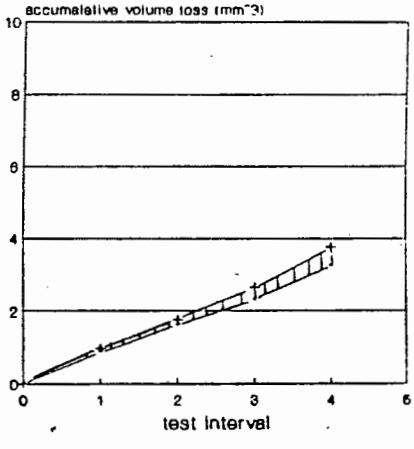

Amended RWR Tests

All alloys were evaluated in terms of their material performance as determined by the standard tests and factors such as strength, weldability and machinability. A short list of alloys comprising LM6+Sr, 5083, 6261, 7017 and 7075 was then selected for amended RWR tests. The relative wear behaviour of these alloys as a function of increased corrosion was established using 3CR12 as reference alloys. An effective increase in the percentage corrosion for successive tests is achieved by keeping the corrosion time and abrasion length constant for all tests, but reducing the severity of abrasion. This is achieved by decreasing load and grit size parameters. Details of test variables are contained in Table 5.6.

TABLE 5.6 : Test Parameters for amended RWR Tests.

| | 4 x 25 cm ABRASION | | | CORROSION TIME |
|---|---|---|---|---|
| | LOAD (kg) | SPEED (m/s) | GRIT SIZE | |
| Test 1 | 3.66 | 0.275 | 80 grit | 4 x 46 hrs |
| Test 2 | 1.33 | 0.275 | 180 grit | 4 x 46 hrs |
| Test 3 | 0.94 | 0.275 | 220 grit | 4 x 46 hrs |
| Test 4 | 0.76 | 0.275 | 220 grit | 4 x 46 hrs |

Figures 5.17 and 5.18 show plots of RWR (relative 3CR12) versus % corrosion 3CR12 for the alloys tested. Scanning electron microscope analysis of wear surfaces after the 24% corrosion tests revealed considerable damage by localised and pitting corrosion in the case of LM6+Sr and 7075. Only isolated pitting of abrasion grooves was observed for the alloys 5083, 6261 and 7017. (See SEM photographs, figs. 5.17 and 5.18).

FIGURE 5.17 : RWR (relative 3CR12) versus % corrosion 3CR12 for the alloys 7017 and 7075. SEM photographs show the wear surfaces after the 24% corrosion test

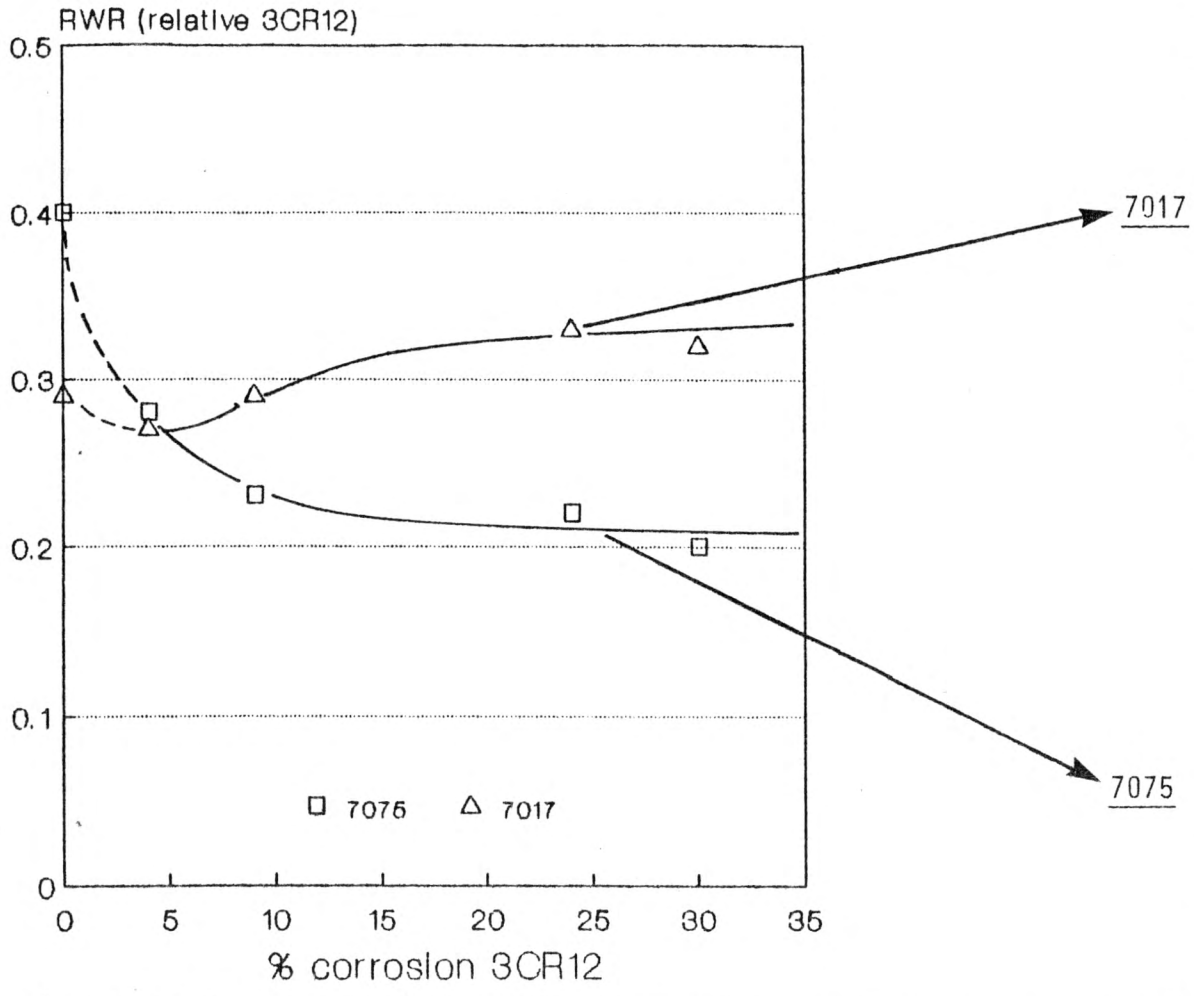


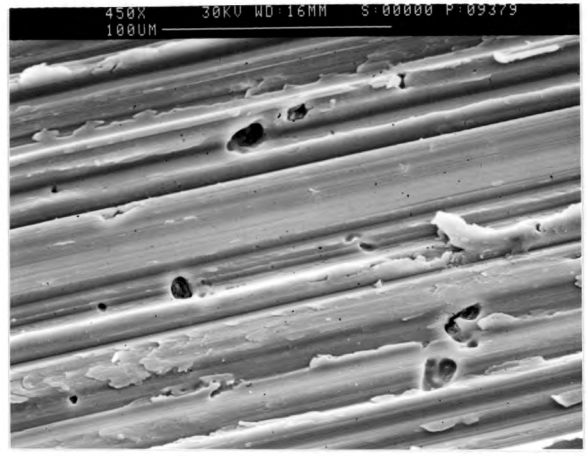


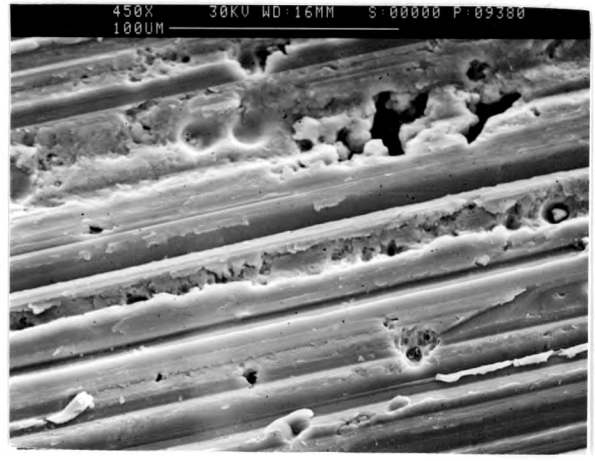


$$\text{RWR (relative 3CR12)} = \frac{\text{total volume loss of 3CR12}}{\text{total volume loss of test material}}$$

% corrosion 3CR12 = % of total volume loss by corrosion for 3CR12

FIGURE 5.18 : RWR (relative 3CR12) versus % corrosion 3CR12 for the alloys 6261, 5083 and LM6+Sr. SEM photographs show the wear surfaces after the 24% corrosion test.

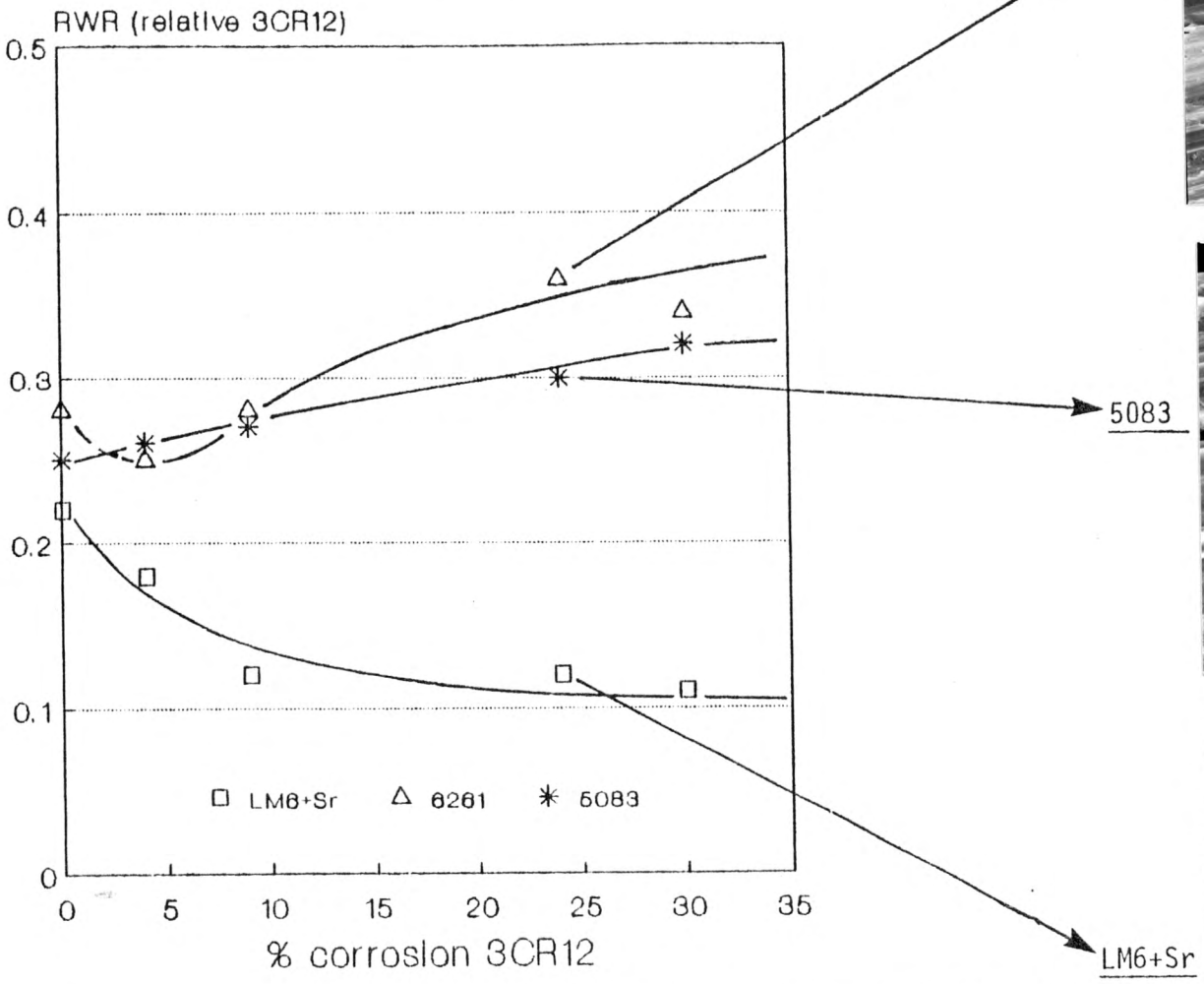


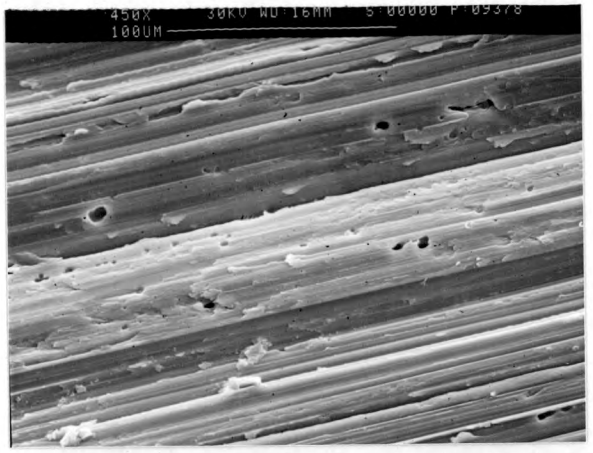


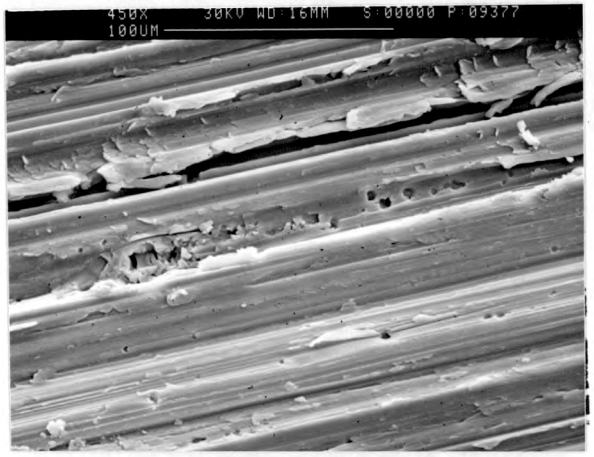


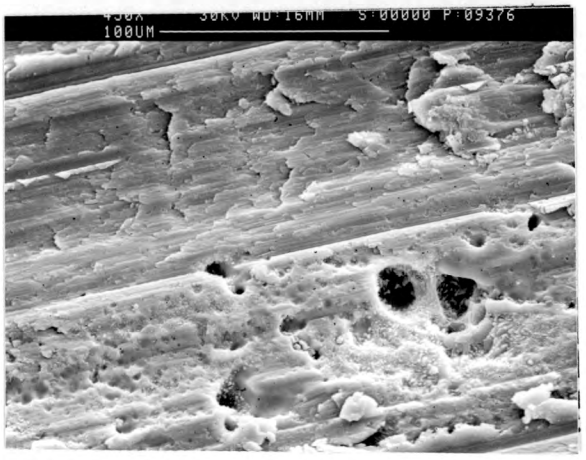


$$\text{RWR (relative 3CR12)} = \frac{\text{total volume loss of 3CR12}}{\text{total volume loss of test material}}$$

$$\text{\% corrosion 3CR12} = \text{\% of total volume loss by corrosion for 3CR12}$$

# CHAPTER 6

## DISCUSSION

Having presented the experimental data obtained for this investigation, it is now possible to analyse and discuss these results in terms of project objectives laid out in Chapter 1. Figure 6.1 gives a diagramatic layout of the discussion path followed in this chapter.

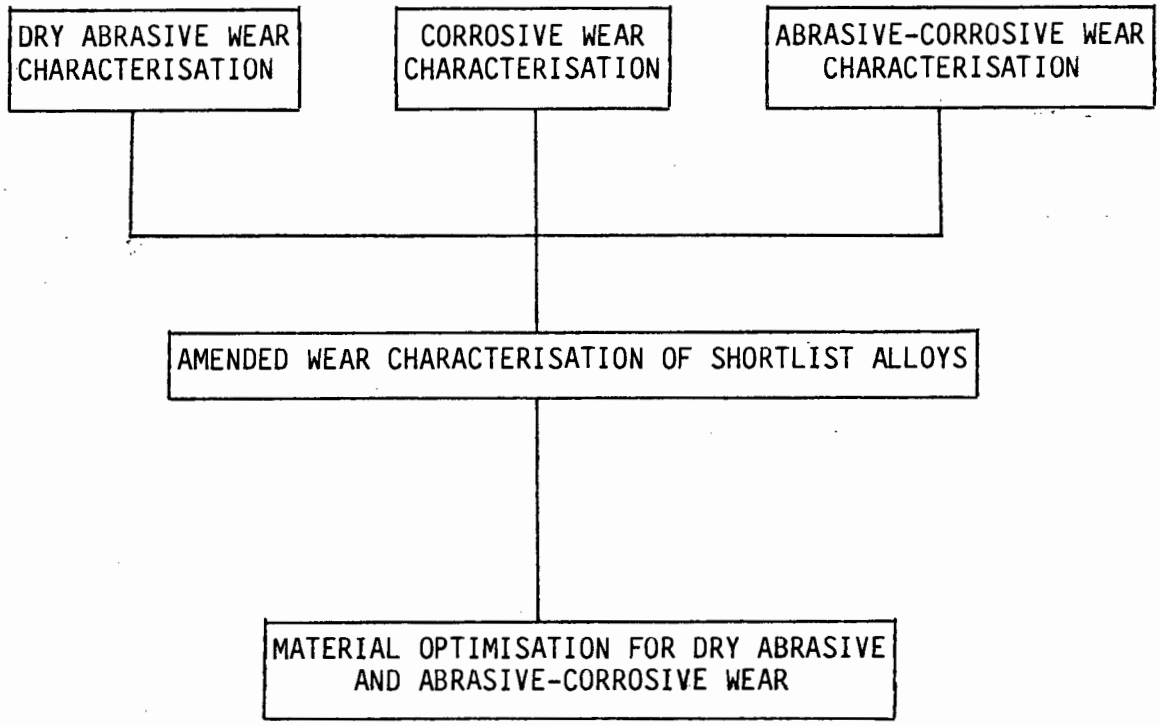


FIGURE 6.1 : Discussion path.

The first step involves the broad wear characterisation of all test alloys using the standard tests devised by previous authors (Noel and Allen, 1981). Using a set of criteria based on material selection in a mining wear environment, a shortlist of alloys is selected for further wear characterisation. Finally, material optimization for dry abrasive and abrasive-corrosive wear is presented.

## 6.1 DRY ABRASIVE WEAR CHARACTERISATION

### 6.1.1 The influence of external factors on dry abrasive wear rates

In a dry abrasive wear environment the external effect of wear performance is determined by load, speed and grit size parameters. For the test ranges set out in Table 3.4, the response of aluminium alloys can be summarised by figs. 6.2, 6.3 and 6.5.

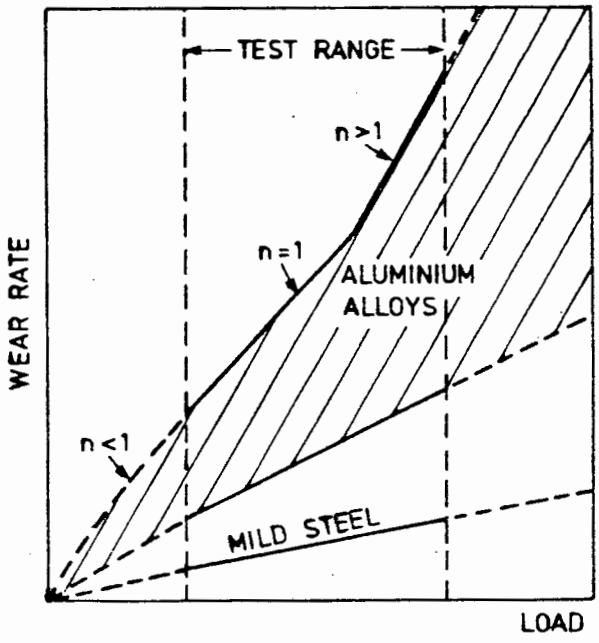


FIGURE 6.2 : Schematic response of aluminium alloys to the external parameter load. The exponent of eqn.(1) depends on sample and grit size. Test range 1.3 to 3.6 kg.

Load

The response of aluminium alloys to load is shown schematically in fig. 6.2. Three regions of the curve can further be identified. For loads smaller than 1000g, wear rate is proportional to the pressure on the sample surface elevated to an exponent slightly less than 1.0.($n<1$). Larsen-Basse (1978) reports similar results using copper samples. The n value of eqn.(1) approaches unity for loads exceeding 1000g and direct proportionality is observed . Eqn.(2) and Table 5.1 describe the relationship mathematically.

Figure 5.1 shows the wear rate of KS1275 and LM6+PC1 to increase linearly with load in two distinct regions marked by a sharp transition point at load 2800g. Jasim and Dwarakadasa (1987) found a similar behaviour for pure aluminium and Al-Si cast alloys. The transition point was found to be specific for each alloy, depending on the properties of the alloy and abrasion conditions, and occurred because of the change over to a more severe wear mechanism. In the case of KS1275 and LM6+PC1, where higher wear rates than the other cast alloys are observed, microstructural properties are such that this transition occurs at lower loads than for the other alloys.

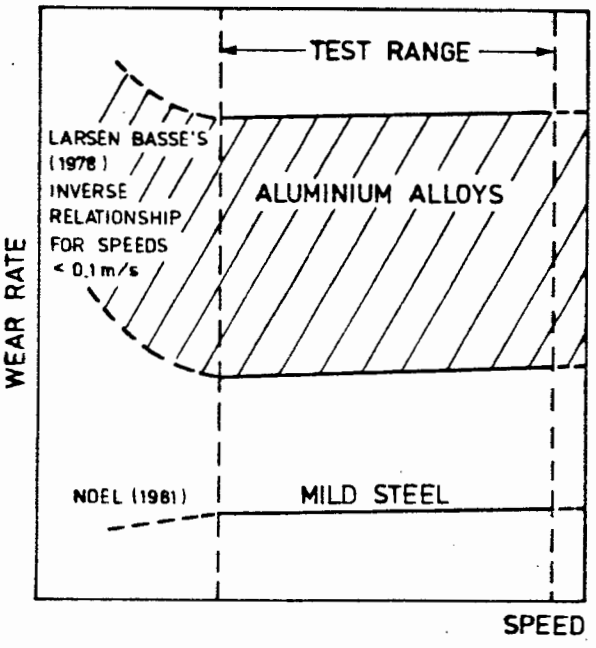


FIGURE 6.3 : Schematic response of aluminium alloys to the external parameter speed. Test range 0.1 to 0.5 m/s.

Speed

Allen, Protheroe and Ball (1981/1982), found the wear rate of austenitic stainless steels to increase over the velocity range 0.02 to 0.45 m/s and ascribed this to an increase in friction temperature leading to easier slip and deformation. A different trend is observed for aluminium alloys. Larsen-Basse and Tanouye (1978) found an inverse relationship between removal rate and sliding velocity at low velocities (0-0.1 m/s). Figure 5.2 shows that wear rate then levels off over the test range 0.1 to 0.5 m/s.

The response of aluminium alloys to velocity as shown schematically in fig. 6.3 can be explained as follows: under low velocity conditions ( 0.1 m/s) an increase in abrasion velocity effects the flow stress by making deformation more difficult. Wear rates are thus reduced. At higher velocities a counter influence to the wear process is introduced. Increased friction temperature leads to easier slip and deformation of the wear material and the reduction in wear rate observed at low velocities is off-set. Constant wear rate is thus observed as a result of the balancing counter effects of strain rate on friction temperature and flow stress as formulated by Allen, Protheroe and Ball (1981/1982) and Larsen-Basse and Tanouye (1978) respectively. Figure 6.4 shows the effect of higher flow stress and friction temperature on wear loss.

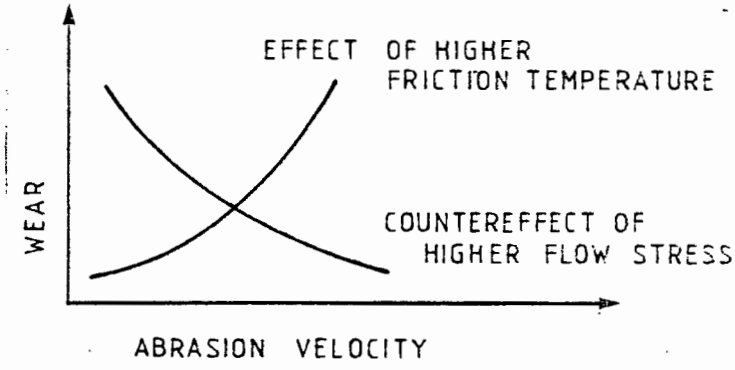


FIGURE 6.4 : Schematic effect of higher flow stress and friction temperature due to increased abrasion velocity on wear loss.

Grit size

Figure 6.5 shows the schematic response of aluminium alloys to grit size. Wear rate is seen to increase rapidly with grit size until a critical grit diameter of 200$\mu$m is reached. Above this value wear increases linearly with grit size; the relationship is then described by eqn. (3). The above trend observed for aluminium alloys and the explanation thereof is in agreement with previous authors. See Chapter 2, p(10).

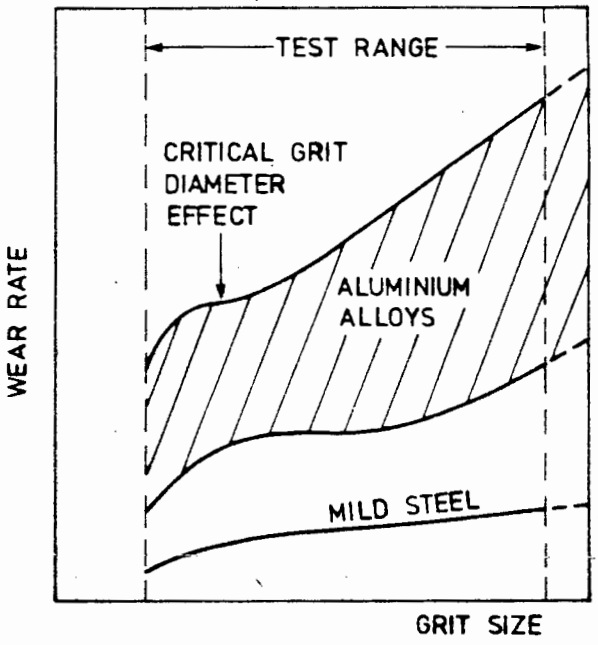


FIGURE 6.5 : Schematic response of aluminium alloys to the external parameter grit size. Test range 120 to 640 $\mu$m.

One exception to the critical grit diameter effect is the 16% silicon cast alloy KS281.1. The wear curve is characterised by a smooth decrease of wear rate for decreasing grit sizes, showing no critical grit diameter. However, for finer grit sizes this decrease accelerates and KS281.1 outperforms other cast alloys for grit sizes below the critical value. See Fig. 5.3(b). Two possible explanations are forwarded : due to the relatively high bulk hardness of KS281.1 as compared to the other cast alloys, attrition of abrasive particles would be more pronounced for finer grit sizes, resulting in lower wear rates for decreasing grit sizes. Silicon dendrites in the cast structure of KS281.1 vary in size from approximately 100-250 $\mu$m and form a hard primary phase of the microstructure. For finer grit sizes these microstructural features become comparable in size to abrasive groove width or depth. Wear rates are then influenced by their individual properties rather than through their effect on bulk properties. (Moore 1980).

### 6.1.2 Relative abrasion resistance and the effect of material properties

Relative abrasion resistance values presented in fig. 6.6 show that aluminium alloys have approximately half or less the abrasion resistance of conventionally used steels such as mild steel

(RAR=1.00) or 3CR12 (RAR=1.22). Heat-treatable alloys have the best abrasion resistance, out-performing cast alloys by a maximum factor of 2½ times.

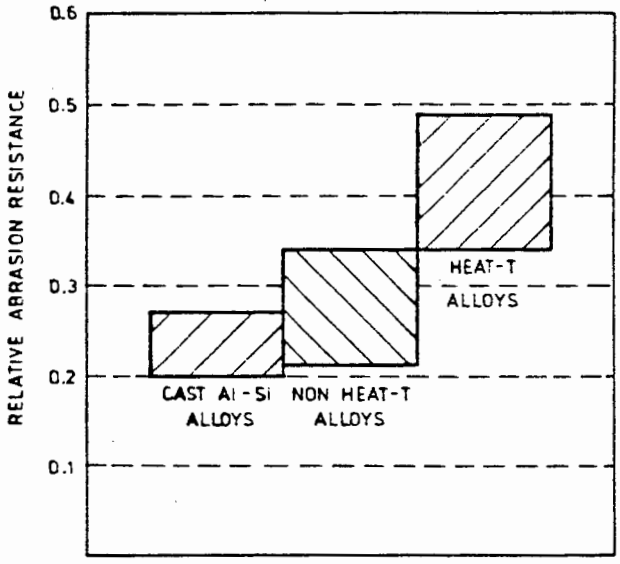


FIGURE 6.6 : Abrasion resistance of aluminium alloys.

An explanation for the distribution of abrasion resistance values is attempted by looking at the material and microstructural properties that influence abrasive wear.

Cast alloys

The poor performance of these alloys can be explained by looking at the microstructural aspects of the wear process. Cast Al-Si alloys consist essentially of a soft Al-matrix with hard silicon-phases distributed throughout the microstructure. See figs. 4.4, 4.5 and Table 5.3. During abrasion the soft and ductile Al-matrix offers little resistance to the ploughing action of abrasive grains, whilst the hard, primary silicon-phases are either plucked out of the Al-matrix without appreciable resistance or removed by brittle microfracture. The weak interfaces of these large, angular and incoherent particles play an additional role in determining poor abrasion resistance. Scanning electron microscope photographs of an abraded surface (fig. 5.3(c)) and a Charpy Impact test fracture surface (fig. 5.9(a)) for the KS281.1 alloy illustrate the brittle-ductile microfracture behaviour.

The two wear modes of ductile and brittle material removal are characterised by Materials A and C respectively in fig. 2.3 (Ball, 1986). High wear rates are predicted in each case. An initial indication of poor microfracture properties was further provided by low values of Charpy Impact toughness. See Appendix A4.

Figure 5.4 shows that the abrasion resistance of Al-Si cast alloys is approximately independent of bulk hardness, a parameter influenced by the amount of silicon phases in the microstructure. For example, KS281.1 contains large primary silicon-dendrites and has a higher bulk hardness than the other cast alloys. However, it is evident from the above discussion that abrasion resistance is primarily determined by the micro-toughness and coherency of second phases, rather than their amount and hardness. Thus, although the amount and distribution of silicon phases varies for the cast alloys tested and result in substantially different hardness values the micro-toughness and coherency properties are not altered significantly and similar abrasion resistance values are observed. A slight improvement in abrasion resistance is observed for the alloy LM6+Sr, where strontium is added to the melt to refine the size and round the shape of silicon-particles, improving coherency and distribution properties.

Wrought alloys

When analysing the abrasive wear resistance of wrought aluminium alloys it is important to distinguish between heat-treatable and non heat-treatable alloys since their properties differ significantly and give rise to different wear performances. A summary of material properties that influence the wear characteristics of these alloys is presented in Table 6.1.

TABLE 6.1 : Material properties of heat-treatable and non heat-treatable alloys.

| MATERIAL PROPERTY | NON HEAT-TREATABLE ALLOYS 1200, 3004, 5xxx | HEAT-TREATABLE ALLOYS 2014, 6xxx, 7xxx |
|---|---|---|
| HARDNESS | Low hardness (38-96 HV30) | Higher hardness (96-189 HV30) |
| CHARPY IMPACT TOUGHNESS | High Charpy Impact values ( 70 Joules) of 1200 and 3004 when compared to mild steel. (37 Joules) Typical ductile fracture characteristics as shown in fig. 5.3(c). | Intermediate range of Charpy Impact values. (6-39 Joules) Brittle-ductile fracture characteristics, depending on the paticular alloy. See fig. 5.3(b) and (d). |
| WORK-HARDENING CAPACITY | Values of HVmax/HVbulk range from 1.3 to 2.2. 3004 shows best work-hardening characteristics. See graph no. 8(b). | Values of HVmax/HVbulk range from 1.2 to 1.5, slightly less than for the heat-treatable alloys. See graph no. 8(a) and Appendix A4. |
| TENSILE STRENGTH | Low tensile strength (100-200 MPa) | Higher tensile strength (250-590 MPa) |

It is evident from the properties in Table 6.1 that non heat-treatable aluminium alloys are soft and ductile metals with relatively low strength and hardness properties. Clearly these materials have poor abrasion resistance because since the stresses and strains required for micro-fracture during abrasion are easily achieved and wear loss occurs by ductile cutting.

Narasimha Rao and Sekhar (1986); Horn and Ziegler (1983) found that the work-hardening index was similar and small for all aluminium alloys and that cold work of non heat-treatable alloys did not improve their abrasion resistance significantly. Table 6.1 shows that HVmax/HVbulk, a measure of work-hardening capacity, is only slightly better for non heat-treatable alloys. A notable exception is the alloy 3004 where a high value of HVmax/HVbulk indicates good work-hardening characteristics. Correspondingly higher abrasion resistance (RAR=0.34) is observed.

Consideration of heat-treatable alloy properties show that artificial ageing treatments improve hardness and strength properties significantly. Improved fracture toughness properties

result in a better combination of hardness, strength and toughness. These alloys resemble Material C characterised by Ball(1986) in Section 2.2.2 more closely and as anticipated, better abrasion resistance is observed.

### 6.1.3 Influence of ageing time on abrasion resistance

In the aforegoing section it was established that the natural strength properties developed by artificial ageing of heat-treatable alloys give rise to better abrasion resistance values. This section discusses the effect of ageing temperature and time on the development of optimum abrasion resistance.

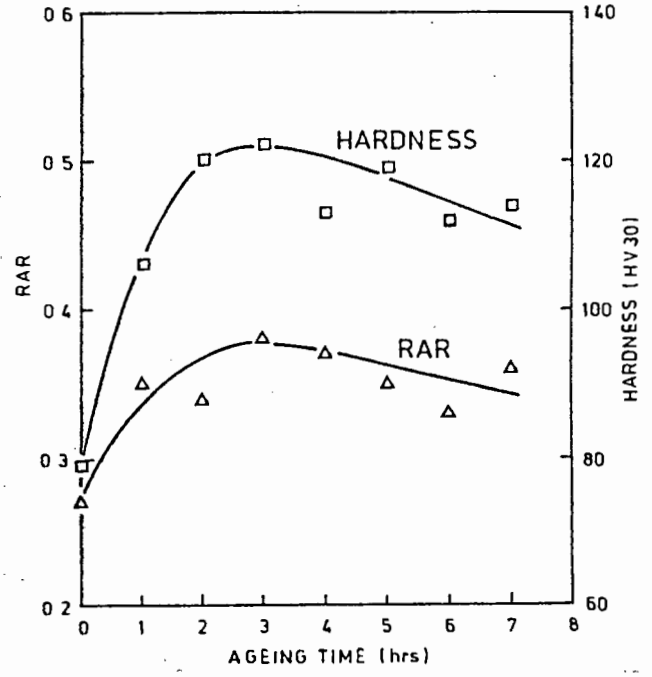


FIGURE 6.7 : Ageing curve of 6082 showing development of optimum RAR and hardness. Ageing temperature = 200°C.

Figure 6.7 shows the development of abrasion resistance and hardness as a function of ageing time for the alloy 6082. It is observed that optimum abrasion resistance and hardness is developed simultaneously, after which a decrease in properties occurs. The following explanation is applicable : After solution treatment alloying elements are in supersaturated solid solution and the

precipitate-free microstructure is soft and ductile, with correspondingly low abrasion resistance. Artificial ageing allows the precipitation of second phase particles to occur and the resulting matrix of solid solution and precipitates is stronger and more resistant to ductile cutting and microfracture during abrasive actions. Consequently, abrasion resistance increases. After the attainment of optimum precipitate size and coherency with the solid solution further ageing results in a decrease of hardness and strength properties as over-coarsening of second phase particles occurs. A decrease in abrasion resistance is then observed.

Similar heat-treatments of the alloys 6261 and 7017 at lower ageing temperatures show that optimum abrasion resistance and hardness properties are attained after longer ageing times (10-12 hrs) since the precipitation reaction occurs more slowly. See fig. 6.8.

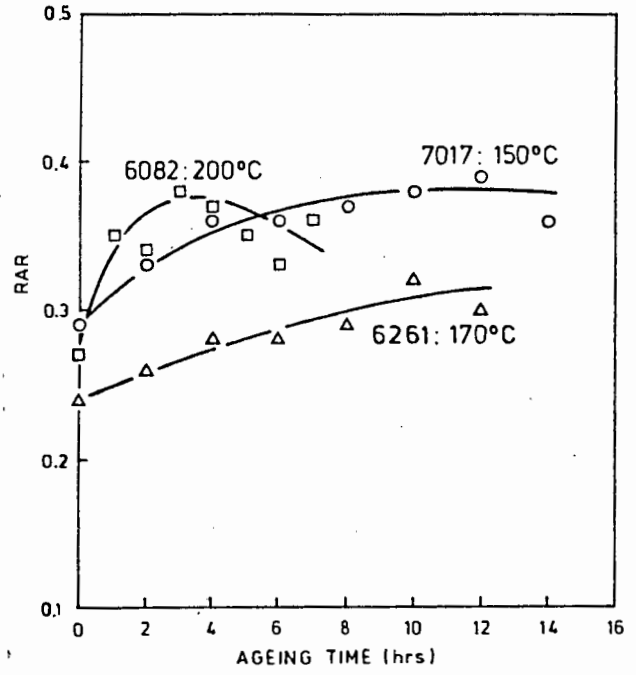


FIGURE 6.8 : Attainment of optimum abrasion resistance at different temperatures for the alloys 6082, 6261 and 7017.

## 6.2 CORROSIVE WEAR CHARACTERISATION

The first step in the corrosive wear characterisation of aluminium alloys was to establish the type of attack that occurs for each alloy under RWR test conditions. Three types of corrosive attack, namely general,

localised and pitting corrosion were found to occur either singularly or in combination. In the discussion that follows reference is made to Table 5.5, a summary of corrosive wear test observations and figs. 5.12, 5.13 and 5.14.

Pitting attack was found to occur for the alloys 1200, 3004, 5083, 6082 and 7017. It was noticed, that although pit size was the same for all these alloys, pit density increased as the number of the alloy series increased. See fig. 5.13(a), (b) and (c). Fig. 5.13(d) also shows that pit nucleation occurs predominantly at small particles contained in the aluminium matrix. The above findings can be explained as follows : in the microstructure of aluminium alloys localised preferential attack at constituent sites will occur if a difference in electrode potential between the solid solution and constituent exists. The magnitude and sign of this difference is given by Table 2.2 and determines both the severity of attack and preferentiality of attack to either the solid solution or constituent. In the case of 1200 alloy a homogenous microstructure with low alloying content and only a very fine distribution of impurity and insoluble phases limits corrosive attack. Pitting is confined to preferential erosion of the solid solution around impurity particles such as $FeAl_3$. Table 2.2 shows that $FeAl_3$ behaves cathodically with respect to aluminium. As the alloy series number increases, alloying content is increased and more second phase particles are present in the aluminium matrix. The number of sites where pitting can be initiated is thus increased and higher pitting densities are observed. Preferential corrosive attack of work hardened scrathed regions did not occur and confirms that pitting attack is predominantly dependent on constituent density for these alloys.

Severe pitting and localised attack was observed for the cast Al-Si alloy LM6+PCl. Fig. 5.14(a) clearly shows preferential attack of the Al-Si solid solution around silicon needles. Table 2.2 verifies that pure silicon has a strong cathodic potential relative to its solid solution. Preferential attack was found to occur at scratched regions. See fig. 5.14(b). During abrasion large silicon needles may be partially plucked out of the aluminium matrix or fractured along different planes. The resulting random allignment and protrusion from the wear groove surface of these particles make the formation of a coherent passivating layer difficult. Corrosion kinetics are adversely affected (as noted by Noel (1981) for mild steel specimens) and selective pitting at abraded regions occurs.

The most severe form of attack was observed for the alloys 2014 and 7075. Due to the high anodic potentials of copper and zinc containing solid solutions of 2014 and 7075 respectively, general and pitting attack is observed for these alloys. Fig. 5.14(c) clearly shows preferential erosion of the solid solution around a particle constituent, breakdown of the surrounding oxide layer and general corrosion of the remaining surface. Fig. 5.14(d) illustrates severe pitting attack. Note again the breakdown of oxide layer in the top left hand corner, giving way to general corrosion.

The three types of corrosive attack described are illustrated in fig. 5.15 and are characterised similarly by Barker (1988) in Section 2.3.3. Comparing figs. 2.10 and 5.15, Materials A, B and C correspond to mild steel, LM6+Sr and 6082 respectively. The general attack of mild steel represents an exaggerated version of corrosive attack for 2014 and 7075.

It is observed from fig. 5.15 that the induction period of 6082 ($t_2$ in fig. 2.10) is poorly defined and can be approximated to a maxium value of 20 hrs. SEM photographs of the wear surfaces (see fig. 5.15(b) and(c)) show that pitting is initiated at constituent sites before 20 hrs corrosion, and although pitting density remains constant, pit size increases for increased exposure times (80 hrs). It can be concluded that localised breakdown of the oxide layer at constituent sites and pitting proceed after a short exposure time. However, since attack occurrs predominantly at constituent sites pitting density remains constant and volume losses at higher exposure times (after 30 hrs) level off.

## 6.3 ABRASIVE-CORROSIVE WEAR CHARACTERISATION

The behaviour of aluminium alloys for this type of wear was characterised by two standard tests, RWR#2 and RWR#1. Section 3.2 reviews the test conditions employed. In the discussion that follows reference is made to fig. 5.15 and fig. 5.16; plots of accumulative abrasion and abrasion-corrosion volume losses for the RWR#1 test. Hatched areas represent the volume lost by corrosion.

For the RWR#2 test alloys were subjected to wear intervals of 1 metre abrasion and 22 hrs corrosion. It was found that abrasion was the predominant wear factor for this test, corrosion intervals causing little wear damage in terms of volume losses. Since it has already been established that aluminium alloys have poor abrasion resistance, it was anticipated that mild steel would out-perform these alloys for the RWR#2 test. A linear relationship between RWR#2 and RAR of slope slightly greater than unity (fig. 5.15) verifies both the close dependence of the RWR#2 test on abrasion resistance and the minor effect of corrosion.

For the RWR#1 test alloys were subjected to wear intervals of 25cm abrasion and 46 hrs corrosion. It was found that corrosion was the predominant wear factor, mild steel showing 86% volume loss by corrosion. Comparing the relative amount of volume lost by corrosion for the various alloys in fig. 5.16, it is clear that aluminium alloys out-perform mild steel for this test because of superior corrosion resistance. Furthermore, results for the RWR#1 test show that as corrosion becomes the more predominant wear factor in an abrasive-corrosive wear environment, overall wear resistance is determined primarily by the corrosion properties of the series of alloys, whilst the dry abrasion properties of individual alloys within that series become less important. Good examples are the two 7-series alloys 7017 and 7075. The relative abrasion resistance of 7075 (RAR=0.49) is 28% higher than that of 7017 (RAR=0.35). It has also been established in Section 6.2 that 7017 has superior corrosion resistance. Corresponding values of 2.24 and 2.21 for the RWR#1 test (see fig. 5.15) show that the advantage of superior abrasion resistance of 7075 is lost as the corrosion properties of the alloy become the main determinant of overall wear resistance.

The 5-series alloys, having excellent corrosion properties show a significant improvement for the RWR#1 test. Figure 5.16(6) shows no recorded volume losses. Despite superior abrasion properties, a significant decrease in wear performance is observed for the 2014 alloy (fig. 5.15(4)) because of its poor corrosion resistance. The abrasive-corrosive wear behaviour under more corrosive conditions is investigated for some of these alloys in Section 6.4.

## 6.4 AMENDED ABRASIVE-CORROSIVE WEAR CHARACTERISTION OF SHORT LIST ALLOYS

A short list of alloys was selected to obtain a good cross-section of the most promising aluminimum alloys, bearing in mind the criteria for material selection in a mining environment. Two main selection criteria were employed :

(i) material performance as determined by the standard abrasion and abrasion-corrosion tests.

(ii) factors such as strength, toughness, weldability, formability and machinability that are important for mining applications.

Using the information contained in Appendices A4 and A5 to evaluate criteria (i) and (ii), it was possible to draw up Table 6.2 of major advantages and disadvantages for the various alloys. The following short list of alloys was selected : LM6+Sr, 5083, 6261, 7017 and 7075. The cast alloy LM6+Sr was included for its excellent casting characteristics and better wear performance relative to the other cast alloys. Although the 1200 and 3004 alloys show high point values for criteria (ii) (see Appendix A5), they were excluded because of poor abrasion resistance and low strength. The Al-Cu alloy 2014 was not included because of poor corrosion resistance and relative non-availability. The two higher strength 6-series alloys 6082 and 6261 have very similar properties. 6261 was selected as the more commonly used alloy. The 7-series alloy 7017 was included for good all-round performance for criteria (i) and (ii). The 7075 alloy has poor corrosion resistance but was included for its excellent abrasion resistance and strength. For further wear tests it also serves as a useful comparison to the 7017 alloy.

TABLE 6.2 : Major advantages and disadvantages

| ALLOY | ADVANTAGES | DISADVANTAGES |
|---|---|---|
| 1200 | very good corrosion resistance<br>excellent weldability &<br>formability | poor abrasion resistance<br>low tensile strength<br>fair machinability |
| 2014 | good abrasion resistance<br>high strength<br>good machinability | poor corrosion resistance<br>fair weldability<br>poor formability |
| 3004 | moderate abrasion resistance<br>very good corrosion resistance<br>excellent weldability<br>very good formability | low tensile strength<br>fair machinability |
| 5xxx | excellent corrosion resist.<br>very good weldability &<br>formability | moderate/poor abrasion resist.<br>moderate tensile strength<br>fair machinability |
| 6xxx | good abrasion resistance<br>good weldability, formability<br>& machinability<br>good strength properties | no major disadvantages |
| 7017 | good corrosion resistance<br>moderate/good abrasion resist.<br>very good weldability<br>good formability & machinability | no major disadvantages |
| 7075 | high tensile strength<br>very good abrasion resist.<br>excellent machinability | poor corrosion resistance<br>fair formability<br>very poor weldability |

It has been established that the short-list alloys out-perform mild steel by a factor of 1.3 to 2.2 for the RWR#1 test. For amended wear tests where the corrosion factor is increased, a new reference alloy with superior strength and corrosion properties to mild steel, namely 3CR12, was selected. 3CR12 is used extensively as a structural and wear application engineering material in the mining industry. Table 6.3 lists the relevant material properties of mild steel and 3CR12. A description of the tests and detailed test parameters are contained in Section 5.5. The following discussion refers figs. 5.17 and 5.18.

TABLE 6.3 : Reference alloys.

| ALLOY | HARDNESS (HV30) | TENSILE STRENGTH (MPa) | RAR | RWR#1 | RWR#2 |
|---|---|---|---|---|---|
| Mild steel | 200 | ±230 | 1.00 | 1.00 | 1.00 |
| 3CR12 | 185 | 530 | 1.22 | 7.63 | 2.25 |

In the abrasive-corrosive tests conducted, load and grit size parameters of abrasive intervals are decreased from Test 1 to Test 4 (see Table 5.6) to facilitate an increased corrosion factor. Two important consequences were anticipated:

(a) as established in Section 6.1, lower dry abrasive wear losses for successive tests would be observed as a result of decreased load and grit size parameters.

(b) damage caused by corrosion intervals may only be partially removed by subsequent abrasion intervals, allowing a semi-continuous corrosive wear process to proceed throughout the test.

The alloys 5083, 6261 and 7017 show an approximately 20% increase in relative wear performance from test 1 to test 4. See figs. 5.17 and 5.18. The following explanation is applicable. It has been established in Section 6.2 that corrosive volume losses for these materials level off after an exposure time of approximately 20 hrs. In the case of Test 1 where abrasive intervals are severe the semi-continuous corrosive wear process described in (b) is minimised and accumulative volume losses can be depicted as shown in fig. 6.9.

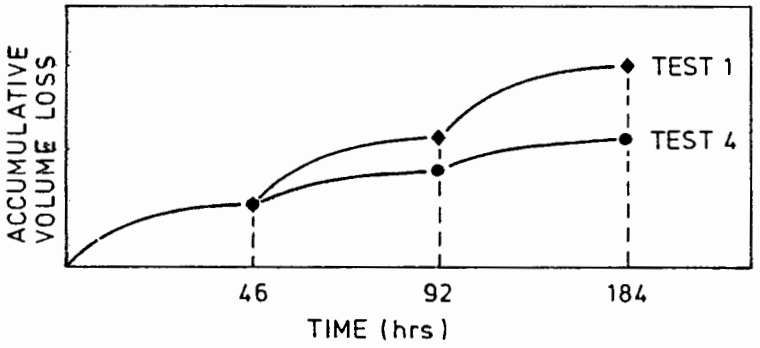


◆ abrasive interval removes wear damage caused by corrosion

● abrasive interval only partially removes corrosive wear damage

FIGURE 6.9 : Schematic graph of accumulative volume losses for Test 1 and Test 4.

In the case of Test 4 less severe abrasive intervals only partially remove wear damage of preceding corrosion intervals and a semi-continuous corrosive wear process is allowed to continue throughout the test. SEM photographs after the 24% corrosion test (test 3) show the minor effect of pitting corrosion. The resulting decrease in accumulative volume losses is shown in fig. 6.9.

Barker (1988) predicts a similar decrease in accumulative volume losses for Material A with induction period $t_1$, by decreasing the corrosive exposure time rather than reducing the severity of abrasive intervals. See fig. 2.12. This method of volume loss reduction is not possible for the above aluminium alloys since their induction period is short and poorly defined.

The cast alloy LM6+Sr and 7075 show the opposite trend. During corrosion intervals, extensive localised and pitting attack of the wear surface takes place and wear losses due to factor (b) increase for successive tests. Corrosive attack is predominant and as a result wear performance is decreased and approximately halved for test 4 in both cases. SEM photographs of the LM6+Sr and 7075 wear surfaces (figs 5.17 and 5.18) show that after the last abrasive interval of test 4, extensive corrosive attack of the wear surface is clearly visible.

## 6.5 MATERIAL OPTIMISATION

This section of the discussion concerns the identification of wear conditions, material properties and heat-treatments that may optimise the wear performance of aluminium alloys in the light of results that were presented and discussed in the previous sections.

### Dry abrasive wear

Wear rate curves for varying load, speed and grit size conditions show that the performance gap between aluminium alloys and mild steel is narrowed appreciably for certain dry abrasive wear environments:

(i) Comparing the coeffcient $S_1$ of eqn.(2) for mild steel and aluminium alloys, it can be seen that relative performance improves as the load decreases.

(ii) For abrasion speeds greater than 0.1 m/s, wear losses are unaffected by further speed increases (verified up to 0.5 m/s). Austenitic stainless steels show a significant increase in wear rates at higher velocities. (Allen, Protheroe and Ball, 1981).

(iii) A critical grit size below which the performance relative to mild steel is improved significantly can be established. This grit size depends on the geometry of the wear situation and is approximately 200 m under the test conditions of this investigation.

If, in a given wear environment, dry abrasive service conditions are identified, the following ranking table for the selection of aluminium alloys is applicable.

TABLE 6.4 : Ranking of aluminium alloys for dry abrasive wear.

| | |
|---|---|
| 7075 | **GOOD ABRASION RESISTANCE** |
| 2014 | |
| 6-series | |
| 7017 | |
| 3004 | |
| 5-series | |
| LM6 cast alloys | |
| KS cast alloys | |
| 1200 | **POOR ABRASION RESISTANCE** |

Corrosive wear

Table 6.5 can be drawn up as a guide to aluminium alloy selection in a corrosive wear environment representative of average mine water conditions.

TABLE 6.5 : Guide for corrosive wear selection.

| | |
|---|---|
| 1-series<br>3-series<br>5-series<br>6-series<br>7017 | ↓ INCREASED PITTING CORROSION WITH LOW VOLUME LOSSES |
| 7075<br>Al-Si cast alloys<br>2-series | ↓ SEVERE LOCALISED AND PITTING CORROSION WITH HIGHER VOLUME LOSSES |

Abrasive-corrosive wear

Under conditions where a semi-continuous abrasive action is interrupted by short corrosion periods, ranking Table 6.6(a) is applicable. In the presence of long corrosion periods that are periodically interrupted by light abrasive actions the selection of alloys according to Table 6.6(b) is recommended. The alloys 7075, 2014 and LM6+Sr show a significant decrease in wear performance (up to 50%) under conditions where corrosion is predominant and should not be considered for an abrasive-corrosive wear evaluation.

TABLE 6.6 : Ranking of aluminium alloys for abrasive-corrosive wear.

| (a) SEMI-CONTINUOUS ABRASION WITH SHORT CORROSION PERIODS | | (b) LONG CORROSION PERIODS WITH LIGHT ABRASIVE INTERVALS |
|---|---|---|
| 7017 | GOOD WEAR RESISTANCE | 6261 |
| 7075 | | 5083 |
| 5-series | | 7017 |
| 6-series | | 3004 |
| 3004 | | 1200 |
| 2014 | | 7075 |
| 1200 | | LM6 cast alloys |
| LM6 cast alloys | | KS cast alloys |
| KS cast alloys | POOR WEAR RESISTANCE | 2014 |

Optimisation of material properties for abrasion resistance

It was established in Section 6.1.2 that the superior abrasion resistance of heat-treatable alloys can be attributed partly to a good combination of tensile strength and hardness. Three factors are important when considering these material properties as a measure of abrasion resistance:

(i) A plot of tensile strength versus abrasion resistance (fig. 5.5 (a)) yields no definite trend and it follows that this property alone does not provide an adequate measure of abrasion resistance.

(ii) Figure 5.4 shows that approximate linear relationship between abrasion resistance and hardness for both heat-treatable and non heat-treatable alloys is identifiable. Bulk hardness thus provides and adequate measure of relative abrasion resistance only when analysed separately for the two classes of wrought alloys.

(iii) It is apparent from fig. 5.5(b) that hardness also gives a good indication of tensile strength for wrought alloys. Eqn.(4) describes the relationship.

Work-hardening capacity was found to be similar and small for all wrought alloys, regardless of their strength value. Figure 5.7 confirms that this material property alone gives no direct indication of abrasion resistance. A noteable exception is the alloy 3004, where superior work-hardening characteristics and correspondingly higher abrasion resistance relative to the other non heat-treatable alloys was observed.

An overview of the microstructures presented in figs 4.4 to 4.11 show that aluminium alloys with a very fine or very coarse distribution of second phase particles have low abrasion resistance. Good examples are the cast and 1-series alloys respectively. Abrasion resistance is optimised by an intermediate size and distribution of second phase particles as exhibited by the heat-treatable alloys.

Another important material property combination is fracture toughness and hardness. Figures 5.8(a) and (b) give plots of abrasion resistance and hardness versus Charpy Impact Energy for wrought alloys. The trends indicated show reasonable comparison with the model presented by Zum Gahr in Section 2.2.2. Lawn and Marshall (1979) used this model to predict optimisation of wear resistance for each of the three regions of fig. 2.4. In Region I wear resistance is optimised by maximising fracture toughness. Over Region II maximisation of the ratio of fracture toughness to hardness is proposed. Optimum wear resistance in Region III is obtained by maximising hardness.

# CHAPTER 7

## CONCLUSIONS

### Effect of external factors on dry abrasive wear rates

(1) Direct proportionality between load and wear rate is observed for aluminium alloys.

(2) Wear rate is approximately independent of speed for the range 0.1 to 0.5m/s. This trend may be attributed to the interaction of strain rate and temperature effects on flow stress.

(3) Aluminium alloys exhibit the critical grit diameter effect and show a linear increase in wear rate for further increases in grit size above the critical value.

### Relative abrasion resistance and the effect of material properties

(1) Cast Al-Si alloys have abrasion resistance approximately 1/4 that of mild steel. Poor microfracture properties are observed as a result of coarse and brittle silicon phases contained in the aluminium matrix of these alloys.

(2) Non heat-treatable wrought alloys such as 1200, 3004 and 5083 exhibit soft ductile deformation characterisitics and also have fairly low abrasion resistance, approximately 1/3 that of mild steel.

(3) In the case of heat-treatable alloys such as 2014, 6082 and 7075 microfracture properties are improved by a better combination of tensile strength, hardness and toughness. Abrasion resistance values approximately 1/3 to 1/2 to that of mild steel are observed.

(4) Aluminium alloys can be ranked for dry abrasive wear according to Table 6.4.

### Corrosive wear resistance

(1) Pitting corrosion for the alloys 1200, 3004, 5083, 6082 and 7017 occurs predominantly at constituent sites due to localised differences in electrode potentials. Higher series alloys with a large number of constituent particles exhibit higher pitting densities.

(2) Severe pitting and localised attack of Al-Si cast alloys is observed as a result of the strong cathodic potential of silicon phases in the aluminium matrix.

(3) Poor corrosion resistance is exhibited by the alloys 2014 and 7075. Due to the high anodic potentials of copper and zinc containing solid solutions respectively they are subject to severe general and pitting attack.

(4) A guide for corrosive selection of aluminium alloys is given by Table 6.5.

Abrasive-corrosive wear resistance

(1) Under abrasive-corrosive conditions the alloys 2014, 7075 and LM6+Sr show a decrease in wear performance due to poor corrosion properties. The most suitable conditions are semi-continuous abrasive intervals interrupted by short corrosion periods.

(2) Under conditions of long corrosion periods with light abrasive intervals the alloys 5083, 6261 and 7017 show a significant improvement in wear performance. This trend is attributed to good corrosion properties where only low volume losses by pitting corrosion are exhibited.

(3) Al-alloys can be ranked for abrasive-corrosive wear according to Table 6.6.

Optimum material properties for abrasion resistance

It can be concluded that the abrasion resistance of wrought alloys may be maximised by designing an aluminium alloy with a good combination of tensile strength, fracture toughness and hardness, together with an intermediate microstructural size distribution of second phase particles in the aluminium matrix. In the case of non heat-treatable alloys where cold work improves abrasive wear performance only marginally, strengthening of the soft aluminium solid solution may be achieved by suitable alloying elements. Ageing of heat-treatable alloys improves abrasion resistance significantly, peak hardness and strength conditions resulting in optimum abrasion properties. It is important that the dry abrasion results be evaluated in accordance with the experimental parameters used since the performance of wrought and cast aluminium alloys vary significantly for different load and speed conditions and different types of abrasives.

## REFERENCES

ALLEN C., BALL A. and NOËL R.E.J. (1984) : "The development of 3CR12 type steels to resist corrosive abrasive environments", Proceedings of Inaugural International 3CR12 Conferences, Johannesburg, March 1984, 433-453.

ALLEN C., PROTHEROE B.E. and BALL A. (1981) : "The selection of abrasion corrosion resistant materials for gold mining equipment", Journal of the South African Institute of Mining and Metallurgy, **81** (10), 289-297.

ALLEN C., PROTHEROE B.E. and BALL A. (1981/1982) : "The abrasive-corrosive wear of stainless steel", Wear, **74** , 287-305.

ASM Metals Handbook (1972) : Atlas of Microstructures of Industrial Alloys, American Society of Metals, Ohio, Vol.7.

AVINET B.W.E., GODDARD J. and WILMAN H. (1960) : "An experimental study of friction and wear during abrasion of metals", Proc. Roy. Soc. (London), Ser.A, 159-179.

BALL A. (1983) : "On the importance of work hardening in the design of wear-resistant materials", Wear, **91** , 201-207.

BALL A. and BLÖM H. (1987) : "The design and performance of steels in an abrasive-corrosive mining environment", IMechE, C189/87, 595-602.

BALL A. and WARD J.J. (1985) : "An approach to material selection for corrosive abrasive wear by systematic in-situ and laboratory testing procedures", Tribology International, **18** (6), 347-351.

BARBOSA M. and SCULLY J.C. (1982) : "The role of repassivation kinetics in the measurement of the pitting potential of AISI 304 stainless steel by the scratch method", Corrosion Science, **22** (11), 1025-1036.

BATCHELOR A.W., STACHOWIAK G.W. (1987) : "Predicting synergism between corrosion and abrasive wear".

CAPENDALE A.E. (1985) : "The influence of water composition on the pitting behaviour of a stainless steel", M.Sc thesis, University of Cape Town.

DUNN D.J. (1985) : "Metal removing mechanisms comprising wear in mineral processing", Proceedings of International Conference on Wear of Materials - 1985, Ludema K.C. (Ed), ASME, New York.

EYRE T.S. (1984) : "Wear of aluminium alloys", Research at Brunel.

FOGEL G. (1980) : "The influence of microstructure on abrasive wear", Msc thesis, University of Cape Town.

HATCH J.E. (1984) : Aluminium : Properties and physical metallurgy, American Society of Metals.

HORN W., ZIEGLER W. (1983) : "The wear behaviour of aluminium alloys", Zeitschrift Metalkunde.

HORNBOGEN E. (1975) : "The role of fracture toughness in the wear of metals", Wear, **33** , 251-259.

LARSEN-BASSE J. (1968) : "Influence of grit diameter and specimen size on wear during sliding abrasion", Wear, **12** , 35-53.

LARSEN-BASSE J. and TANOUYE P.A. (1978) : "Strain rate effects in low speed two-body abrasion", Journal of Lubrication Technology, **100** (4), 181-184.

LENEL U.R. and KNOTT B.R. (1986) : "Wear resistance of steels designed for use in severe abrasion-corrosion conditions", Paper presented at International Conference on Wear of Materials - 1987, Ludema K.C. (Ed), ASME, New York, 635-643.

MALAN S.F., PATERSON A.E. (1986) : "Introduction to Aluminium", Aluminium Federation of S.A.

MING-KAI TSE, NAM P. SUH (1977) : "Chemical effects in sliding wear of aluminium", Wear, **44** , 145-162.

MOHAMMED JASIM K., DWARAKADASA E.S. (1987) : "Wear in Al-Si alloys under dry sliding conditions", Wear, **119** , 119-130.

MOORE J.J., IWASAKI I., NATARAJAN K.A., PEREZ R. and ADAM K. (1984) : "The effect of grinding ball composition and mineral slurry environment on grinding media wear", IMechE, C352/84, 215-226.

MOORE M.A. (1974) : "A review of two-body abrasive wear", Wear, **27** , 1-17.

MOORE M.A. 91980) : "Abrasive Wear", Paper presented at the Fundamentals of Friction and Wear of Materials, Materials Science Seminar, American Society of Metals, Pittsburgh, Pennsylvainia.

MOORE M.A. and DOUTHWAITE R.M. (1976) : "Plastic deformation below worn surfaces", Metallurgical Transactions A, **7A** , 1833-1839.

MOORE M.A., RICHARDSON R.C.D. and ATTWOOD D.G. (1972) : "The limiting strength of worn metal surfaces", Metallurgical Transactions, **3** , 2485-2491.

MULHEARN P.J. and SAMUELS L.E. (1962) : "The abrasion of metals: A model of the process", Wear, **5** , 478-498.

MURRAY M.J., MUTTON P.J. and WATSON J.D. (1979) : "Abrasive wear mechanisms in steels", Proceedings of International Conference on Wear of Materials - 1979, Ludema K.C., Glaeser W.A. and Rhee S.K. (Eds), ASME, New York, 257-265.

MUTTON P.J. and WATSON J.D. (1978) : "Some effects of microstructure on the abrasion resistance of metals", Wear, **48** , 385-398.

NAVARIMHA RAO K., SEKHAR J.A. (1986) : "Comparative wear behaviour of aluminium alloys", Journal of Materials Science Letters, 5.

NOËL R.E.J. (1981) : "The abrasive-corrosive wear behaviour of metals", M.Sc (Eng) thesis, University of Cape Town.

NOËL R.E.J. and BALL A. (1983) : "On the synergistic effects of abrasion and corrosion during wear", Wear, **87** , 351-361.

NOËL R.E.J., ALLEN C. and BALL A. (1984) : "The development and use of in-situ and laboratory tests as a guide to the selection of materials for the gold mining industry", IMechE, C358/84, 23-28.

OKABAYASHI K., KAWAMOTO M., NOTANI H. (1966) : "Study on the wear of casting aluminium alloys (III)", Light Metals - Japan.

POLMEAR I.J. (1986) : Light Alloys, Edward Arnold Publishers Ltd., London.

PRAMILA BAI B.N., BISWAS S.K. (1984) : "Mechanism of wear in dry sliding of a hypoeutectic aluminium alloy", Lubrication Engineering, **43** , 57-61.

PROTHEROE B.E., BALL A. and HEATHCOCK C.J. (1982) : "The development of wear resistant alloys for the South African gold mining industry", Proceedings of International Confernce on Recent Developments in Speciality Steels and Hard Materials, Comins N.R. and Clarke J.B. (Eds), CSIR, Pretoria, 289-298.

ROBINSON S. (1987): "An introduction to aluminium", Hulett Aluminium Limited.

SCHUMACHER W. (1985) : "Corrosion wear synergy of alloy and stainless steels", Proceddings of International Conference on Wear of Materials - 1985, Ludema K.C. (Ed), ASME, New York.

ZUM-GAHR K.H. (1981/1982) : "Formation of wear debris by the abrasion of ductile metals", Wear, **74** , 353-373.

ZUM-GAHR K.H. (1988) : "Modelling of two-body abrasive wear", Wear, **124** 87-103.

ZUM-GAHR K.H. (1987) : Microstructure and wear of materials, Elsevier Science Publishing Company Inc., New York.

APPENDIX A1 : Standard test procedures

RAR test procedure

1. Standard specimen size : 10 x 10 x 15 mm (can be longer or shorter)
2. Run-in 10 x 10 face on used abrasive belt under load until evenly abraded
3. Note direction of abrasion (leading edge)
4. Clean sample ultrasonically in alcohol, dry it, cool it to room temperature
5. Weigh specimen to 0.01 mg
6. At abrasion rig: clamp specimen in holder, check abrasion direction and specimen height
7. On a fresh 80 grit belt line up specimen at start line
8. Load is 32.1 kPa (3.21 kg for 10 x 10 mm face)
9. Abrade sample for three full rounds (Length = 3 x 1.22 m = 3.66 m)
10. Unclamp specimen from holder
11. Repeat items 4 to 10 four times (total of 14.64 m abrasion, 4 readings)

Remember always to include at least one mild steel specimen as standard in a test batch.

RWR#1 test procedure

1. Specimen as for R.A.R. test, unabraded sides must be free from corrosion, preferably polished to 800 grit
2. Run-in, clean and weigh specimen as for R.A.R. test.
3. Coat the five unabraded sides of specimen with laquer (at present, we use Plascon Incralac laquer CAB 7-51L)
4. At corrosion rig:
   - Make sure rig is clean (rust, algae)
   - Fill main tank with destilled water, rinse rig for one hour, empty it again
   - Fill tank with the following solution:
     14 l dest. water + 6.79 g $CaCl_2$ + 14.55 g $Na_2SO_4$
   - Switch on pump and heater, let system equilibrate to 30°C
   - Load sample holder: abraded surfaces flush with test plate, leading edge of sample aligned to flow of water
   - Start test
5. After 46 hours: Take specimen out of rig
6. Ultrasonically clean a) 1 min in acetone
   b) 5 min in 10% diamonium hydrogen citrate + $H_2O$
   c) 1 min in alcohol, dry and cool to room temperature
7. Weigh specimen to 0.01 mg
8. At abrasion rig: Clamp specimen in, correctly aligned
9. Set rig on Ref. 25 cm, abrade specimen on fresh abrasive for exactly 25 cm
10. Ultrasonically clean specimen in alcohol, dry, cool and weigh to 0.01 mg
11. Coat unabraded sides with laquer
12. Clean filter of corrosion test rig in diluted HCl
13. Load sample correctly aligned into holder, restart corrosion rig (solution remains the same for whole test)
14. Repeat items 5 to 13 four times, total 8 days corrosion and 1 m abrasion
    Check ocasionally for temperature and cleanness of filter.

Always include at least one mild steel sample as standard in test batch.

RWR#2 test procedure

Procedure remains exactly the same.
The following parameters change : time in corrosion rig = 22 hours (not 46)
abrasion path length = 1 m (not 25 cm)

Total test is four days corrosion and four meter abrasion.

Always include at least one mild steel sample as standard in test batch.

APPENDIX A2 : AFSA data on alloying elements.

| ALLOY | ALLOYING ELEMENTS (% wt) | | | | | | | | |
|---|---|---|---|---|---|---|---|---|---|
| | Cu | Fe | Mg | Mn | Si | Ti | Zn | Cr | Other |
| 1200 | 0.05 | 0.7 | - | 0.05 | 0.5 | - | 0.1 | - | 0.15 |
| 2014 | 3.9-5.0 | 0.7 | 0.2-0.8 | 0.4-1.2 | 0.5-1 | 0.5 | 0.20 | 0.01 | 0.15 |
| 3004 | 0.05 | 0.42 | 0.85-1.05 | 1.0-1.2 | 0.15-0.21 | 0.05 | - | 0.1 | 0.1 |
| 5083 | 0.1 | 0.4 | 4.0-4.9 | 0.5-1.0 | 0.40 | 0.15 | 0.2 | 0.25 | 0.15 |
| 5251 | 0.1 | 0.2-0.5 | 1.9-2.3 | 0.30-0.45 | 0.1-0.3 | 0.2 | 0.03 | - | 0.1 |
| 6063 | 0.1 | 0.35 | 0.45-0.9 | 0.1 | 0.3-0.6 | 0.2 | 0.10 | - | 0.15 |
| 6082 | 0.1 | 0.50 | 0.5-1.2 | 0.4-1.0 | 0.7-1.3 | 0.1 | 0.2 | 0.25 | 0.15 |
| 6261 | 0.15-0.4 | 0.40 | 0.7-1.0 | 0.20-0.35 | 0.40-0.70 | 0.10 | 0.20 | 0.10 | 0.15 |
| 7017 | 0.10-0.15 | 0.3 | 2.4-2.7 | 0.2-0.3 | 0.15 | 0.2 | 4.8-5.2 | 0.1 | 0.1 |
| 7075 | 1.2-2.0 | 0.50 | 2.1-2.9 | 0.30 | 0.40 | 0.2 | 5.1-6.1 | 0.28 | 0.15 |
| | | | | | | | | | |
| | | | | | | | | | |
| | | | | | | | | | Ni |
| KS281.1 | 1.03 | 0.43 | 1.10 | 0.12 | 16.73 | 0.08 | 0.07 | - | 0.96 |
| LM6+Sr | 0.05 | 0.30 | 0.06 | 0.11 | 12.37 | 0.03 | 0.03 | - | 0.01 |
| LM6+PC1 | 0.03 | 0.43 | 0.03 | 0.13 | 12.85 | 0.05 | 0.02 | - | 0.01 |
| KS1275 | 1.02 | 0.46 | 1.09 | 0.11 | 12.50 | 0.09 | 0.08 | - | 0.92 |

APPENDIX A3 : Mechanical properties, fabrication routes and temper conditions.

| ALLOY | 0.2 % PROOF STRESS (MPa) | TENSILE STRENGTH (MPa) | % ELONGATION | FABRICATION ROUTE | TEMPER DESIGNATION |
|---|---|---|---|---|---|
| 1200 | - | 95-120 | 9% | R | H2 |
| 2014 | 480 | 520 | - | E&F | T6 |
| 3004 | 145 | 190-240 | - | R | H2 |
| 5083 | 175 | 295 | 10% | R | H2 |
| 5251 | 170 | 230 | 13% | R | H2 |
| 6063 | 205 | 245 | 13% | R | T6 |
| 6082 | 320 | 345 | 12% | R | T6 |
| 6261 | 290 | 318 | 10% | R | T6 |
| 7017 | 531 | 553 | 13% | R | T6 |
| 7075 | 540 | 590 | 7% | R | T6 |
| KS281.1 | - | 190-220 | 0.5% | - | as cast |
| LM6+Sr | - | 220-240 | 9-12% | - | as cast |
| LM6+PC1 | - | 220-240 | 9-12% | - | as cast |
| KS1275 | - | 177 | 0.5% | - | as cast |

Temper desigations
T6 = Solution heat-treated and artifically aged
H2 = ½ hard coldworked

Fabrication routes
R = rolled
E&F = extruded and forged

APPENDIX A4 : Results of standard tests.

| ALLOY | MECHANICAL AND PHYSICAL PROPERTIES | | | | STANDARD WEAR TESTS | | |
|---|---|---|---|---|---|---|---|
| | Density ($g/cm^3$) | Hardness (HV30) | Charpy Impact Energy (J) | Work hardening capacity (HV max/HV bulk) | RAR | RWR#1 | RWR#2 |
| 1200 | 2.69 | 38 | 76 | 1.5 | 0.22 | 1.30 | 0.37 |
| 2014 | 2.79 | 160 | 6 | 1.3 | 0.40 | 1.39 | 0.61 |
| 3004 | 2.71 | 62 | 71 | 2.2 | 0.34 | 1.49 | 0.50 |
| 5083 | 2.65 | 96 | 25 | 1.3 | 0.31 | 2.14 | 0.56 |
| 5251 | 2.66 | 84 | - | - | 0.31 | 1.98 | 0.58 |
| 6063 | 2.69 | 83 | 39 | - | 0.41 | 1.85 | 0.54 |
| 6082 | 2.70 | 95 | 15 | 1.2 | 0.40 | 1.90 | 0.55 |
| 6261 | 2.70 | 115 | 15 | - | 0.34 | 1.95 | 0.57 |
| 7017 | 2.74 | 145 | 29 | 1.5 | 0.35 | 2.24 | 0.60 |
| 7075 | 2.79 | 189 | - | - | 0.49 | 2.21 | 0.70 |
| KS281.1 | 2.65 | 140 | 2 | - | 0.25 | 0.89 | 0.36 |
| KS1275 | 2.68 | 100 | 1 | - | 0.20 | 0.84 | 0.33 |
| LM6+Sr | 2.65 | 69 | 4 | - | 0.27 | 1.33 | 0.43 |
| LM6+PCl | 2.65 | 73 | 3 | - | 0.21 | 1.11 | 0.36 |
| MS | 7.78 | 200 | 37 | - | 1.00 | 1.00 | 1.00 |
| 3CR12 | 7.68 | 185 | 75 | - | 1.22 | 7.63 | 2.25 |

APPENDIX A5 : AFSA manufacturing data

| ALLOY | CORROSION RESISTANCE | WELDABILITY | FORMABILITY | MACHINABILITY | TOTAL POINT VALUE |
|---|---|---|---|---|---|
| 1200 | 4 | 5 | 5 | 2 | 16 |
| 2014 | 1 | 2 | 1 | 3 | 7 |
| 3004 | 4 | 5 | 4 | 2 | 15 |
| 5083 | 5 | 3 | 3 | 2 | 13 |
| 5251 | 5 | 4 | 4 | 2 | 15 |
| 6063 | 4 | 3 | 3 | 3 | 13 |
| 6082 | 3 | 3 | 3 | 3 | 12 |
| 6261 | 3 | 3 | 3 | 3 | 12 |
| 7017 | 3 | 4 | 3 | 3 | 13 |
| 7075 | 1 | 0 | 2 | 5 | 8 |

Comparative ratings :

| | |
|---|---|
| Excellent | = 5 |
| Very good | = 4 |
| Good | = 3 |
| Fair | = 2 |
| Poor | = 1 |
| Not recommended | = 0 |